



Search for new phenomena in three- or four-lepton events in pp collisions at $\sqrt{s} = 13$ TeV with the ATLAS detector

The ATLAS Collaboration*



ARTICLE INFO

Article history:

Received 1 July 2021

Received in revised form 3 December 2021

Accepted 6 December 2021

Available online 14 December 2021

Editor: M. Doser

ABSTRACT

A search with minimal model dependence for physics beyond the Standard Model in events featuring three or four charged leptons (3ℓ and 4ℓ , $\ell = e, \mu$) is presented. The analysis aims to be sensitive to a wide range of potential new-physics theories simultaneously. This analysis uses data from pp collisions delivered by the Large Hadron Collider at a centre-of-mass energy of $\sqrt{s} = 13$ TeV and recorded with the ATLAS detector, corresponding to the full Run 2 dataset of 139 fb^{-1} . The 3ℓ and 4ℓ phase space is divided into 22 event categories according to the number of leptons in the event, the missing transverse momentum, the invariant mass of the leptons, and the presence of leptons originating from a Z -boson candidate. These event categories are analysed independently for the presence of deviations from the Standard Model. No statistically significant deviations from the Standard Model predictions are observed. Upper limits for all signal regions are reported in terms of the visible cross-section.

Crown Copyright © 2021 Published by Elsevier B.V. This is an open access article under the CC BY license (<http://creativecommons.org/licenses/by/4.0/>). Funded by SCOAP³.

1. Introduction

Despite the success of the Standard Model (SM) [1–4] in describing the interactions of elementary particles, there remain observations that suggest the existence of additional phenomena [5–9]. Many theories of physics beyond the Standard Model (BSM theories) have been proposed that feature final states in high-energy proton–proton (pp) collisions with exactly three or four leptons (3ℓ and 4ℓ , where $\ell = e, \mu$ in this paper). An example is supersymmetry (SUSY), where neutralino and chargino production [10] yields three leptons and a neutrino through an intermediate WZ state, and where di-Higgs production [11] yields four or more leptons. Furthermore, enhanced flavour-changing decay cross-section of top quarks at the loop level may lead to anomalous production of 3ℓ final states with respect to the SM [12]. Multiple types of seesaw models can produce multilepton final states alongside neutrinos [13–17]. Adding an additional Higgs triplet to the SM Lagrangian [18,19] potentially leads to a doubly charged Higgs particle [20,21] which can decay into two leptons, leading to a four-lepton final state if produced in pairs. Theories predicting such a particle include left–right symmetric models [22,23], scalar singlet dark matter [24] and the Zee–Babu model [25]. Conclusive evidence for any of these BSM theories has thus far been elusive. Many dedicated analyses within the LHC experimental collaborations are being performed to search for such evidence. However, the vast number of theories means that it would be difficult to perform a dedicated analysis for each model. This motivates the desire

to establish instead a search that does not rely on a specific model for its signal description (henceforth called ‘model-independent’), which can cover a wide range of signatures to seek indicators of exotic physics.

The analysis presented here is committed to investigating a large phase space while making few prior assumptions about the nature of new-physics processes. As such, it is expected to be sensitive to a large number of signals that could be populating the ATLAS data, albeit with a lower sensitivity than a dedicated analysis could achieve. Partial overlap with dedicated analyses is expected, but since these are typically tuned to specific models they do not consider the full phase space. For instance, Ref. [26] also studies 4ℓ final states, but does not consider events with low four-lepton invariant masses and missing transverse momenta. The present analysis does not attempt to exploit very distinctive features, such as e.g. resonances in invariant-mass distributions, and instead entails a substantially more inclusive selection than is typical of searches for specific BSM theories. Nevertheless, a comparison with a few benchmark models indicates that its sensitivity is not greatly reduced compared to that of more dedicated searches.

The analysis aims to uncover evidence of BSM physics. Failing that, it can provide a set of upper limits on the visible cross-section, which can be reinterpreted as upper limits on BSM models of interest. The upper limits on two benchmark models derived in this fashion, a Type-III seesaw model [27] and a doubly-charged Higgs model [28] are compared with those obtained using dedicated analyses.

For this analysis, the full pp dataset collected by the ATLAS experiment during the 2015–2018 data-taking period is used, cor-

* E-mail address: atlas.publications@cern.ch.

responding to an integrated luminosity of 139 fb^{-1} delivered by the LHC. Events featuring exactly three or four charged leptons are categorised into signal regions based on the invariant mass of the leptons, the missing transverse momentum and the presence of a lepton pair compatible with originating from a Z -boson decay. The observations in such regions are individually used to probe for the presence of a BSM signal. Control regions are established to extract a normalisation of the most prominent SM backgrounds, which are leptonically decaying WZ and ZZ diboson pairs, and for the estimation of the contribution from interactions producing lepton candidates from heavy-flavor hadrons decays or hadronic particles misidentified as leptons. In each region, a SM-only hypothesis is compared with a hypothesis assuming the SM plus an additional number of BSM events as a free parameter.

A previous general multilepton search with the ATLAS detector was performed using 20.3 fb^{-1} of pp collisions at $\sqrt{s} = 8 \text{ TeV}$ [29]. Compared to that search, the current analysis uses a larger dataset collected at $\sqrt{s} = 13 \text{ TeV}$ and assigns 4ℓ events to multiple separate regions, but does not consider hadronic τ -lepton decays. A strategy for a general search was outlined in Ref. [30] using 3.2 fb^{-1} of data at $\sqrt{s} = 13 \text{ TeV}$. That search uses fewer data events and a coarser background estimation, but offers a broader selection of final states, including multilepton final states, and performs tests with additional variables. Furthermore, a similar search, also testing multilepton final states, has been performed by the CMS Collaboration with 137 fb^{-1} of pp collisions at $\sqrt{s} = 13 \text{ TeV}$ [31].

2. ATLAS detector

The ATLAS experiment [32] at the LHC is a multipurpose particle detector with a forward-backward symmetric cylindrical geometry and a near 4π coverage in solid angle.¹ It consists of an inner tracking detector (ID) surrounded by a thin superconducting solenoid providing a 2 T axial magnetic field, electromagnetic and hadron calorimeters, and a muon spectrometer. The inner tracking detector covers the pseudorapidity range $|\eta| < 2.5$. It consists of silicon pixel (with the insertable B-layer installed before Run 2 [33,34]), silicon microstrip, and transition radiation tracking detectors. In the range $|\eta| < 3.2$, hermetic lead/liquid-argon (LAr) sampling calorimeters provide electromagnetic (EM) energy measurements with high granularity. The central region, $|\eta| < 1.8$, is additionally instrumented with a thin LAr presampling detector to correct for energy losses in the inactive material in front of the detector. A steel/scintillator-tile hadronic calorimeter covers the central pseudorapidity range $|\eta| < 1.7$. The endcap and forward regions are instrumented with LAr calorimeters for both the EM and hadronic energy measurements up to $|\eta| = 4.9$. The muon spectrometer surrounds the calorimeters. It consists of three large superconducting air-core toroidal magnets with eight coils each. The field integral of the toroids ranges between 2.0 and 6.0 Tm across most of the detector. The muon spectrometer includes three layers of precision tracking chambers, allowing precise muon momentum measurements up to $|\eta| = 2.7$, and fast detectors for triggering up to $|\eta| = 2.4$. A two-level trigger system [35] is used to select events. The first-level trigger is implemented in hardware and uses a subset of the detector information to accept events at a rate below 100 kHz. This is followed by a software-based trigger

that reduces the accepted event rate to 1 kHz on average depending on the data-taking conditions.

3. Data and simulated events

This analysis uses pp collision data at a centre-of-mass energy of $\sqrt{s} = 13 \text{ TeV}$, collected by the ATLAS detector and corresponding to a total integrated luminosity of 139 fb^{-1} . Only data recorded during stable beam conditions with all ATLAS detector subsystems operational [36] have been included. Dilepton triggers [37,38] covering all lepton flavour combinations (ee , $e\mu$ and $\mu\mu$) are used. The transverse momentum (p_T) requirements of these triggers depend on the data-taking period. For the dielectron trigger, these requirements are 12 GeV in 2015, 17 GeV in 2016, and 24 GeV in 2017–18. For the dimuon trigger, they are 18 and 8 GeV in 2015 and 22 and 8 GeV in 2016–18.² For the mixed-flavour trigger, the p_T requirement is 17 GeV for the electron and 14 GeV for the muon. These trigger choices correspond to the dilepton triggers with the lowest p_T requirements available during each data-taking year.

Expected event rates due to SM processes that can result in 3ℓ and 4ℓ final states were estimated using a combination of Monte Carlo (MC) event generation and data-driven techniques. Event generators based on MC methods were used to estimate the total expected contributions from SM processes producing only prompt leptons.³ The dominant SM backgrounds are the production of two vector bosons decaying leptonically: WZ for the 3ℓ final states and ZZ for the 4ℓ final states. Subleading prompt-lepton backgrounds that contribute are triboson production, and processes which include at least one top quark: $t\bar{t}X$ ($X = W, Z, H$), tZ , $t\bar{t}WW$ and $t\bar{t}\bar{t}$.

All diboson and triboson (VV and VVV , where $V = W, Z$) production, including off-shell production, was simulated with the SHERPA 2.2.2 [39] generator. The NNPDF3.0nnlo set of PDFs was used [40], along with the dedicated set of tuned parton-shower parameters developed by the SHERPA authors. The matrix element calculations were matched and merged with the SHERPA parton shower [41] based on Catani–Seymour dipole factorisation [42,43] using the MEPS@NLO prescription [44–47]. Diboson events were generated at next-to-leading-order (NLO) accuracy in QCD for up to one additional parton and at leading-order (LO) accuracy for two and three additional parton emissions. Electroweak $VVjj$ ($j = \text{jet}$) events were generated at LO. This contribution includes Higgs boson production through vector-boson fusion (with $H \rightarrow ZZ$). It also includes triboson processes where one boson decays hadronically, including $VH \rightarrow VVV \rightarrow VVjj$. Loop-induced production of ZZ events via gluon-gluon fusion was simulated using matrix elements accurate at LO for up to one additional parton emission for both the fully leptonic and semileptonic final states. This contribution includes $gg \rightarrow H \rightarrow ZZ$.

Triboson events were generated at NLO for the inclusive process and at LO for up to two additional parton emissions. The virtual QCD corrections were provided by the OPENLOOPS library [48–50]. This process includes only on-shell fully leptonic decays.

The production of $t\bar{t}V$, $t\bar{t}WW$, tZq and $t\bar{t}\bar{t}$ events was modelled using the MADGRAPH5_aMC@NLO v2.3 [51] (v2.2 for $t\bar{t}WW$) generator, while $t\bar{t}H$ events [52] were modelled using the POWHEGBOX [53–56] v2 generator with the h_{damp} parameter set to $1.5 m_{\text{top}}$ [57]. Events were generated at NLO for $t\bar{t}V$ and $t\bar{t}H$. The tZq , $t\bar{t}WW$ and $t\bar{t}\bar{t}$ processes were modelled at LO with their cross-sections normalised to NLO predictions [51]. The

¹ ATLAS uses a right-handed coordinate system with its origin at the nominal interaction point (IP) in the centre of the detector and the z -axis along the beam pipe. The x -axis points from the IP to the centre of the LHC ring, and the y -axis points upwards. Cylindrical coordinates (r, ϕ) are used in the transverse plane, ϕ being the azimuthal angle around the z -axis. The pseudorapidity is defined in terms of the polar angle θ as $\eta = -\text{Ln}(\tan(\theta/2))$. Angular distance is measured in units of $\Delta R \equiv \sqrt{(\Delta\eta)^2 + (\Delta\phi)^2}$.

² At least one muon must pass the higher p_T requirement and a second muon at least the lower p_T requirement.

³ A lepton is prompt if none of the particles in its production chain, traced back to the interaction point of the pp collision, are hadrons.

NNPDF3.0n1o [40] PDF was used. The events were interfaced to PYTHIA8.210 (8.230 for tZq) [58] using a set of tuned parameters called the A14 tune [59] and the NNPDF2.31o [40] PDF set. Collectively, these events are referred to as the top-quark background.

Additional processes involving Higgs boson production, apart from those mentioned above, have been found to yield negligible contributions and are not considered explicitly.

For model-specific interpretation of the analysis, signal samples were generated for Type-III seesaw model heavy leptons and doubly charged Higgs ($H^{\pm\pm}$) particles decaying leptonically. The simplified Type-III seesaw model was included in the MADGRAPH5_aMC@NLO v2.3.3 generator at LO with an implementation using FeynRules [60], described in Ref. [27]. Implementation details are described in Ref. [17]. Samples of $H^{\pm\pm}$ events were generated at LO using the left-right-symmetry package of PYTHIA8.186, which provides the $H^{\pm\pm}$ scenario described in Ref. [28]. Implementation details are described in Ref. [21]. The parton shower was provided by PYTHIA8.230 (PYTHIA8.186) for the Type-III seesaw ($H^{\pm\pm}$) model using the NNPDF2.31o PDF set and the A14 tune [59]. Cross-sections for both samples were normalised to NLO.

The ATLAS detector simulation [61] employing the GEANT4 [62] framework was used to model the detector response in MC events. The effect of pile-up was incorporated into the simulation by overlaying additional inelastic pp events onto hard-scatter events. These were generated with PYTHIA8 [58] using the A3 tune [63] and the MSTW2008LO [64] PDF set. Events were simulated with discrete values for the expected mean number of interactions and then weighted to match the distribution that is observed per bunch crossing in data.

4. Object selection

All events in the analysis are required to have a primary vertex, defined as the vertex with the highest value of $\sum p_T^2$ of its associated tracks, which must include at least two with $p_T > 0.5$ GeV. Electron and muon candidates are required to originate from the primary vertex.

Requirements common to both electron and muon candidates are $p_T > 25$ GeV and $|\eta| < 2.47$. For the purposes of matching tracks to the primary vertex, the track impact parameters⁴ d_0 and z_0 must satisfy $|d_0|/\sigma(d_0) < 5(3)$ for electrons (muons) and $|z_0 \sin \theta| < 0.5$ mm. Furthermore, electron and muon candidates are subjected to identification criteria, for which multiple working points are provided [65,66]. The identification is performed using quality cuts where each working point offers a different trade-off between the rate of false positives and false negatives delivered by the algorithm.

Electron candidates are reconstructed using energy clusters measured in the EM calorimeter matched to reconstructed tracks [65]. The identification for the nominal selection in this analysis is based on a combination of detailed tracking and calorimeter information combined into a likelihood discriminant. The Tight [65] working point is used. The range $1.37 < |\eta| < 1.52$ has a significant amount of non-sensitive material in front of the calorimeter, and is therefore excluded.

Muon candidates are reconstructed by combining measurements in the ID and the muon spectrometer [67]. For this analysis, the Medium identification working point is used for most muon candidates [66], which requires an ID track matched with multiple muon spectrometer precision hits. For muon candidates with $p_T > 300$ GeV, the High- p_T working point [66] is used, which

places a tighter requirement on the number of muon spectrometer hits, ensuring optimal momentum resolution for highly energetic muons.

Both the electron and muon candidates are required to be isolated in the ID. To determine isolation, a cone is placed around the object's track, with an opening angle which is the smaller of $\Delta R = 0.2$ (0.3) for electrons (muons) and $10 \text{ GeV}/p_{T,\ell}$. The scalar p_T sum of all tracks (excluding the lepton itself) within this cone, I_R , must satisfy $I_R/p_{T,\ell} < 0.06$. For muon candidates with $p_T > 50$ GeV, the opening angle of the isolation cone is always $\Delta R = 0.2$. Electron candidates must also pass a calorimeter-based isolation requirement of $I_R/p_{T,\ell} < 0.06$, this time taking the sum of calorimeter energy deposits as I_R , within a cone of $\Delta R = 0.2$.

The constituents for jet reconstruction are identified by combining measurements from both the ID and the calorimeter using a particle-flow algorithm [68]. Jet candidates are reconstructed from these particle-flow objects using the anti- k_t algorithm [69,70] with a radius parameter $R = 0.4$. The jet energy scale (JES) and resolution (JER) [71] are corrected to particle level using MC simulation. Jets are furthermore required to have $p_T > 20$ GeV and $|\eta| < 2.5$. The jet vertex tagger (JVT) [72] is used to test jets that have $p_T < 60$ GeV and $|\eta| < 2.4$ to suppress those originating from pile-up.

Objects found to have very collinear tracks are considered to be overlapping. Overlaps are resolved through a sequence of rules. This procedure prevents double-counting of particles interacting with different parts of the detector, and provides an optimal classification of these particles. If a muon candidate is found to have a shared ID track with an electron candidate, the electron candidate is rejected. If two electron candidates have shared ID tracks, the one with the lower p_T is rejected. Jets are rejected if they are within $\Delta R' = 0.2$ (for overlap removal, the pseudorapidity in ΔR is substituted with the rapidity, defined as $y = -\ln \frac{E+p_z}{E-p_z}$) of a lepton candidate, except if the candidate is a muon and three or more collinear tracks are found. Subsequently, lepton candidates that are within $\Delta R' = 0.4$ of any remaining jets are removed.

The missing transverse momentum (E_T^{miss}) [73] in a given reconstructed event is computed as a combination of a hard term, the magnitude of the negative vector sum of the p_T of all reconstructed leptons and jets, and a soft term, computed from the momenta of inner-detector tracks that are not matched to any of the selected objects but do originate from the primary vertex.

5. Analysis strategy

Selected events are separated into different categories, referred to as regions, to maximise the sensitivity to a relatively broad range of potential new phenomena. Signal regions (SRs) are defined as regions to be probed for the presence of such signatures. Criteria that separate these SRs are the number of leptons, the E_T^{miss} and the presence of an on-Z lepton pair: a same-flavour and oppositely charged (SFOC) lepton pair with a dilepton mass within 10 GeV of the Z-boson mass of 91.2 GeV.⁵ Control regions (CRs) are defined so as to be dominated by particular SM processes which have been well-studied in the ATLAS experiment [74,75]. The full list of regions with their selection criteria, apart from the splitting into different invariant-mass ranges, is shown in Table 1. All regions are orthogonal to each other, so no event is assigned to more than one region. The CRs are used to extract the normalisation of the main background processes from data and to constrain the size of the systematic uncertainties of the analysis. Validation

⁴ The d_0 is the transverse impact parameter: the distance of the track from the beam line at the position of closest approach (PCA) in the plane perpendicular to the beam line, while $\sigma(d_0)$ is its uncertainty. The z_0 is the z coordinate of the PCA where $|d_0|/\sigma(d_0)$ is measured, relative to that of the primary vertex.

⁵ A lepton that does not form an on-Z lepton pair with any other lepton in the event is called off-Z.

Table 1

Overview of the regions defined for this analysis. The - symbols indicate that no requirements are made on the variable for that particular region. Additional requirements on SRs, described in the *Other* column, veto events that are used in the CR/VRs from entering into the SRs. The *Z*-pairs column denotes the number of non-overlapping lepton pairs that are same-flavour and oppositely charged and have a dilepton invariant mass within 10 GeV of the *Z*-boson mass of 91.2 GeV. The off-flavour ℓ is the lepton in the 3ℓ event that has a different flavour from the other two leptons; cuts requiring an off-flavour ℓ are not applied if all three leptons are of the same flavour.

Region	Particles	E_T^{miss}	<i>Z</i> -pairs	Other
Signal regions				
3ℓ	3ℓ	< 50 GeV	1	veto event if $m_T < 80$ GeV for off- <i>Z</i> ℓ
	3ℓ	> 50 GeV	1	veto event if $m_T < 80$ GeV for off- <i>Z</i> ℓ
	3ℓ	< 50 GeV	0	veto event if $m_T < 40$ GeV for off-flavour ℓ
	3ℓ	> 50 GeV	0	veto event if $m_T < 40$ GeV for off-flavour ℓ
<i>3ℓ SRs are divided into m_{inv} ranges of 0–200, 200–400, 400–600 and >600 GeV.</i>				
4ℓ	4ℓ	< 50 GeV	1	-
	4ℓ	> 50 GeV	1	-
	4ℓ	-	0	-
<i>4ℓ SRs are divided in m_{inv} ranges of 0–400 and >400 GeV.</i>				
Fake-Factor Estimation Regions				
<i>e</i> -fakes	$1e$	< 25 GeV	-	jets ≥ 1
μ -fakes	1μ	< 40 GeV	-	jets ≥ 2 , at least 1 jet $p_T > 35$ GeV, $ \Delta\phi(\mu, j) > 2.7$
Validation regions				
3ℓ On- <i>Z</i>	$ee\mu + e\mu\mu$	-	1	off-flavour ℓ : $m_T < 40$ GeV
3ℓ Off- <i>Z</i>	$ee\mu + e\mu\mu$	-	0	2 SFOC leptons off-flavour ℓ : $m_T < 40$ GeV
Control regions				
<i>WZ</i>	3ℓ	-	1	off- <i>Z</i> ℓ : $40 < m_T < 80$ GeV
<i>ZZ</i>	4ℓ	-	2	

regions (VRs) are used to confirm that the predictions for SM background processes are well-modelled.

A large group of BSM models predict the existence of at least one additional heavy lepton beyond the SM (e.g. Ref. [27]), either charged or neutral. Such theories often feature final states with one or more neutrinos, which due to being invisible to the detector translates into a non-zero E_T^{miss} . This motivates a selection of SRs separated by a E_T^{miss} cut. A threshold of $E_T^{\text{miss}} = 50$ GeV was chosen, which splits the phase space into regions where the E_T^{miss} originates mostly from detector resolution effects and regions where the E_T^{miss} is likely to be due to objects invisible to the detector.

SRs are also categorised according to the presence or absence of at least one on-*Z* lepton pair, and are called on-*Z* and off-*Z* SRs respectively. No selection based on charge and flavour is made for these SRs beyond the SFOC pair needed for the on-*Z* region. Certain heavy BSM particles are expected to decay into lepton pairs without first decaying to an intermediate *Z*-boson (e.g. Ref. [28]). Off-*Z* SRs are expected to be sensitive to such signals while excluding the main prompt-lepton background contribution (leptonically decaying *WZ* and *ZZ* vector-boson pairs, which are likely to be on-*Z*). Furthermore, on-*Z* SRs include the few events where three leptons combine into multiple valid on-*Z* pairs.

SRs are further split according to the distribution of the invariant mass (m_{inv}) of all leptons in the event. Four divisions are established to construct the 3ℓ regions: 0–200 GeV, 200–400 GeV, 400–600 GeV, and >600 GeV. Two divisions are established for the 4ℓ regions: 0–400 GeV and >400 GeV. This leads to 22 SRs in total.

Two CRs are defined: a 3ℓ CR for the *WZ* background and a 4ℓ CR for the *ZZ* background. The *WZ* control region requires an on-*Z* lepton pair and a third off-*Z* lepton which has a transverse mass (m_T , defined as $m_T = [2p_T^{\ell} E_T^{\text{miss}} (1 - \cos(\Delta\phi(\ell, E_T^{\text{miss}})))]^{1/2}$), of $40 < m_T < 80$ GeV, which captures leptons originating from a *W*-boson decay. The *ZZ* control region requires four leptons to form two on-*Z* lepton pairs. The SRs are separated from the *WZ* CR through their flavour composition or by requiring $m_T > 80$ GeV,

and from the *ZZ* CR by vetoing events with 4 on-*Z* leptons. Both CRs are used to constrain the two normalisation factors of their corresponding backgrounds. These normalisation factors are free parameters in the statistical analysis.

A data-driven technique is used to estimate backgrounds with at least one fake lepton, referred to as the fake-lepton background, in the SRs, CRs and VRs. Fake leptons are either non-prompt leptons or hadrons misidentified as leptons by the detector. The primary sources of such events are the *Z* + jets and $t\bar{t}$ processes which have two prompt leptons and at least one fake lepton. The yield of fake-lepton background events is measured separately for electrons and muons using the fake-factor method, which is described in Ref. [29]. Dedicated regions containing a single lepton candidate are established using data collected by the single-lepton triggers. Selection requirements for these regions are imposed to ensure a large number of events with fake leptons, in order to reduce the statistical uncertainty of this contribution. Requirements are based on the E_T^{miss} of the event ($E_T^{\text{miss}} < 25$ GeV for electrons, $E_T^{\text{miss}} < 40$ GeV for muons) and on the number of jets in the event (≥ 1 for the electron region, ≥ 2 for the muon region). For the muon, there must also be at least one jet (j) with $p_T > 35$ GeV and $\Delta\phi(\mu, j) > 2.7$, called the tag jet. For each region, an adjacent ‘anti-ID’ region is established, with orthogonal selection criteria of the identification and isolation algorithms. The anti-ID regions admit non-isolated electrons and muons, as well as isolated but Loose [65] electrons, but veto events which satisfy the nominal selection criteria. The anti-ID selection is tuned for a large number of fake leptons, while the stringent working points of the nominal selection suppress these fake leptons, to ensure the analysis is robust against fake-lepton contamination. A ratio is computed from the event rates of these two regions. This ratio is called the fake factor and is parameterised as a function of the p_T and η of the lepton. An anti-ID region is also established for each signal, control and validation region of the analysis. These anti-ID regions use the same selection criteria, except that one or more of their leptons passes the alternative identification and isolation requirements. Using the fake factor, the yield of fake-lepton background

events is extrapolated from each anti-ID region to its nominal counterpart. Prompt backgrounds, estimated through MC methods and normalised to their theoretical cross sections, are subtracted from observed data in the fake-factor estimation regions prior to calculation of the fake factor, and in the anti-ID regions prior to extrapolation.

Certain subselections of $ee\mu + e\mu\mu$ events are designated as on- Z and off- Z VRs. These are used to check that the computed fake factors transfer correctly from the regions where they are calculated to the regions in which they are applied. The on- Z and off- Z VRs consist of different ratios of fake-lepton sources: the on- Z VR is more sensitive to Z +jets events than the off- Z region, while the reverse is true for $t\bar{t}$ events. Furthermore, both VRs have a substantial WZ contribution which can be validated. In the off- Z VR the proper modelling of the WZ MC simulation of off-shell Z decays is confirmed. For this VR, a SFOC pair of off- Z leptons is required. Both validation regions target, through a m_T requirement of $m_T(\ell, E_T^{\text{miss}}) < 40$ GeV, a third lepton that is likely to be fake. Only mixed-flavour final states are selected for these VRs so that the choice of the third lepton, assumed to be the fake lepton (or the lepton due to W -boson decay), is unambiguous.

6. Systematic uncertainties

Systematic uncertainties affect the precision of the predicted background contributions. Two classes of systematic uncertainties are defined: detector-related uncertainties, referred to as 'experimental', and uncertainties in MC modelling of the processes, referred to as 'theoretical'.

6.1. Experimental uncertainties

Multiple experimental uncertainties have been considered for this analysis, although only a small number of them have a significant impact on the results. These uncertainties are discussed below.

The uncertainty in the combined 2015–2018 integrated luminosity [76] is 1.7%, obtained using the LUCID-2 detector [77] for the primary luminosity measurements. Uncertainties in the reweighting procedure applied to the simulation to bring its pile-up multiplicity distribution into agreement with that in the data are also included, ranging between 0.5% and 1%.

For the leptons, uncertainties due to the measured momentum resolution and scale are taken into account [65,78]. Uncertainties in the reconstruction, identification and isolation efficiency scale factors that are used to correct for the difference between the MC simulation and data are also included. The impact of this set of uncertainties on the expected yield for the signal regions varies between 1% and 2%.

Sets of uncertainties in the jet energy scale and resolution are also included. These were derived from information taken from test-beam data, LHC collision data and simulation [71,79]. These uncertainties are small for all signal regions, with an impact between 0.2% and 0.9%.

Uncertainties associated with the above objects are propagated to an uncertainty in the hard term of the E_T^{miss} computation. Further uncertainties affecting the E_T^{miss} that are included are uncertainties in the offset and resolution of the soft term [80]. The impact of these ranges between no impact (for the 4ℓ , off- Z region, which is insensitive to E_T^{miss}) and 4% for the 4ℓ , on- Z , $E_T^{\text{miss}} > 50$ GeV region.

Several systematic uncertainties on the fake factors are considered. First, there is an uncertainty due to limited number of events in the single-lepton region where the fake factors are calculated. Then, there is an uncertainty in the MC modelling of the dominant background contributions in the single-lepton region (the W +jets

and Z +jets contributions). The fake-lepton background estimate is compared with an estimate obtained when using fake factors that consider events with and without b -jets [81], with the difference between the two estimates taken as an uncertainty. Finally, two uncertainties are included to address the bias caused by imposing a E_T^{miss} upper bound in the fake-lepton estimation regions, and by a p_T requirement on the tag jet in the fake-muon estimation regions. These uncertainties are estimated by varying the requirements on these variables upwards and downwards by 10 GeV. The impact of the fake-factor uncertainties on the total background prediction ranges between 0.1% (for the 4ℓ regions, where there are very few fake-lepton events) and 1.6%.

6.2. Theoretical uncertainties

Theoretical uncertainties affect the MC-based background estimate of the multiboson and top-quark backgrounds. The main theoretical uncertainties considered for this analysis originate from the missing higher orders in the perturbative expansion of the partonic cross-section, from PDF uncertainties and the choice of PDF, and from the uncertainty in the strong coupling constant (α_s). The analysis follows the PDF4LHC recommendations [82] for the computation of these uncertainties. These uncertainties are uncorrelated between different background contributions. Other uncertainties such as matching and merging uncertainties, hadronisation and parton-shower uncertainties are not included as this analysis is not directly sensitive to jets.

For the diboson and triboson processes, the contribution of missing higher-order diagrams is estimated by observing the differences in the cross-section prediction when varying the renormalisation scale μ_r and factorisation scale μ_f . These scales are independently varied upwards and downwards by a factor of two [83], leaving out predictions where the terms are scaled in opposite directions. This leads to a total of seven scale variations. The total uncertainty is taken as the envelope of all variations, picking the variation with the largest value in each individual m_{inv} bin and region.

For the $t\bar{t}X$ ($X = W, Z, H$) contributions to the top-quark background, the uncertainty due to missing higher orders is estimated in the same way as for the diboson and triboson uncertainties, using the envelope of the seven variations of μ_r and μ_f , while the PDF uncertainty is taken as the standard deviation of 100 replica variations. The impact of uncertainties in α_s is taken from Ref. [84]. Predictions from alternative generators for $t\bar{t}W$ and $t\bar{t}Z$ processes (SHERPA [39] for $t\bar{t}W$, MADGRAPH5_aMC@NLO [51] interfaced with HERWIG 7 [85] for $t\bar{t}Z$) are used in assessing an uncertainty due to the choice of generator; this uncertainty is found to have no impact on the final result. For the rare top-quark processes tZq , $t\bar{t}WW$ and $t\bar{t}t\bar{t}$, the scale and PDF uncertainties are taken as those associated with the computed NLO cross-section values reported in Ref. [51]. A more precise estimation of these uncertainties is considered unnecessary due to the minute contribution of these rare top-quark processes to the total background yield of this analysis.

The impact of the scale uncertainties on the total background estimate ranges between 5% and 15%; the SRs with high E_T^{miss} and m_{inv} requirements are at the high end of this range as the impact of higher-order diagrams is especially large there. The impact of the PDF uncertainty is around 2%–3%, with higher values (up to 6%) in higher m_{inv} bins. The impact of the α_s uncertainty is 1%–2%.

In general, the dominant sources of systematic uncertainty for this analysis are the theoretical uncertainties. Of these, the μ_r and μ_f scale uncertainty of the diboson backgrounds (WZ for the 3ℓ SRs, ZZ of the 4ℓ SRs) has the largest effect. However, many SRs are still statistically limited. This is the case for the 4ℓ SRs (except for the 4ℓ , on- Z SRs with $m_{\text{inv}} < 400$ GeV); for the two 3ℓ SRs

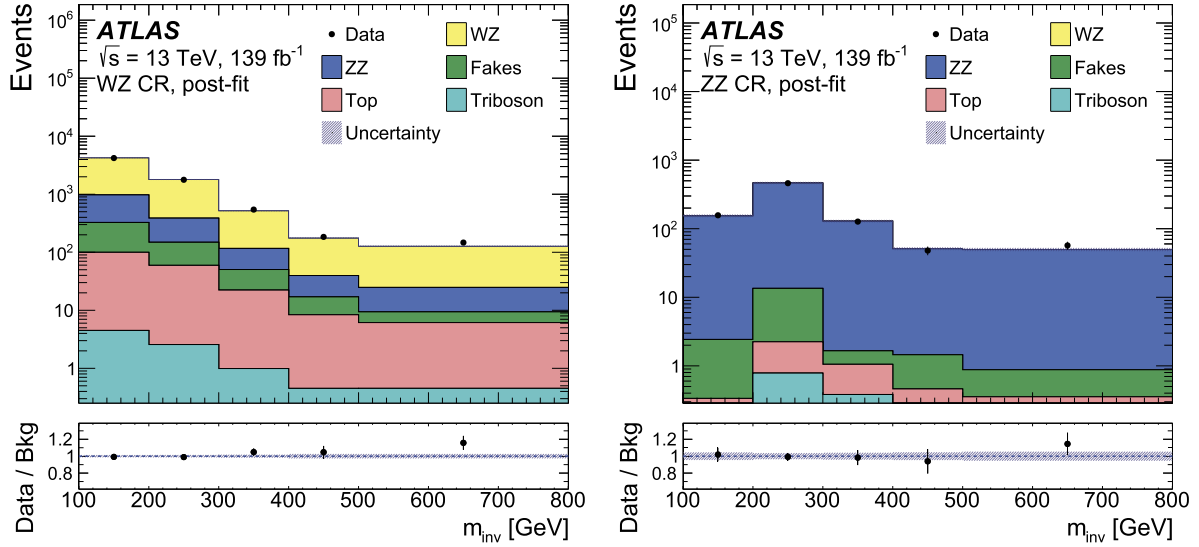


Fig. 1. Comparison between data and prediction for the m_{inv} distribution of the WZ (left) and ZZ (right) control regions after the fit to the data. The rightmost bin is inclusive and contains all events with $m_{\text{inv}} > 500$ GeV. ‘Fakes’ refers to the fake-lepton background. The hatched grey area shows the combination of all uncertainties in the analysis.

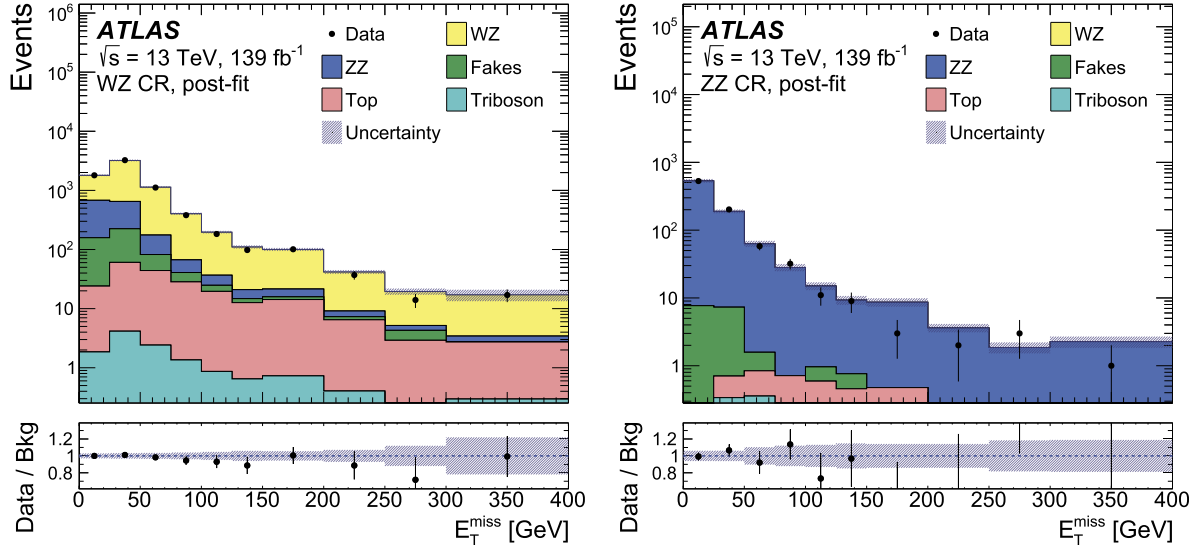


Fig. 2. Comparison between data and prediction for the E_T^{miss} distribution of the WZ (left) and ZZ (right) control regions after the fit to the data. The rightmost bin is inclusive and contains all events with $E_T^{\text{miss}} > 300$ GeV. ‘Fakes’ refers to the fake-lepton background. The hatched grey area shows the combination of all uncertainties in the analysis.

where $E_T^{\text{miss}} < 50$ GeV and $m_{\text{inv}} > 400$ GeV; and for the 3ℓ , off-Z, $E_T^{\text{miss}} > 50$ GeV SR with $m_{\text{inv}} > 600$ GeV.

7. Statistical analysis and results

Each of the 22 SRs is treated in an individual, together with the CRs, cut-and-count experiment, and a statistical analysis is performed independently for each region. For each of these analyses, the parameter of interest is the number of signal events in the corresponding SR: N_S . The same WZ and ZZ control regions are used for all statistical analyses as well.

This analysis employs a maximum-likelihood technique, using the profile likelihood ratio (see, e.g., Ref. [86]) to estimate N_S while also accounting for the various systematic uncertainties affecting the background predictions, which enter the likelihood expression as nuisance parameters (NP) $\vec{\theta}$. The likelihood for each SR is the product of Poisson probability terms $\mathcal{P}(n|\mu)$ for the single SR and

multiple control region bins. The predicted number of events in each region is expressed in terms of the WZ and ZZ background normalisation factors k_{WZ} and k_{ZZ} , the nuisance parameters and, in the case of the SR, N_S . For each systematic uncertainty, indexed by l , the likelihood formula is multiplied by a constraint term, which is a standard Gaussian response function $\mathcal{G}(0|\theta_l, \sigma_l)$ with mean and standard deviation equal to the central value of the nuisance parameter and its uncertainty, respectively. The likelihood therefore takes the form:

$$\begin{aligned}
 L = & \mathcal{P}(N_{\text{SR}}|N_S + k_{WZ}N_{WZ}^{\text{SR}}(\vec{\theta}) + k_{ZZ}N_{ZZ}^{\text{SR}}(\vec{\theta})) + \sum_{j \in \text{bg}} N_j^{\text{SR}}(\vec{\theta}) \\
 & \times \prod_{i \in WZ, ZZ \text{ CR bins}} \mathcal{P}(N_i | k_{WZ}N_{WZ}^i(\vec{\theta}) + k_{ZZ}N_{ZZ}^i(\vec{\theta})) \\
 & + \sum_{j \in \text{bg}} N_j^i(\vec{\theta}) \times \prod_{l \in \text{NP}} \mathcal{G}(0|\theta_l, \sigma_l),
 \end{aligned}$$

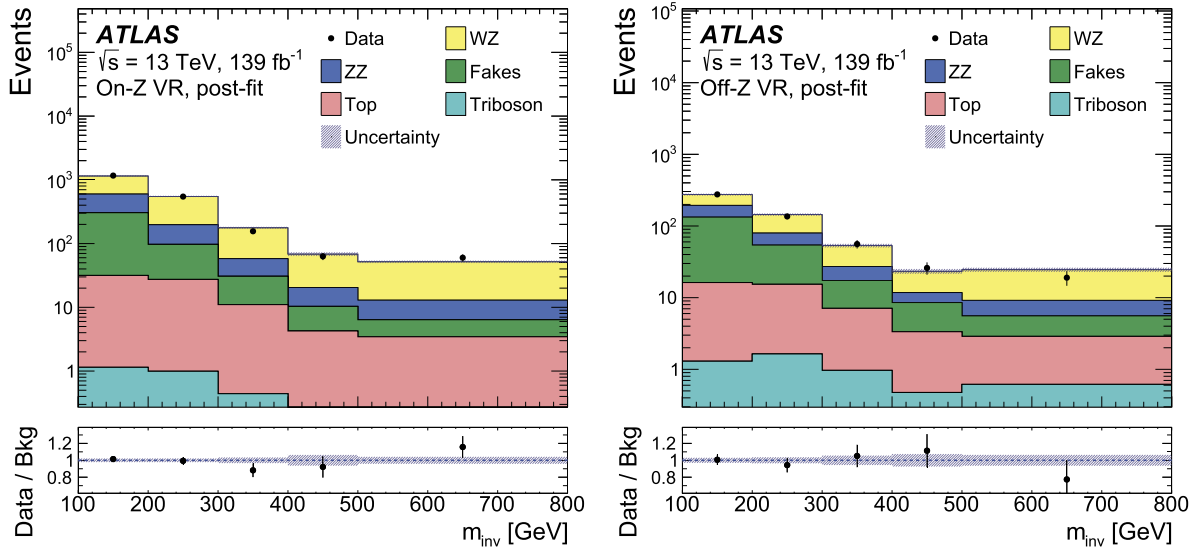


Fig. 3. Comparison between data and prediction for the m_{inv} distribution of the on-Z (left) and off-Z (right) validation regions after the fit to the data. The rightmost bin is inclusive and contains all events with $m_{\text{inv}} > 500$ GeV. ‘Fakes’ refers to the fake-lepton background. The hatched grey area shows the combination of all uncertainties in the analysis.

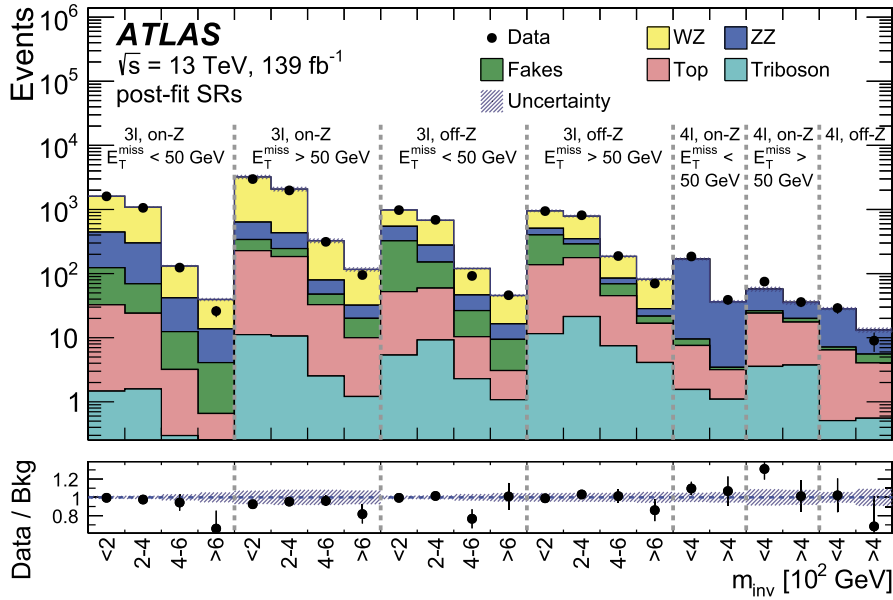


Fig. 4. Comparison between data and prediction in each signal region of this analysis after the profile likelihood fit has been performed. ‘Fakes’ refers to the fake-lepton background. The hatched grey area shows the combination of all uncertainties in the analysis.

where the index j runs over all background contributions other than WZ and ZZ . Many sources of uncertainty affect the predictions in both the SR and the CRs. The correlations between predictions in the different regions are accounted for by a common dependence on the associated nuisance parameter(s). The impact of these may vary between control and signal regions, particularly for the dominant systematic uncertainties (which are the diboson scale uncertainties).

7.1. Likelihood fit to data

Figs. 1–3 show comparisons between data and predictions for CRs and VRs after performing a likelihood fit to the CRs. The values of the normalisation factors are obtained from a binned CR-only fit (i.e. its likelihood formula does not include a term for any signal region) to the distributions in Fig. 1. The normalisation factors

are found to be 0.98 ± 0.07 for the WZ background, consistent with the generator cross-section, and 1.05 ± 0.09 for the ZZ background, which is consistent with previous measurements of the event yield of on-shell ZZ decays [75]. Furthermore, the VRs show good agreement between data and background, indeed validating the off-shell WZ modelling and the understanding of the fake-lepton background.

Fig. 4 shows all SRs with the observed data and post-fit background yields. The event yields obtained by comparing the measured data with the expected background are shown, after performing the fitting procedure, in Table 2 for the 3 ℓ signal regions, and in Table 3 for the 4 ℓ signal regions.

The assumed number of signal events N_S is allowed to float freely. It is determined independently for each SR and is not required to be positive. Given that the SR is not binned, it does not add further degrees of freedom and hence does not constrain the

Table 2

Summary of the event yields for all background contributions to the 3ℓ signal regions after the combined likelihood fit has been performed. The observed data for each signal region are also given. 'Fakes' refers to the fake-lepton background. The 'Total' row gives the sum of event counts of all individual Standard Model contributions. The 'Signal' row gives the remaining discrepancy between the sum of backgrounds and observed data. The total uncertainty in the event yield is given for each background contribution, for the total Standard Model prediction and for the best-fit value of the signal contribution. It should be noted that the uncertainty in the total background prediction cannot be obtained as a sum in quadrature of the uncertainties in its contributions, due to statistical correlations.

3ℓ , On-Z, $E_T^{\text{miss}} < 50$ GeV				
Sample	<200 GeV	200–400 GeV	400–600 GeV	>600 GeV
Top	31.1 ± 3.2	22.5 ± 2.8	2.9 ± 0.5	0.53 ± 0.11
Triboson	1.47 ± 0.16	1.58 ± 0.18	0.30 ± 0.05	0.13 ± 0.02
WZ	1168 ± 25	787 ± 19	89.6 ± 3.3	25.8 ± 1.7
ZZ	320 ± 13	230 ± 9	29.4 ± 1.5	9.6 ± 0.9
Fakes	91 ± 9	45 ± 7	9.2 ± 2.5	3.4 ± 0.9
Total	1612 ± 26	1087 ± 19	131 ± 4	39.5 ± 2.1
Data	1604	1061	124	26
Signal	-8 ± 48	-26 ± 38	-7 ± 12	-13 ± 5

3ℓ , On-Z, $E_T^{\text{miss}} > 50$ GeV				
Sample	<200 GeV	200–400 GeV	400–600 GeV	>600 GeV
Top	217 ± 19	174 ± 18	30.2 ± 3.4	8.8 ± 1.2
Triboson	11.2 ± 1.4	10.6 ± 1.4	2.5 ± 0.4	1.21 ± 0.21
WZ	2589 ± 216	1650 ± 162	246 ± 25	84 ± 8
ZZ	295 ± 41	186 ± 24	32 ± 4	12.1 ± 1.5
Fakes	112 ± 16	61 ± 11	14.8 ± 3.3	10.0 ± 1.8
Total	3224 ± 235	2082 ± 172	325 ± 27	116 ± 9
Data	2982	1985	313	95
Signal	-242 ± 249	-97 ± 183	-12 ± 33	-21 ± 13

3ℓ , Off-Z, $E_T^{\text{miss}} < 50$ GeV				
Sample	<200 GeV	200–400 GeV	400–600 GeV	>600 GeV
Top	47 ± 4	50 ± 5	8.1 ± 0.8	2.00 ± 0.27
Triboson	5.4 ± 0.5	9.2 ± 0.9	2.29 ± 0.26	1.08 ± 0.17
WZ	437 ± 9	401 ± 10	73.7 ± 3.0	29.1 ± 1.2
ZZ	222 ± 11	126 ± 7	19.9 ± 1.5	7.0 ± 0.9
Fakes	272 ± 16	92 ± 10	16.1 ± 3.0	6.3 ± 1.4
Total	983 ± 19	679 ± 14	120 ± 4	45.5 ± 2.1
Data	978	689	92	46
Signal	-5 ± 37	10 ± 30	-28 ± 10	0 ± 7

3ℓ , Off-Z, $E_T^{\text{miss}} > 50$ GeV				
Sample	<200 GeV	200–400 GeV	400–600 GeV	>600 GeV
Top	126 ± 11	156 ± 14	38 ± 4	12.6 ± 1.7
Triboson	11.6 ± 1.3	21.4 ± 2.8	7.5 ± 1.1	4.1 ± 0.6
WZ	445 ± 34	439 ± 30	101 ± 6	53 ± 4
ZZ	107 ± 12	59 ± 6	15.6 ± 1.7	6.7 ± 0.8
Fakes	263 ± 19	112 ± 14	24 ± 4	4.9 ± 1.2
Total	953 ± 44	788 ± 38	186 ± 9	81 ± 5
Data	944	813	188	70
Signal	-9 ± 55	25 ± 48	2 ± 16	-11 ± 10

backgrounds further; the post-fit background values for every SR are therefore always the same as those of the CR-only fit, with N_S adjusted to make up for the difference between the total background and the observed data in the SR.

For each SR a fit finds the number of signal events (\hat{N}_S) and, from the parabolic behaviour of the log-likelihood around its maximum, its associated uncertainty ($\Delta\hat{N}_S$). From these values a significance can be computed, defined as $Z = \hat{N}_S/\Delta\hat{N}_S$ so that negative significance is associated with negative signal yields. The signifi-

cances for all SRs are given in Table 4. In this analysis, all SRs have a significance below $|Z| < 3$.

7.2. Visible cross-section limits

No significant excess was found in any of the signal regions. Limits on the number of signal events are set. The CL_S method [87] is used to ascertain upper limits in the signal regions. Assumptions made about the test statistic are based on the works of Wilks [88]

Table 3

Summary of the event yields for all background contributions to the 4ℓ signal regions after the combined likelihood fit has been performed. The observed data for each signal region are also given. ‘Fakes’ refers to the fake-lepton background. The ‘Total’ row gives the sum of event counts of all individual Standard Model contributions. The ‘Signal’ row gives the remaining discrepancy between the sum of backgrounds and observed data. The total uncertainty in the event yield is given for each background contribution, for the total Standard Model prediction and for the best-fit value of the signal contribution. It should be noted that the uncertainty in the total background prediction cannot be obtained as a sum in quadrature of the uncertainties in its contributions, due to statistical correlations.

$4\ell, \text{On-Z}, E_T^{\text{miss}} < 50 \text{ GeV}$			$4\ell, \text{On-Z}, E_T^{\text{miss}} > 50 \text{ GeV}$		
Sample	0–400 GeV	>400 GeV	Sample	0–400 GeV	>400 GeV
Top	6.0 ± 0.8	2.1 ± 0.4	Top	20.6 ± 2.2	13.8 ± 1.7
Triboson	1.56 ± 0.15	1.10 ± 0.12	Triboson	3.6 ± 0.5	3.7 ± 0.6
ZZ	159 ± 8	33.1 ± 1.9	ZZ	31 ± 4	15.6 ± 1.8
Fakes	1.9 ± 2.1	0.3 ± 0.7	Fakes	2.2 ± 1.5	2.5 ± 1.3
Total	169 ± 8	36.5 ± 2.1	Total	57 ± 5	35.5 ± 2.9
Data	185	39	Data	75	36
Signal	16 ± 16	2 ± 7	Signal	18 ± 10	0 ± 7

$4\ell, \text{Off-Z}$		
Sample	0–400 GeV	>400 GeV
Top	5.9 ± 0.7	3.5 ± 0.5
Triboson	0.51 ± 0.06	0.55 ± 0.08
ZZ	21.3 ± 0.9	7.6 ± 0.4
Fakes	0.7 ± 1.1	1.5 ± 1.0
Total	28.4 ± 1.6	13.2 ± 1.2
Data	29	9
Signal	1 ± 6	-4.2 ± 3.1

Table 4

Local significance of the value of the parameter of interest for each signal region after performing the combined likelihood fit, defined as $Z = \hat{N}_S / \Delta \hat{N}_S$.

SR	0–200 GeV	200–400 GeV	400–600 GeV	>600 GeV
$3\ell, \text{On-Z}, E_T^{\text{miss}} < 50 \text{ GeV}$	–0.2	–0.7	–0.6	–2.5
$3\ell, \text{On-Z}, E_T^{\text{miss}} > 50 \text{ GeV}$	–1.0	–0.5	–0.4	–1.6
$3\ell, \text{Off-Z}, E_T^{\text{miss}} < 50 \text{ GeV}$	–0.1	0.3	–2.7	0.1
$3\ell, \text{Off-Z}, E_T^{\text{miss}} > 50 \text{ GeV}$	–0.2	0.5	0.2	–1.2

SR	0–400 GeV	>400 GeV
$4\ell, \text{On-Z}, E_T^{\text{miss}} < 50 \text{ GeV}$	1.0	0.4
$4\ell, \text{On-Z}, E_T^{\text{miss}} > 50 \text{ GeV}$	1.8	0.1
$4\ell, \text{Off-Z}$	0.1	–1.3

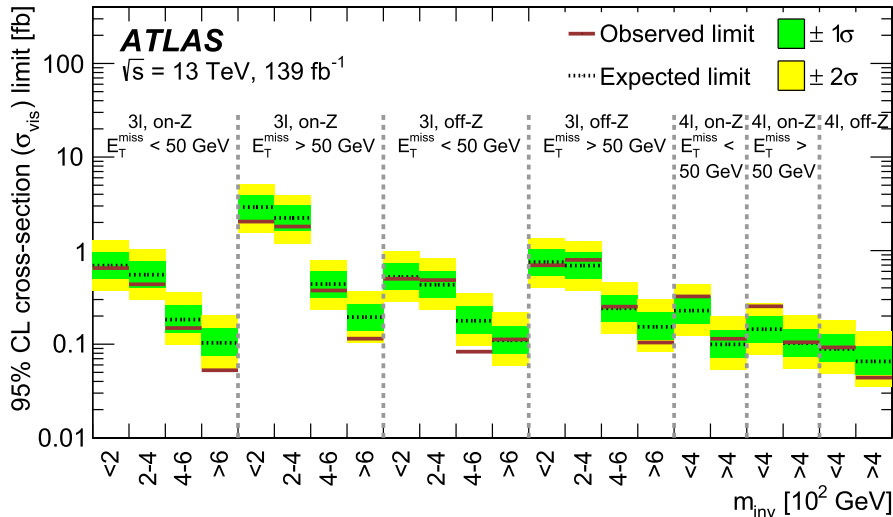


Fig. 5. The expected and observed 95% CL upper limits for each signal region of this analysis expressed in terms of the visible cross-section σ_{vis} .

Table 5

Expected and observed cross-section exclusion limits at 95% CL for representative mass values of the two selected models. Also the most sensitive bin, which was used to obtain these limits for each case, is listed, along with the signal acceptance times efficiency in this region (denoted by $A \times \epsilon$).

Model	Mass [GeV]	Best single SR	m_{inv}	$A \times \epsilon$	σ_{exp}^{95} [fb]	σ_{obs}^{95} [fb]
Type-III Seesaw	400	3ℓ , Off-Z, $E_{\text{T}}^{\text{miss}} > 50$ GeV	> 600 GeV	0.0036	41	${}_{-11}^{+17}$
	700	3ℓ , Off-Z, $E_{\text{T}}^{\text{miss}} > 50$ GeV	> 600 GeV	0.012	12	${}_{-3}^{+5}$
$H^{\pm\pm}$	300	4ℓ , Off-Z	> 400 GeV	0.37	0.18	${}_{-0.05}^{+0.08}$
	500	4ℓ , Off-Z	> 400 GeV	0.40	0.16	${}_{-0.05}^{+0.07}$

and Wald [89]. Specifically, it is assumed that the test statistic asymptotically approaches a χ^2 distribution with one degree of freedom for a large number of events [90].

Expected and observed 95% CL upper limits are presented for the visible cross-section σ_{vis} , which is calculated by dividing the upper limit on the total number of events (N_{95}) by the integrated luminosity \mathcal{L} of the collected data: $\sigma_{\text{vis}} = N_{95}/\mathcal{L}$. These limits are given for all SRs in Fig. 5. Visible cross-section limits in this figure can be reinterpreted as limits on specific physics models as long as the selection efficiency and acceptance of the model (including any uncertainties in these values) for a specific SR definition used in this analysis is known. By dividing the visible cross-section limits given here by this efficiency and acceptance, upper limits on the cross-section can be derived from this analysis.

7.3. Model-specific limits

The results are interpreted for two particular BSM models previously studied by dedicated analyses. The purpose of this interpretation is to compare the results obtained by this model-independent search with those from a dedicated search. Studied models are the Type-III seesaw model described in Ref. [17] and the search for doubly charged Higgs boson production described in Ref. [21]. The chosen parameters of the models studied in this section are at parity with the referenced analyses, but only two representative particle mass hypotheses are chosen for each models: 400 GeV and 700 GeV for the heavy lepton in the Type-III seesaw model, and 300 GeV and 500 GeV for the $H^{\pm\pm}$ particles. These masses are chosen to cover a range of masses corresponding to the simulated models available and the published limits available for comparison.

The signal regions and background predictions remain the same as described earlier in this Letter. Using these models, all of the signal regions in these analyses are studied to find the region with the best limit-setting power, judged by the value of the expected limit. The best signal region and the corresponding expected and observed limits found by this analysis are given in Table 5. To convert the limits from the model-independent analysis to limits on the cross-section of the signal model considered, only a correction for acceptance effects and selection efficiency is applied. This procedure ignores uncertainties in these quantities; however, the experimental uncertainties on the expected signal yields in the most sensitive regions are not larger than a few percent.

The Type-III seesaw model analysis [17] presents an expected 95% CL cross-section upper limit of $22_{-6.4}^{+8.5}$ fb for $m_L = 400$ GeV and $7.5_{-1.8}^{+3.1}$ fb for $m_L = 700$ GeV for the full Run 2 dataset with an integrated luminosity of 139 fb^{-1} , although it only tests dilepton final states. These limits are more stringent than those derived with the analysis presented in this paper that correspond to 41 and 12 fb, respectively. The doubly-charged Higgs boson analysis [21] presents an expected 95% CL cross-section upper limit for the four-lepton final state of $0.16_{-0.07}^{+0.14}$ fb for $m_{H^{\pm\pm}} = 300$ GeV and $0.14_{-0.07}^{+0.13}$ fb for $m_{H^{\pm\pm}} = 500$ GeV. These limits are comparable to those when using the best limit of a single SR of this analysis.

However, the upper limits in Ref. [21] are obtained using only 2015 and 2016 ATLAS data, corresponding to an integrated luminosity of 36.1 fb^{-1} .

8. Conclusion

In this paper, a model-independent search targeting final states with three or four light leptons is presented using 139 fb^{-1} of $\sqrt{s} = 13$ TeV pp collision data collected by the ATLAS detector at the LHC from 2015 to 2018. The analysis offers a wide coverage of the 3ℓ and 4ℓ phase space. The measured data of 3ℓ and 4ℓ events is tested for potential indicators of physics beyond the Standard Model. By categorising the targeted phase space according to the number of leptons, the missing transverse momentum, the presence of a lepton pair originating from a Z-boson decay, and the invariant mass of the leptons in the event, a total of 22 signal regions are defined. Each signal region is analysed independently using a profile likelihood fit. Control regions were established to extract the normalisations of the primary background processes.

No significant deviations from the Standard Model expectation are found in the data. In the absence of a detected signal, upper limits at the 95% CL are provided in terms of the visible cross-sections. The expected upper limits can be interpreted by dedicated analyses as long as the efficiency and acceptance of their signal model in a particular signal region is known. The analysis is interpreted using simulated signal models for heavy leptons from the Type-III seesaw mechanism [17] and a doubly charged Higgs boson model [21].

Declaration of competing interest

The authors declare that they have no known competing financial interests or personal relationships that could have appeared to influence the work reported in this paper.

Acknowledgements

We thank CERN for the very successful operation of the LHC, as well as the support staff from our institutions without whom ATLAS could not be operated efficiently.

We acknowledge the support of ANPCyT, Argentina; YerPhI, Armenia; ARC, Australia; BMWFW and FWF, Austria; ANAS, Azerbaijan; SSTC, Belarus; CNPq and FAPESP, Brazil; NSERC, NRC and CFI, Canada; CERN; ANID, Chile; CAS, MOST and NSFC, China; Min-ciencias, Colombia; MSMT CR, MPO CR and VSC CR, Czech Republic; DNR and DNSRC, Denmark; IN2P3-CNRS and CEA-DRF/IRFU, France; SRNSFG, Georgia; BMBF, HGF and MPG, Germany; GSRI, Greece; RGC and Hong Kong SAR, China; ISF and Benozijyo Center, Israel; INFN, Italy; MEXT and JSPS, Japan; CNRST, Morocco; NWO, Netherlands; RCN, Norway; MEIn, Poland; FCT, Portugal; MNE/IFA, Romania; JINR; MES of Russia and NRC KI, Russian Federation; MESTD, Serbia; MSSR, Slovakia; ARRS and MIZŠ, Slovenia; DSI/NRF, South Africa; MICINN, Spain; SRC and Wallenberg Foundation, Sweden; SERI, SNSF and Cantons of Bern and Geneva, Switzerland; MOST, Taiwan; TAEK, Turkey; STFC, United Kingdom; DOE

and NSF, United States of America. In addition, individual groups and members have received support from BCKDF, CANARIE, Compute Canada and CRC, Canada; COST, ERC, ERDF, Horizon 2020 and Marie Skłodowska-Curie Actions, European Union; Investissements d'Avenir Labex, Investissements d'Avenir Idex and ANR, France; DFG and AvH Foundation, Germany; Herakleitos, Thales and Aristeia programmes co-financed by EU-ESF and the Greek NSRF, Greece; BSF-NSF and GIF, Israel; Norwegian Financial Mechanism 2014-2021, Norway; NCN and NAWA, Poland; La Caixa Banking Foundation, CERCA Programme Generalitat de Catalunya and PROMETEO and GenT Programmes Generalitat Valenciana, Spain; Göran Gustafssons Stiftelse, Sweden; The Royal Society and Leverhulme Trust, United Kingdom.

The crucial computing support from all WLCG partners is acknowledged gratefully, in particular from CERN, the ATLAS Tier-1 facilities at TRIUMF (Canada), NDGF (Denmark, Norway, Sweden), CC-IN2P3 (France), KIT/GridKA (Germany), INFN-CNAF (Italy), NL-T1 (Netherlands), PIC (Spain), ASGC (Taiwan), RAL (UK) and BNL (USA), the Tier-2 facilities worldwide and large non-WLCG resource providers. Major contributors of computing resources are listed in Ref. [91].

References

- [1] S. Glashow, Partial-symmetries of weak interactions, *Nucl. Phys.* 22 (1961) 579.
- [2] S. Weinberg, A model of leptons, *Phys. Rev. Lett.* 19 (1967) 1264.
- [3] G. 't Hooft, Renormalizable Lagrangians for massive Yang-Mills fields, *Nucl. Phys. B* 35 (1971) 167.
- [4] G. 't Hooft, M. Veltman, Regularization and renormalization of gauge fields, *Nucl. Phys. B* 44 (1972) 189.
- [5] V. Trimble, Existence and nature of dark matter in the universe, *Annu. Rev. Astron. Astrophys.* 25 (1987) 425.
- [6] A.G. Riess, et al., Observational evidence from supernovae for an accelerating universe and a cosmological constant, *Astron. J.* 116 (1998) 1009.
- [7] Super-Kamiokande Collaboration, Evidence for oscillation of atmospheric neutrinos, *Phys. Rev. Lett.* 81 (1998) 1562, arXiv:hep-ex/9807003.
- [8] SNO Collaboration, Direct evidence for neutrino flavor transformation from neutral-current interactions in the Sudbury neutrino observatory, *Phys. Rev. Lett.* 89 (2002) 011301, arXiv:nucl-ex/0204008.
- [9] A.D. Sakharov, Violation of CP invariance, C asymmetry, and baryon asymmetry of the universe, *Sov. Phys. Usp.* 34 (1991) 392.
- [10] ATLAS Collaboration, Search for chargino-neutralino production with mass splittings near the electroweak scale in three-lepton final states in $\sqrt{s} = 13$ TeV pp collisions with the ATLAS detector, *Phys. Rev. D* 101 (2020) 072001, arXiv:1912.08479 [hep-ex].
- [11] P. Huang, Y.H. Ng, Di-Higgs production in SUSY models at the LHC, arXiv:1910.13968 [hep-ph], 2019.
- [12] Y. Afik, S. Bar-Shalom, A. Soni, J. Wudka, New flavor physics in di- and trilepton events from single-top at the LHC and beyond, *Phys. Rev. D* 103 (2021) 075031, arXiv:2101.05286 [hep-ph].
- [13] F. del Aguila, J. Aguilar-Saavedra, Distinguishing seesaw models at LHC with multi-lepton signals, *Nucl. Phys. B* 813 (2009) 22, arXiv:0808.2468 [hep-ph].
- [14] E. Ma, Pathways to naturally small neutrino masses, *Phys. Rev. Lett.* 81 (1998) 1171, arXiv:hep-ph/9805219.
- [15] P.-H. Gu, H. Zhang, S. Zhou, Minimal type II seesaw model, *Phys. Rev. D* 74 (2006) 076002, arXiv:hep-ph/0606302.
- [16] R. Franceschini, T. Hambye, A. Strumia, Type-III seesaw mechanism at CERN LHC, *Phys. Rev. D* 78 (2008) 033002, arXiv:0805.1613 [hep-ph].
- [17] ATLAS Collaboration, Search for type-III seesaw heavy leptons in dilepton final states in pp collisions at $\sqrt{s} = 13$ TeV with the ATLAS detector, *Eur. Phys. J. C* 81 (2020) 218, arXiv:2008.07949 [hep-ex].
- [18] H. Georgi, M. Machacek, Doubly charged Higgs bosons, *Nucl. Phys. B* 262 (1985) 463.
- [19] N.G. Deshpande, J.F. Gunion, B. Kayser, F. Olness, Left-right-symmetric electroweak models with triplet Higgs field, *Phys. Rev. D* 44 (1991) 837.
- [20] P. Bhupal Dev, M.J. Ramsey-Musolf, Y. Zhang, Doubly-charged scalars in the type II seesaw mechanism: fundamental symmetry tests and high-energy searches, *Phys. Rev. D* 98 (2018) 055013, arXiv:1806.08499 [hep-ph].
- [21] ATLAS Collaboration, Search for doubly charged Higgs boson production in multi-lepton final states with the ATLAS detector using proton-proton collisions at $\sqrt{s} = 13$ TeV, *Eur. Phys. J. C* 78 (2018) 199, arXiv:1710.09748 [hep-ex].
- [22] J.F. Gunion, J. Grifols, A. Mendez, B. Kayser, F. Olness, Higgs bosons in left-right-symmetric models, *Phys. Rev. D* 40 (1989) 1546.
- [23] N. Setzer, S. Spinner, Running with triplets: how slepton masses change with doubly-charged Higgs bosons, *Phys. Rev. D* 75 (2007) 117701, arXiv:hep-ph/0612318.
- [24] S. Bhattacharya, S. Jana, S. Nandi, Neutrino masses and scalar singlet dark matter, *Phys. Rev. D* 95 (2017) 055003, arXiv:1609.03274 [hep-ph].
- [25] M. Nebot, J.F. Oliver, D. Palao, A. Santamaria, Prospects for the Zee-Babu model at the CERN LHC and low energy experiments, *Phys. Rev. D* 77 (2008) 093013, arXiv:0711.0483 [hep-ph].
- [26] ATLAS Collaboration, Search for supersymmetry in events with four or more charged leptons in 139 fb^{-1} of $\sqrt{s} = 13$ TeV pp collisions with the ATLAS detector, *J. High Energy Phys.* 07 (2021) 167, arXiv:2103.11684 [hep-ex].
- [27] C. Biggio, F. Bonnet, Implementation of the type III seesaw model in FeynRules/MadGraph and prospects for discovery with early LHC data, *Eur. Phys. J. C* 72 (2011) 1899, arXiv:1107.3463 [hep-ph].
- [28] K. Huitu, J. Maalampi, A. Pietila, M. Raidal, Doubly charged Higgs at LHC, *Nucl. Phys. B* 487 (1997) 27, arXiv:hep-ph/9606311.
- [29] ATLAS Collaboration, Search for new phenomena in events with three or more charged leptons in pp collisions at $\sqrt{s} = 8$ TeV with the ATLAS detector, *J. High Energy Phys.* 08 (2015) 138, arXiv:1411.2921 [hep-ex].
- [30] ATLAS Collaboration, A strategy for a general search for new phenomena using data-derived signal regions and its application within the ATLAS experiment, *Eur. Phys. J. C* 79 (2019) 120, arXiv:1807.07447 [hep-ex].
- [31] CMS Collaboration, Search for physics beyond the standard model in multilepton final states in proton-proton collisions at $\sqrt{s} = 13$ TeV, *J. High Energy Phys.* 03 (2020) 051, arXiv:1911.04968 [hep-ex].
- [32] ATLAS Collaboration, The ATLAS experiment at the CERN large hadron collider, *J. Instrum.* 3 (2008) S08003.
- [33] ATLAS Collaboration, ATLAS insertable B-layer technical design report, ATLAS-TDR-19; CERN-LHCC-2010-013, <https://cds.cern.ch/record/1291633>, 2010, Addendum: ATLAS-TDR-19-ADD-1; CERN-LHCC-2012-009 <https://cds.cern.ch/record/1451888>, 2012.
- [34] B. Abbott, et al., Production and integration of the ATLAS insertable B-layer, *J. Instrum.* 13 (2018) T05008, arXiv:1803.00844 [physics.ins-det].
- [35] ATLAS Collaboration, Operation of the ATLAS trigger system in Run 2, *J. Instrum.* 15 (2020) P10004, arXiv:2007.12539 [hep-ex].
- [36] ATLAS Collaboration, ATLAS data quality operations and performance for 2015-2018 data-taking, *J. Instrum.* 15 (2020) P04003, arXiv:1911.04632 [physics.ins-det].
- [37] ATLAS Collaboration, Performance of electron and photon triggers in ATLAS during LHC Run 2, *Eur. Phys. J. C* 80 (2020) 47, arXiv:1909.00761 [hep-ex].
- [38] ATLAS Collaboration, Performance of the ATLAS muon triggers in Run 2, *J. Instrum.* 15 (2020) P09015, arXiv:2004.13447 [hep-ex].
- [39] E. Bothmann, et al., Event generation with Sherpa 2.2, *SciPost Phys.* 7 (2019) 034, arXiv:1905.09127 [hep-ph].
- [40] R.D. Ball, et al., Parton distributions for the LHC run II, *J. High Energy Phys.* 04 (2015) 040, arXiv:1410.8849 [hep-ph].
- [41] S. Schumann, F. Krauss, A parton shower algorithm based on Catani-Seymour dipole factorisation, *J. High Energy Phys.* 03 (2008) 038, arXiv:0709.1027 [hep-ph].
- [42] J.-C. Winter, F. Krauss, G. Soff, A modified cluster-hadronization model, *Eur. Phys. J. C* 36 (2004) 381, arXiv:hep-ph/0311085.
- [43] T. Gleisberg, S. Höche, Comix, a new matrix element generator, *J. High Energy Phys.* 12 (2008) 039, arXiv:0808.3674 [hep-ph].
- [44] S. Höche, F. Krauss, M. Schönherr, F. Siegert, A critical appraisal of NLO + PS matching methods, *J. High Energy Phys.* 09 (2012) 049, arXiv:1111.1220 [hep-ph].
- [45] S. Höche, F. Krauss, M. Schönherr, F. Siegert, QCD matrix elements + parton showers. The NLO case, *J. High Energy Phys.* 04 (2013) 027, arXiv:1207.5030 [hep-ph].
- [46] S. Catani, F. Krauss, B.R. Webber, R. Kuhn, QCD matrix elements + parton showers, *J. High Energy Phys.* 11 (2001) 063, arXiv:hep-ph/0109231.
- [47] S. Höche, F. Krauss, S. Schumann, F. Siegert, QCD matrix elements and truncated showers, *J. High Energy Phys.* 05 (2009) 053, arXiv:0903.1219 [hep-ph].
- [48] F. Buccioni, et al., OpenLoops 2, *Eur. Phys. J. C* 79 (2019) 866, arXiv:1907.13071 [hep-ph].
- [49] F. Cascioli, P. Maierhöfer, S. Pozzorini, Scattering amplitudes with open loops, *Phys. Rev. Lett.* 108 (2012) 111601, arXiv:1111.5206 [hep-ph].
- [50] A. Denner, S. Dittmaier, L. Hofer, Collier: a fortran-based complex one-loop library in extended regularizations, *Comput. Phys. Commun.* 212 (2017) 220, arXiv:1604.06792 [hep-ph].
- [51] J. Alwall, et al., The automated computation of tree-level and next-to-leading order differential cross sections, and their matching to parton shower simulations, *J. High Energy Phys.* 07 (2014) 079, arXiv:1405.0301 [hep-ph].
- [52] ATLAS Collaboration, Observation of Higgs boson production in association with a top quark pair at the LHC with the ATLAS detector, *Phys. Lett. B* 784 (2018) 173, arXiv:1806.00425 [hep-ex].
- [53] S. Frixione, P. Nason, G. Ridolfi, A positive-weight next-to-leading-order Monte Carlo for heavy flavour hadroproduction, *J. High Energy Phys.* 09 (2007) 126, arXiv:0707.3088 [hep-ph].
- [54] P. Nason, A new method for combining NLO QCD with shower Monte Carlo algorithms, *J. High Energy Phys.* 11 (2004) 040, arXiv:hep-ph/0409146.
- [55] S. Frixione, P. Nason, C. Oleari, Matching NLO QCD computations with parton shower simulations: the POWHEG method, *J. High Energy Phys.* 11 (2007) 070, arXiv:0709.2092 [hep-ph].

- [56] S. Alioli, P. Nason, C. Oleari, E. Re, A general framework for implementing NLO calculations in shower Monte Carlo programs: the POWHEG BOX, *J. High Energy Phys.* 06 (2010) 043, arXiv:1002.2581 [hep-ph].
- [57] ATLAS Collaboration, Studies on top-quark Monte Carlo modelling for Top2016, ATLAS-PHYS-PUB-2016-020, <https://cds.cern.ch/record/2216168>, 2016.
- [58] T. Sjöstrand, et al., An introduction to PYTHIA 8.2, *Comput. Phys. Commun.* 191 (2015) 159, arXiv:1410.3012 [hep-ph].
- [59] ATLAS Collaboration, ATLAS Pythia 8 tunes to 7 TeV data, ATLAS-PHYS-PUB-2014-021, <https://cds.cern.ch/record/1966419>, 2014.
- [60] A. Alloul, N.D. Christensen, C. Degrande, C. Duhr, B. Fuks, FeynRules 2.0 - a complete toolbox for tree-level phenomenology, *Comput. Phys. Commun.* 185 (2013) 2250, arXiv:1310.1921 [hep-ph].
- [61] ATLAS Collaboration, The ATLAS simulation infrastructure, *Eur. Phys. J. C* 70 (2010) 823, arXiv:1005.4568 [physics.ins-det].
- [62] GEANT4 Collaboration, S. Agostinelli, et al., Geant4 - a simulation toolkit, *Nucl. Instrum. Methods Phys. Res., Sect. A* 506 (2003) 250.
- [63] ATLAS Collaboration, The Pythia 8 A3 tune description of ATLAS minimum bias and inelastic measurements incorporating the Donnachie-Landshoff diffractive model, ATLAS-PHYS-PUB-2016-017, <https://cds.cern.ch/record/2206965>, 2016.
- [64] A.D. Martin, W.J. Stirling, R.S. Thorne, G. Watt, Parton distributions for the LHC, *Eur. Phys. J. C* 63 (2009) 189, arXiv:0901.0002 [hep-ph].
- [65] ATLAS Collaboration, Electron and photon performance measurements with the ATLAS detector using the 2015-2017 LHC proton-proton collision data, *J. Instrum.* 14 (2019) P12006, arXiv:1908.00005 [hep-ex].
- [66] ATLAS Collaboration, Muon reconstruction and identification efficiency in ATLAS using the full Run 2 pp collision data set at $\sqrt{s} = 13$ TeV, *Eur. Phys. J. C* 81 (2020) 578, arXiv:2012.00578 [hep-ex].
- [67] T. Cornelissen, et al., Concepts, Design and Implementation of the ATLAS New Tracking (NEWT), Tech. Rep., ATLAS-SOFT-PUB-2007-007, CERN, 2007, <https://cds.cern.ch/record/1020106>.
- [68] ATLAS Collaboration, Jet reconstruction and performance using particle flow with the ATLAS detector, *Eur. Phys. J. C* 77 (2017) 466, arXiv:1703.10485 [hep-ex].
- [69] M. Cacciari, G.P. Salam, G. Soyez, The anti- k_r jet clustering algorithm, *J. High Energy Phys.* 04 (2008) 063, arXiv:0802.1189 [hep-ph].
- [70] M. Cacciari, G.P. Salam, G. Soyez, FastJet user manual, *Eur. Phys. J. C* 72 (2012) 1896, arXiv:1111.6097 [hep-ph].
- [71] ATLAS Collaboration, Jet energy scale and resolution measured in proton-proton collisions at $\sqrt{s} = 13$ TeV with the ATLAS detector, *Eur. Phys. J. C* 81 (2020) 689, arXiv:2007.02645 [hep-ex].
- [72] ATLAS Collaboration, Performance of pile-up mitigation techniques for jets in pp collisions at $\sqrt{s} = 8$ TeV using the ATLAS detector, *Eur. Phys. J. C* 76 (2016) 581, arXiv:1510.03823 [hep-ex].
- [73] ATLAS Collaboration, Performance of missing transverse momentum reconstruction with the ATLAS detector using proton-proton collisions at $\sqrt{s} = 13$ TeV, *Eur. Phys. J. C* 78 (2018) 903, arXiv:1802.08168 [hep-ex].
- [74] ATLAS Collaboration, Measurement of $W^{\pm}Z$ production cross sections and gauge boson polarisation in pp collisions at $\sqrt{s} = 13$ TeV with the ATLAS detector, *Eur. Phys. J. C* 79 (2019) 535, arXiv:1902.05759 [hep-ex].
- [75] ATLAS Collaboration, Measurements of differential cross-sections in four-lepton events in 13 TeV proton-proton collisions with the ATLAS detector, *J. High Energy Phys.* 07 (2021) 005, arXiv:2103.01918 [hep-ex].
- [76] ATLAS Collaboration, Luminosity determination in pp collisions at $\sqrt{s} = 13$ TeV using the ATLAS detector at the LHC, ATLAS-CONF-2019-021, <https://cds.cern.ch/record/2677054>, 2019.
- [77] G. Avoni, et al., The new LUCID-2 detector for luminosity measurement and monitoring in ATLAS, *J. Instrum.* 13 (2018) P07017.
- [78] ATLAS Collaboration, Muon reconstruction performance of the ATLAS detector in proton-proton collision data at $\sqrt{s} = 13$ TeV, *Eur. Phys. J. C* 76 (2016) 292, arXiv:1603.05598 [hep-ex].
- [79] ATLAS Collaboration, Jet energy scale measurements and their systematic uncertainties in proton-proton collisions at $\sqrt{s} = 13$ TeV with the ATLAS detector, *Phys. Rev. D* 96 (2017) 072002, arXiv:1703.09665 [hep-ex].
- [80] ATLAS Collaboration, E_T^{miss} performance in the ATLAS detector using 2015-2016 LHC pp collisions, ATLAS-CONF-2018-023, <https://cds.cern.ch/record/2625233>, 2018.
- [81] ATLAS Collaboration, ATLAS b -jet identification performance and efficiency measurement with $t\bar{t}$ events in pp collisions at $\sqrt{s} = 13$ TeV, *Eur. Phys. J. C* 79 (2019) 970, arXiv:1907.05120 [hep-ex].
- [82] J. Butterworth, et al., PDF4LHC recommendations for LHC Run II, *J. Phys. G* 43 (2016) 023001, arXiv:1510.03865 [hep-ph].
- [83] E. Bothmann, M. Schönherr, S. Schumann, Reweighting QCD matrix-element and parton-shower calculations, *Eur. Phys. J. C* 76 (2016) 590, arXiv:1606.08753 [hep-ph].
- [84] D. de Florian, et al., Handbook of LHC Higgs cross sections: 4. Deciphering the nature of the Higgs sector, arXiv:1610.07922 [hep-ph], 2016.
- [85] M. Bähr, et al., Herwig++ physics and manual, *Eur. Phys. J. C* 58 (2008) 639, arXiv:0803.0883 [hep-ph].
- [86] A. Stuart, K. Ord, S. Arnold (Eds.), Kendall's Advanced Theory of Statistics: Classical Inference & the Linear Model, vol. 2A, 6th ed., Oxford University Press, 1999.
- [87] A.L. Read, Presentation of search results: the CL_s technique, *J. Phys. G* 28 (2002) 2693.
- [88] S. Wilks, The large-sample distribution of the likelihood ratio for testing composite hypotheses, *Ann. Math. Stat.* 9 (1938) 60.
- [89] A. Wald, Tests of statistical hypotheses concerning several parameters when the number of observations is large, *Trans. Am. Math. Soc.* 54 (1943) 426, <http://www.jstor.org/stable/1990256>.
- [90] G. Cowan, K. Cranmer, E. Gross, O. Vitells, Asymptotic formulae for likelihood-based tests of new physics, *Eur. Phys. J. C* 71 (2011) 1554, arXiv:1007.1727 [physics.data-an]; Erratum: *Eur. Phys. J. C* 73 (2013) 2501.
- [91] ATLAS Collaboration, ATLAS computing acknowledgements, ATLAS-SOFT-PUB-2021-003, <https://cds.cern.ch/record/2776662>.

The ATLAS Collaboration

G. Aad⁹⁹, B. Abbott¹²⁵, D.C. Abbott¹⁰⁰, A. Abed Abud³⁴, K. Abeling⁵¹, D.K. Abhayasinghe⁹¹, S.H. Abidi²⁷, O.S. AbouZeid³⁸, H. Abramowicz¹⁵⁸, H. Abreu¹⁵⁷, Y. Abulaiti⁵, A.C. Abusleme Hoffman^{143a}, B.S. Acharya^{64a,64b,p}, B. Achkar⁵¹, L. Adam⁹⁷, C. Adam Bourdarios⁴, L. Adamczyk^{81a}, L. Adamek¹⁶³, J. Adelman¹¹⁸, A. Adiguzel^{11c,ae}, S. Adorni⁵², T. Adye¹⁴⁰, A.A. Affolder¹⁴², Y. Afik¹⁵⁷, C. Agapopoulou⁶², M.N. Agarar¹², J. Agarwala^{68a,68b}, A. Aggarwal¹¹⁶, C. Agheorghiesei^{25c}, J.A. Aguilar-Saavedra^{136f,136a,ad}, A. Ahmad³⁴, F. Ahmadov⁷⁷, W.S. Ahmed¹⁰¹, X. Ai⁴⁴, G. Aielli^{71a,71b}, S. Akatsuka⁸³, M. Akbiyik⁹⁷, T.P.A. Åkesson⁹⁴, A.V. Akimov¹⁰⁸, K. Al Khoury³⁷, G.L. Alberghi^{21b}, J. Albert¹⁷², M.J. Alconada Verzini⁸⁶, S. Alderweireldt⁴⁸, M. Aleksa³⁴, I.N. Aleksandrov⁷⁷, C. Alexa^{25b}, T. Alexopoulos⁹, A. Alfonsi¹¹⁷, F. Alfonsi^{21b,21a}, M. Alhroob¹²⁵, B. Ali¹³⁸, S. Ali¹⁵⁵, M. Aliev¹⁶², G. Alimonti^{66a}, C. Allaire³⁴, B.M.M. Allbrooke¹⁵³, P.P. Allport¹⁹, A. Aloisio^{67a,67b}, F. Alonso⁸⁶, C. Alpigiani¹⁴⁵, E. Alunno Camelia^{71a,71b}, M. Alvarez Estevez⁹⁶, M.G. Alviggi^{67a,67b}, Y. Amaral Coutinho^{78b}, A. Ambler¹⁰¹, L. Ambroz¹³¹, C. Amelung³⁴, D. Amidei¹⁰³, S.P. Amor Dos Santos^{136a}, S. Amoroso⁴⁴, C.S. Amrouche⁵², C. Anastopoulos¹⁴⁶, N. Andari¹⁴¹, T. Andeen¹⁰, J.K. Anders¹⁸, S.Y. Andreev^{43a,43b}, A. Andreazza^{66a,66b}, V. Andrei^{59a}, S. Angelidakis⁸, A. Angerami³⁷, A.V. Anisenkov^{119b,119a}, A. Annovi^{69a}, C. Antel⁵², M.T. Anthony¹⁴⁶, E. Antipov¹²⁶, M. Antonelli⁴⁹, D.J.A. Antrim¹⁶, F. Anulli^{70a}, M. Aoki⁷⁹, J.A. Aparisi Pozo¹⁷⁰, M.A. Aparo¹⁵³, L. Aperio Bella⁴⁴, N. Aranzabal³⁴, V. Araujo Ferraz^{78a}, C. Arcangeletti⁴⁹, A.T.H. Arce⁴⁷, E. Arena⁸⁸, J-F. Arguin¹⁰⁷, S. Argyropoulos⁵⁰, J.-H. Arling⁴⁴, A.J. Armbruster³⁴, A. Armstrong¹⁶⁷, O. Arnaez¹⁶³, H. Arnold³⁴, Z.P. Arrubarrena Tame¹¹¹, G. Artoni¹³¹, H. Asada¹¹⁴, K. Asai¹²³, S. Asai¹⁶⁰, N.A. Asbah⁵⁷, E.M. Asimakopoulou¹⁶⁸, L. Asquith¹⁵³, J. Assahsah^{33d},

K. Assamagan²⁷, R. Astalos^{26a}, R.J. Atkin^{31a}, M. Atkinson¹⁶⁹, N.B. Atlay¹⁷, H. Atmani^{58b},
 P.A. Atmasiddha¹⁰³, K. Augsten¹³⁸, S. Auricchio^{67a,67b}, V.A. Austrup¹⁷⁸, G. Avolio³⁴, M.K. Ayoub^{13c},
 G. Azuelos^{107,ak}, D. Babal^{26a}, H. Bachacou¹⁴¹, K. Bachas¹⁵⁹, F. Backman^{43a,43b}, A. Badea⁵⁷,
 P. Bagnaia^{70a,70b}, H. Bahrasemani¹⁴⁹, A.J. Bailey¹⁷⁰, V.R. Bailey¹⁶⁹, J.T. Baines¹⁴⁰, C. Bakalis⁹,
 O.K. Baker¹⁷⁹, P.J. Bakker¹¹⁷, E. Bakos¹⁴, D. Bakshi Gupta⁷, S. Balaji¹⁵⁴, R. Balasubramanian¹¹⁷,
 E.M. Baldin^{119b,119a}, P. Balek¹³⁹, E. Ballabene^{66a,66b}, F. Balli¹⁴¹, W.K. Balunas¹³¹, J. Balz⁹⁷, E. Banas⁸²,
 M. Bandieramonte¹³⁵, A. Bandyopadhyay¹⁷, L. Barak¹⁵⁸, E.L. Barberio¹⁰², D. Barberis^{53b,53a},
 M. Barbero⁹⁹, G. Barbour⁹², K.N. Barends^{31a}, T. Barillari¹¹², M-S. Barisits³⁴, J. Barkeloo¹²⁸,
 T. Barklow¹⁵⁰, B.M. Barnett¹⁴⁰, R.M. Barnett¹⁶, A. Baroncelli^{58a}, G. Barone²⁷, A.J. Barr¹³¹,
 L. Barranco Navarro^{43a,43b}, F. Barreiro⁹⁶, J. Barreiro Guimarães da Costa^{13a}, U. Barron¹⁵⁸, S. Barsov¹³⁴,
 F. Bartels^{59a}, R. Bartoldus¹⁵⁰, G. Bartolini⁹⁹, A.E. Barton⁸⁷, P. Bartos^{26a}, A. Basalaeu⁴⁴, A. Basan⁹⁷,
 I. Bashta^{72a,72b}, A. Bassalat⁶², M.J. Basso¹⁶³, C.R. Basson⁹⁸, R.L. Bates⁵⁵, S. Batlamous^{33e}, J.R. Batley³⁰,
 B. Batool¹⁴⁸, M. Battaglia¹⁴², M. Bauce^{70a,70b}, F. Bauer^{141,*}, P. Bauer²², H.S. Bawa²⁹, A. Bayirli^{11c},
 J.B. Beacham⁴⁷, T. Beau¹³², P.H. Beauchemin¹⁶⁶, F. Becherer⁵⁰, P. Bechtel²², H.P. Beck^{18,r}, K. Becker¹⁷⁴,
 C. Becot⁴⁴, A.J. Beddall^{11a}, V.A. Bednyakov⁷⁷, C.P. Bee¹⁵², T.A. Beermann¹⁷⁸, M. Begalli^{78b}, M. Begel²⁷,
 A. Behera¹⁵², J.K. Behr⁴⁴, C. Beirao Da Cruz E Silva³⁴, J.F. Beirer^{51,34}, F. Beisiegel²², M. Belfkir⁴,
 G. Bella¹⁵⁸, L. Bellagamba^{21b}, A. Bellerive³², P. Bellos¹⁹, K. Beloborodov^{119b,119a}, K. Belotskiy¹⁰⁹,
 N.L. Belyaev¹⁰⁹, D. Benckekroun^{33a}, Y. Benhammou¹⁵⁸, D.P. Benjamin⁵, M. Benoit²⁷, J.R. Bensinger²⁴,
 S. Bentvelsen¹¹⁷, L. Beresford¹³¹, M. Beretta⁴⁹, D. Berge¹⁷, E. Bergeaas Kuutmann¹⁶⁸, N. Berger⁴,
 B. Bergmann¹³⁸, L.J. Bergsten²⁴, J. Beringer¹⁶, S. Berlendis⁶, G. Bernardi¹³², C. Bernius¹⁵⁰,
 F.U. Bernlochner²², T. Berry⁹¹, P. Berta⁴⁴, A. Berthold⁴⁶, I.A. Bertram⁸⁷, O. Bessidskaia Bylund¹⁷⁸,
 S. Bethke¹¹², A. Betti⁴⁰, A.J. Bevan⁹⁰, S. Bhatta¹⁵², D.S. Bhattacharya¹⁷³, P. Bhattarai²⁴, V.S. Bhopatkar⁵,
 R. Bi¹³⁵, R.M. Bianchi¹³⁵, O. Biebel¹¹¹, R. Bielski³⁴, N.V. Biesuz^{69a,69b}, M. Biglietti^{72a}, T.R.V. Billoud¹³⁸,
 M. Bindi⁵¹, A. Bingul^{11d}, C. Bini^{70a,70b}, S. Biondi^{21b,21a}, C.J. Birch-sykes⁹⁸, G.A. Bird^{19,140}, M. Birman¹⁷⁶,
 T. Bisanz³⁴, J.P. Biswal², D. Biswas^{177,k}, A. Bitadze⁹⁸, C. Bittrich⁴⁶, K. Bjørke¹³⁰, I. Bloch⁴⁴, C. Blocker²⁴,
 A. Blue⁵⁵, U. Blumenschein⁹⁰, J. Blumenthal⁹⁷, G.J. Bobbink¹¹⁷, V.S. Bobrovnikov^{119b,119a}, D. Bogavac¹²,
 A.G. Bogdanchikov^{119b,119a}, C. Boehm^{43a}, V. Boisvert⁹¹, P. Bokan⁴⁴, T. Bold^{81a}, M. Bomben¹³²,
 M. Bona⁹⁰, M. Boonekamp¹⁴¹, C.D. Booth⁹¹, A.G. Borbély⁵⁵, H.M. Borecka-Bielska¹⁰⁷, L.S. Borgna⁹²,
 G. Borissov⁸⁷, D. Bortoletto¹³¹, D. Boscherini^{21b}, M. Bosman¹², J.D. Bossio Sola¹⁰¹, K. Bouaouda^{33a},
 J. Boudreau¹³⁵, E.V. Bouhova-Thacker⁸⁷, D. Boumediene³⁶, R. Bouquet¹³², A. Boveia¹²⁴, J. Boyd³⁴,
 D. Boye²⁷, I.R. Boyko⁷⁷, A.J. Bozson⁹¹, J. Bracinik¹⁹, N. Brahimi^{58d,58c}, G. Brandt¹⁷⁸, O. Brandt³⁰,
 F. Braren⁴⁴, B. Brau¹⁰⁰, J.E. Brau¹²⁸, W.D. Breaden Madden⁵⁵, K. Brendlinger⁴⁴, R. Brenner¹⁷⁶,
 L. Brenner³⁴, R. Brenner¹⁶⁸, S. Bressler¹⁷⁶, B. Brickwedde⁹⁷, D.L. Briglin¹⁹, D. Britton⁵⁵, D. Britzger¹¹²,
 I. Brock²², R. Brock¹⁰⁴, G. Brooijmans³⁷, W.K. Brooks^{143d}, E. Brost²⁷, P.A. Bruckman de Renstrom⁸²,
 B. Brüers⁴⁴, D. Bruncko^{26b}, A. Bruni^{21b}, G. Bruni^{21b}, M. Bruschi^{21b}, N. Bruscino^{70a,70b},
 L. Bryngemark¹⁵⁰, T. Buanes¹⁵, Q. Buat¹⁵², P. Buchholz¹⁴⁸, A.G. Buckley⁵⁵, I.A. Budagov⁷⁷,
 M.K. Bugge¹³⁰, O. Bulekov¹⁰⁹, B.A. Bullard⁵⁷, T.J. Burch¹¹⁸, S. Burdin⁸⁸, C.D. Burgard⁴⁴, A.M. Burger¹²⁶,
 B. Burghgrave⁷, J.T.P. Burr⁴⁴, C.D. Burton¹⁰, J.C. Burzynski¹⁰⁰, V. Büscher⁹⁷, P.J. Bussey⁵⁵, J.M. Butler²³,
 C.M. Buttar⁵⁵, J.M. Butterworth⁹², W. Buttinger¹⁴⁰, C.J. Buxo Vazquez¹⁰⁴, A.R. Buzykaev^{119b,119a},
 G. Cabras^{21b}, S. Cabrera Urbán¹⁷⁰, D. Caforio⁵⁴, H. Cai¹³⁵, V.M.M. Cairo¹⁵⁰, O. Cakir^{3a}, N. Calace³⁴,
 P. Calafiura¹⁶, G. Calderini¹³², P. Calfayan⁶³, G. Callea⁵⁵, L.P. Caloba^{78b}, A. Caltabiano^{71a,71b},
 S. Calvente Lopez⁹⁶, D. Calvet³⁶, S. Calvet³⁶, T.P. Calvet⁹⁹, M. Calvetti^{69a,69b}, R. Camacho Toro¹³²,
 S. Camarda³⁴, D. Camarero Munoz⁹⁶, P. Camarri^{71a,71b}, M.T. Camerlingo^{72a,72b}, D. Cameron¹³⁰,
 C. Camincher¹⁷², M. Campanelli⁹², A. Camplani³⁸, V. Canale^{67a,67b}, A. Canesse¹⁰¹, M. Cano Bret⁷⁵,
 J. Cantero¹²⁶, Y. Cao¹⁶⁹, M. Capua^{39b,39a}, R. Cardarelli^{71a}, F. Cardillo¹⁷⁰, G. Carducci^{39b,39a}, T. Carli³⁴,
 G. Carlino^{67a}, B.T. Carlson¹³⁵, E.M. Carlson^{172,164a}, L. Carminati^{66a,66b}, M. Carnesale^{70a,70b},
 R.M.D. Carney¹⁵⁰, S. Caron¹¹⁶, E. Carquin^{143d}, S. Carrá⁴⁴, G. Carratta^{21b,21a}, J.W.S. Carter¹⁶³,
 T.M. Carter⁴⁸, D. Casadei^{31c}, M.P. Casado^{12,h}, A.F. Casha¹⁶³, E.G. Castiglia¹⁷⁹, F.L. Castillo^{59a},
 L. Castillo Garcia¹², V. Castillo Gimenez¹⁷⁰, N.F. Castro^{136a,136e}, A. Catinaccio³⁴, J.R. Catmore¹³⁰,
 A. Cattai³⁴, V. Cavaliere²⁷, N. Cavalli^{21b,21a}, V. Cavasinni^{69a,69b}, E. Celebi^{11b}, F. Celli¹³¹, K. Cerny¹²⁷,
 A.S. Cerqueira^{78a}, A. Cerri¹⁵³, L. Cerrito^{71a,71b}, F. Cerutti¹⁶, A. Cervelli^{21b}, S.A. Cetin^{11b}, Z. Chadi^{33a},
 D. Chakraborty¹¹⁸, M. Chala^{136f}, J. Chan¹⁷⁷, W.S. Chan¹¹⁷, W.Y. Chan⁸⁸, J.D. Chapman³⁰,
 B. Chargeishvili^{156b}, D.G. Charlton¹⁹, T.P. Charman⁹⁰, M. Chatterjee¹⁸, C.C. Chau³², S. Chekanov⁵,

S.V. Chekulaev^{164a}, G.A. Chelkov^{77.ag}, A. Chen¹⁰³, B. Chen¹⁵⁸, C. Chen^{58a}, C.H. Chen⁷⁶, H. Chen^{13c}, H. Chen²⁷, J. Chen^{58a}, J. Chen³⁷, J. Chen²⁴, S. Chen¹³³, S.J. Chen^{13c}, X. Chen^{13b}, Y. Chen^{58a}, Y.-H. Chen⁴⁴, C.L. Cheng¹⁷⁷, H.C. Cheng^{60a}, H.J. Cheng^{13a}, A. Cheplakov⁷⁷, E. Cheremushkina⁴⁴, R. Cherkaoui El Moursli^{33e}, E. Cheu⁶, K. Cheung⁶¹, L. Chevalier¹⁴¹, V. Chiarella⁴⁹, G. Chiarelli^{69a}, G. Chiodini^{65a}, A.S. Chisholm¹⁹, A. Chitan^{25b}, I. Chiu¹⁶⁰, Y.H. Chiu¹⁷², M.V. Chizhov^{77,t}, K. Choi¹⁰, A.R. Chomont^{70a,70b}, Y. Chou¹⁰⁰, Y.S. Chow¹¹⁷, L.D. Christopher^{31e}, M.C. Chu^{60a}, X. Chu^{13a,13d}, J. Chudoba¹³⁷, J.J. Chwastowski⁸², D. Cieri¹¹², K.M. Ciesla⁸², V. Cindro⁸⁹, I.A. Cioară^{25b}, A. Ciocio¹⁶, F. Ciotto^{67a,67b}, Z.H. Citron^{176,l}, M. Citterio^{66a}, D.A. Ciubotaru^{25b}, B.M. Ciungu¹⁶³, A. Clark⁵², P.J. Clark⁴⁸, S.E. Clawson⁹⁸, C. Clement^{43a,43b}, L. Clissa^{21b,21a}, Y. Coadou⁹⁹, M. Cokal^{64a,64c}, A. Coccaro^{53b}, J. Cochran⁷⁶, R.F. Coelho Barrue^{136a}, R. Coelho Lopes De Sa¹⁰⁰, S. Coelli^{66a}, H. Cohen¹⁵⁸, A.E.C. Coimbra³⁴, B. Cole³⁷, J. Collot⁵⁶, P. Conde Muiño^{136a,136h}, S.H. Connell^{31c}, I.A. Connelly⁵⁵, E.I. Conroy¹³¹, F. Conventi^{67a,al}, H.G. Cooke¹⁹, A.M. Cooper-Sarkar¹³¹, F. Cormier¹⁷¹, L.D. Corpe³⁴, M. Corradi^{70a,70b}, E.E. Corrigan⁹⁴, F. Corriveau^{101,aa}, M.J. Costa¹⁷⁰, F. Costanza⁴, D. Costanzo¹⁴⁶, B.M. Cote¹²⁴, G. Cowan⁹¹, J.W. Cowley³⁰, J. Crane⁹⁸, K. Cranmer¹²², R.A. Creager¹³³, S. Crépe-Renaudin⁵⁶, F. Crescioli¹³², M. Cristinziani¹⁴⁸, M. Cristoforetti^{73a,73b,b}, V. Croft¹⁶⁶, G. Crosetti^{39b,39a}, A. Cueto⁴, T. Cuhadar Donszelmann¹⁶⁷, H. Cui^{13a,13d}, A.R. Cukierman¹⁵⁰, W.R. Cunningham⁵⁵, S. Czekierda⁸², P. Czodrowski³⁴, M.M. Czurylo^{59b}, M.J. Da Cunha Sargedas De Sousa^{58a}, J.V. Da Fonseca Pinto^{78b}, C. Da Via⁹⁸, W. Dabrowski^{81a}, T. Dado⁴⁵, S. Dahbi^{31e}, T. Dai¹⁰³, C. Dallapiccola¹⁰⁰, M. Dam³⁸, G. D'amen²⁷, V. D'Amico^{72a,72b}, J. Damp⁹⁷, J.R. Dandoy¹³³, M.F. Daneri²⁸, M. Danninger¹⁴⁹, V. Dao³⁴, G. Darbo^{53b}, S. Darmora⁵, A. Dattagupta¹²⁸, S. D'Auria^{66a,66b}, C. David^{164b}, T. Davidek¹³⁹, D.R. Davis⁴⁷, B. Davis-Purcell³², I. Dawson⁹⁰, K. De⁷, R. De Asmundis^{67a}, M. De Beurs¹¹⁷, S. De Castro^{21b,21a}, N. De Groot¹¹⁶, P. de Jong¹¹⁷, H. De la Torre¹⁰⁴, A. De Maria^{13c}, D. De Pedis^{70a}, A. De Salvo^{70a}, U. De Sanctis^{71a,71b}, M. De Santis^{71a,71b}, A. De Santo¹⁵³, J.B. De Vivie De Regie⁵⁶, D.V. Dedovich⁷⁷, J. Degens¹¹⁷, A.M. Deiana⁴⁰, J. Del Peso⁹⁶, Y. Delabat Diaz⁴⁴, F. Deliot¹⁴¹, C.M. Delitzsch⁶, M. Della Pietra^{67a,67b}, D. Della Volpe⁵², A. Dell'Acqua³⁴, L. Dell'Asta^{66a,66b}, M. Delmastro⁴, P.A. Delsart⁵⁶, S. Demers¹⁷⁹, M. Demichev⁷⁷, S.P. Denisov¹²⁰, L. D'Eramo¹¹⁸, D. Derendarz⁸², J.E. Derkaoui^{33d}, F. Derue¹³², P. Dervan⁸⁸, K. Desch²², K. Dette¹⁶³, C. Deutsch²², P.O. Deviveiros³⁴, F.A. Di Bello^{70a,70b}, A. Di Ciaccio^{71a,71b}, L. Di Ciaccio⁴, C. Di Donato^{67a,67b}, A. Di Girolamo³⁴, G. Di Gregorio^{69a,69b}, A. Di Luca^{73a,73b}, B. Di Micco^{72a,72b}, R. Di Nardo^{72a,72b}, C. Diaconu⁹⁹, F.A. Dias¹¹⁷, T. Dias Do Vale^{136a}, M.A. Diaz^{143a}, F.G. Diaz Capriles²², J. Dickinson¹⁶, M. Didenko¹⁷⁰, E.B. Diehl¹⁰³, J. Dietrich¹⁷, S. Díez Cornell⁴⁴, C. Díez Pardos¹⁴⁸, A. Dimitrievska¹⁶, W. Ding^{13b}, J. Dingfelder²², S.J. Dittmeier^{59b}, F. Dittus³⁴, F. Djama⁹⁹, T. Djobava^{156b}, J.I. Djuvsland¹⁵, M.A.B. Do Vale¹⁴⁴, D. Dodsworth²⁴, C. Doglioni⁹⁴, J. Dolejsi¹³⁹, Z. Dolezal¹³⁹, M. Donadelli^{78c}, B. Dong^{58c}, J. Donini³⁶, A. D'onofrio^{13c}, M. D'onofrio⁸⁸, J. Dopke¹⁴⁰, A. Doria^{67a}, M.T. Dova⁸⁶, A.T. Doyle⁵⁵, E. Drechsler¹⁴⁹, E. Dreyer¹⁴⁹, T. Dreyer⁵¹, A.S. Drobac¹⁶⁶, D. Du^{58b}, T.A. du Pree¹¹⁷, F. Dubinin¹⁰⁸, M. Dubovsky^{26a}, A. Dubreuil⁵², E. Duchovni¹⁷⁶, G. Duckeck¹¹¹, O.A. Ducu^{34,25b}, D. Duda¹¹², A. Dudarev³⁴, M. D'uffizi⁹⁸, L. Duflot⁶², M. Dührssen³⁴, C. Dülsen¹⁷⁸, A.E. Dumitriu^{25b}, M. Dunford^{59a}, S. Dungs⁴⁵, A. Duperrin⁹⁹, H. Duran Yildiz^{3a}, M. Düren⁵⁴, A. Durglishvili^{156b}, B. Dutta⁴⁴, D. Duvnjak¹, G.I. Dyckes¹³³, M. Dyndal^{81a}, S. Dysch⁹⁸, B.S. Dziedzic⁸², B. Eckerova^{26a}, M.G. Eggleston⁴⁷, E. Egidio Purcino De Souza^{78b}, L.F. Ehrke⁵², T. Eifert⁷, G. Eigen¹⁵, K. Einsweiler¹⁶, T. Ekelof¹⁶⁸, Y. El Ghazali^{33b}, H. El Jarrari^{33e}, A. El Moussaouy^{33a}, V. Ellajosyula¹⁶⁸, M. Ellert¹⁶⁸, F. Ellinghaus¹⁷⁸, A.A. Elliot⁹⁰, N. Ellis³⁴, J. Elmsheuser²⁷, M. Elsing³⁴, D. Emelianov¹⁴⁰, A. Emerman³⁷, Y. Enari¹⁶⁰, J. Erdmann⁴⁵, A. Ereditato¹⁸, P.A. Erland⁸², M. Errenst¹⁷⁸, M. Escalier⁶², C. Escobar¹⁷⁰, O. Estrada Pastor¹⁷⁰, E. Etzion¹⁵⁸, G. Evans^{136a}, H. Evans⁶³, M.O. Evans¹⁵³, A. Ezhilov¹³⁴, F. Fabbri⁵⁵, L. Fabbri^{21b,21a}, V. Fabiani¹¹⁶, G. Facini¹⁷⁴, R.M. Fakhruddinov¹²⁰, S. Falciano^{70a}, P.J. Falke²², S. Falke³⁴, J. Faltova¹³⁹, Y. Fan^{13a}, Y. Fang^{13a}, Y. Fang^{13a}, G. Fanourakis⁴², M. Fanti^{66a,66b}, M. Faraj^{58c}, A. Farbin⁷, A. Farilla^{72a}, E.M. Farina^{68a,68b}, T. Farooque¹⁰⁴, S.M. Farrington⁴⁸, P. Farthouat³⁴, F. Fassi^{33e}, D. Fassouliotis⁸, M. Fauci Giannelli^{71a,71b}, W.J. Fawcett³⁰, L. Fayard⁶², O.L. Fedin^{134,q}, M. Feickert¹⁶⁹, L. Feligioni⁹⁹, A. Fell¹⁴⁶, C. Feng^{58b}, M. Feng^{13b}, M.J. Fenton¹⁶⁷, A.B. Fenyuk¹²⁰, S.W. Ferguson⁴¹, J. Ferrando⁴⁴, A. Ferrari¹⁶⁸, P. Ferrari¹¹⁷, R. Ferrari^{68a}, D. Ferrere⁵², C. Ferretti¹⁰³, F. Fiedler⁹⁷, A. Filipčič⁸⁹, F. Filthaut¹¹⁶, M.C.N. Fiolhais^{136a,136c,a}, L. Fiorini¹⁷⁰, F. Fischer¹¹¹, W.C. Fisher¹⁰⁴, T. Fitschen¹⁹, I. Fleck¹⁴⁸, P. Fleischmann¹⁰³, T. Flick¹⁷⁸, B.M. Flierl¹¹¹, L. Flores¹³³, L.R. Flores Castillo^{60a}, F.M. Follega^{73a,73b}, N. Fomin¹⁵, J.H. Foo¹⁶³, G.T. Forcolin^{73a,73b}, B.C. Forland⁶³,

A. Formica ¹⁴¹, F.A. Förster ¹², A.C. Forti ⁹⁸, E. Fortin ⁹⁹, M.G. Foti ¹³¹, D. Fournier ⁶², H. Fox ⁸⁷,
 P. Francavilla ^{69a,69b}, S. Francescato ^{70a,70b}, M. Franchini ^{21b,21a}, S. Franchino ^{59a}, D. Francis ³⁴, L. Franco ⁴,
 L. Franconi ¹⁸, M. Franklin ⁵⁷, G. Frattari ^{70a,70b}, A.C. Freegard ⁹⁰, P.M. Freeman ¹⁹, B. Freund ¹⁰⁷,
 W.S. Freund ^{78b}, E.M. Freundlich ⁴⁵, D. Froidevaux ³⁴, J.A. Frost ¹³¹, Y. Fu ^{58a}, M. Fujimoto ¹²³,
 E. Fullana Torregrosa ¹⁷⁰, T. Fusayasu ¹¹³, J. Fuster ¹⁷⁰, A. Gabrielli ^{21b,21a}, A. Gabrielli ³⁴, P. Gadow ⁴⁴,
 G. Gagliardi ^{53b,53a}, L.G. Gagnon ¹⁶, G.E. Gallardo ¹³¹, E.J. Gallas ¹³¹, B.J. Gallop ¹⁴⁰, R. Gamboa Goni ⁹⁰,
 K.K. Gan ¹²⁴, S. Ganguly ¹⁷⁶, J. Gao ^{58a}, Y. Gao ⁴⁸, Y.S. Gao ^{29,n}, F.M. Garay Walls ^{143a}, C. García ¹⁷⁰,
 J.E. García Navarro ¹⁷⁰, J.A. García Pascual ^{13a}, M. Garcia-Sciveres ¹⁶, R.W. Gardner ³⁵, D. Garg ⁷⁵,
 S. Gargiulo ⁵⁰, C.A. Garner ¹⁶³, V. Garonne ¹³⁰, S.J. Gasiorowski ¹⁴⁵, P. Gaspar ^{78b}, G. Gaudio ^{68a},
 P. Gauzzi ^{70a,70b}, I.L. Gavrilenko ¹⁰⁸, A. Gavrilyuk ¹²¹, C. Gay ¹⁷¹, G. Gaycken ⁴⁴, E.N. Gazis ⁹,
 A.A. Geanta ^{25b}, C.M. Gee ¹⁴², C.N.P. Gee ¹⁴⁰, J. Geisen ⁹⁴, M. Geisen ⁹⁷, C. Gemme ^{53b}, M.H. Genest ⁵⁶,
 S. Gentile ^{70a,70b}, S. George ⁹¹, T. Gerasis ⁴², L.O. Gerlach ⁵¹, P. Gessinger-Befurt ⁹⁷,
 M. Ghasemi Bostanabad ¹⁷², M. Ghneimat ¹⁴⁸, A. Ghosh ¹⁶⁷, A. Ghosh ⁷⁵, B. Giacobbe ^{21b}, S. Giagu ^{70a,70b},
 N. Giangiacomi ¹⁶³, P. Giannetti ^{69a}, A. Giannini ^{67a,67b}, S.M. Gibson ⁹¹, M. Gignac ¹⁴², D.T. Gil ^{81b},
 B.J. Gilbert ³⁷, D. Gillberg ³², G. Gilles ¹⁷⁸, N.E.K. Gillwald ⁴⁴, D.M. Gingrich ^{2,ak}, M.P. Giordani ^{64a,64c},
 P.F. Giraud ¹⁴¹, G. Giugliarelli ^{64a,64c}, D. Giugni ^{66a}, F. Giuli ^{71a,71b}, I. Gkialas ^{8,i}, E.L. Gkougkousis ¹²,
 P. Gkoutoumis ⁹, L.K. Gladilin ¹¹⁰, C. Glasman ⁹⁶, G.R. Gledhill ¹²⁸, M. Glisic ¹²⁸, I. Gnesi ^{39b,d},
 M. Goblirsch-Kolb ²⁴, D. Godin ¹⁰⁷, S. Goldfarb ¹⁰², T. Golling ⁵², D. Golubkov ¹²⁰, J.P. Gombas ¹⁰⁴,
 A. Gomes ^{136a,136b}, R. Goncalves Gama ⁵¹, R. Gonçalo ^{136a,136c}, G. Gonella ¹²⁸, L. Gonella ¹⁹,
 A. Gongadze ⁷⁷, F. Gonnella ¹⁹, J.L. Gonski ³⁷, S. González de la Hoz ¹⁷⁰, S. Gonzalez Fernandez ¹²,
 R. Gonzalez Lopez ⁸⁸, C. Gonzalez Renteria ¹⁶, R. Gonzalez Suarez ¹⁶⁸, S. Gonzalez-Sevilla ⁵²,
 G.R. Gonzalvo Rodriguez ¹⁷⁰, R.Y. González Andana ^{143a}, L. Goossens ³⁴, N.A. Gorasia ¹⁹,
 P.A. Gorbounov ¹²¹, H.A. Gordon ²⁷, B. Gorini ³⁴, E. Gorini ^{65a,65b}, A. Gorišek ⁸⁹, A.T. Goshaw ⁴⁷,
 M.I. Gostkin ⁷⁷, C.A. Gottardo ¹¹⁶, M. Gouighri ^{33b}, V. Goumarre ⁴⁴, A.G. Goussiou ¹⁴⁵, N. Govender ^{31c},
 C. Goy ⁴, I. Grabowska-Bold ^{81a}, K. Graham ³², E. Gramstad ¹³⁰, S. Grancagnolo ¹⁷, M. Grandi ¹⁵³,
 V. Gratchev ¹³⁴, P.M. Gravila ^{25f}, F.G. Gravili ^{65a,65b}, H.M. Gray ¹⁶, C. Grefe ²², I.M. Gregor ⁴⁴, P. Grenier ¹⁵⁰,
 K. Grevtsov ⁴⁴, C. Grieco ¹², N.A. Grieser ¹²⁵, A.A. Grillo ¹⁴², K. Grimm ^{29,m}, S. Grinstein ^{12,x}, J.-F. Grivaz ⁶²,
 S. Groh ⁹⁷, E. Gross ¹⁷⁶, J. Grosse-Knetter ⁵¹, Z.J. Grout ⁹², C. Grud ¹⁰³, A. Grummer ¹¹⁵, J.C. Grundy ¹³¹,
 L. Guan ¹⁰³, W. Guan ¹⁷⁷, C. Gubbels ¹⁷¹, J. Guenther ³⁴, J.G.R. Guerrero Rojas ¹⁷⁰, F. Guescini ¹¹²,
 D. Guest ¹⁷, R. Gugel ⁹⁷, A. Guida ⁴⁴, T. Guillemin ⁴, S. Guindon ³⁴, J. Guo ^{58c}, L. Guo ⁶², Y. Guo ¹⁰³,
 R. Gupta ⁴⁴, S. Gurbuz ²², G. Gustavino ¹²⁵, M. Guth ⁵⁰, P. Gutierrez ¹²⁵, L.F. Gutierrez Zagazeta ¹³³,
 C. Gutschow ⁹², C. Guyot ¹⁴¹, C. Gwenlan ¹³¹, C.B. Gwilliam ⁸⁸, E.S. Haaland ¹³⁰, A. Haas ¹²²,
 M. Habedank ¹⁷, C. Haber ¹⁶, H.K. Hadavand ⁷, A. Hadeef ⁹⁷, M. Haleem ¹⁷³, J. Haley ¹²⁶, J.J. Hall ¹⁴⁶,
 G. Halladjian ¹⁰⁴, G.D. Hallowell ⁹⁹, L. Halser ¹⁸, K. Hamano ¹⁷², H. Hamdaoui ^{33e}, M. Hamer ²²,
 G.N. Hamity ⁴⁸, K. Han ^{58a}, L. Han ^{13c}, L. Han ^{58a}, S. Han ¹⁶, Y.F. Han ¹⁶³, K. Hanagaki ^{79,v}, M. Hance ¹⁴²,
 M.D. Hank ³⁵, R. Hankache ⁹⁸, E. Hansen ⁹⁴, J.B. Hansen ³⁸, J.D. Hansen ³⁸, M.C. Hansen ²², P.H. Hansen ³⁸,
 K. Hara ¹⁶⁵, T. Harenberg ¹⁷⁸, S. Harkusha ¹⁰⁵, Y.T. Harris ¹³¹, P.F. Harrison ¹⁷⁴, N.M. Hartman ¹⁵⁰,
 N.M. Hartmann ¹¹¹, Y. Hasegawa ¹⁴⁷, A. Hasib ⁴⁸, S. Hassani ¹⁴¹, S. Haug ¹⁸, R. Hauser ¹⁰⁴, M. Havranek ¹³⁸,
 C.M. Hawkes ¹⁹, R.J. Hawkings ³⁴, S. Hayashida ¹¹⁴, D. Hayden ¹⁰⁴, C. Hayes ¹⁰³, R.L. Hayes ¹⁷¹,
 C.P. Hays ¹³¹, J.M. Hays ⁹⁰, H.S. Hayward ⁸⁸, S.J. Haywood ¹⁴⁰, F. He ^{58a}, Y. He ¹⁶¹, Y. He ¹³², M.P. Heath ⁴⁸,
 V. Hedberg ⁹⁴, A.L. Heggelund ¹³⁰, N.D. Hehir ⁹⁰, C. Heidegger ⁵⁰, K.K. Heidegger ⁵⁰, W.D. Heidorn ⁷⁶,
 J. Heilman ³², S. Heim ⁴⁴, T. Heim ¹⁶, B. Heinemann ^{44,ai}, J.G. Heinlein ¹³³, J.J. Heinrich ¹²⁸, L. Heinrich ³⁴,
 J. Hejbal ¹³⁷, L. Helary ⁴⁴, A. Held ¹²², S. Hellesund ¹³⁰, C.M. Helling ¹⁴², S. Hellman ^{43a,43b}, C. Helsens ³⁴,
 R.C.W. Henderson ⁸⁷, L. Henkelmann ³⁰, A.M. Henriques Correia ³⁴, H. Herde ¹⁵⁰,
 Y. Hernández Jiménez ¹⁵², H. Herr ⁹⁷, M.G. Herrmann ¹¹¹, T. Herrmann ⁴⁶, G. Herten ⁵⁰,
 R. Hertenberger ¹¹¹, L. Hervas ³⁴, N.P. Hessey ^{164a}, H. Hibi ⁸⁰, S. Higashino ⁷⁹, E. Higón-Rodríguez ¹⁷⁰,
 K.K. Hill ²⁷, K.H. Hiller ⁴⁴, S.J. Hillier ¹⁹, M. Hils ⁴⁶, I. Hinchliffe ¹⁶, F. Hinterkeuser ²², M. Hirose ¹²⁹,
 S. Hirose ¹⁶⁵, D. Hirschbuehl ¹⁷⁸, B. Hiti ⁸⁹, O. Hladik ¹³⁷, J. Hobbs ¹⁵², R. Hobincu ^{25e}, N. Hod ¹⁷⁶,
 M.C. Hodgkinson ¹⁴⁶, B.H. Hodgkinson ³⁰, A. Hoecker ³⁴, J. Hofer ⁴⁴, D. Hohn ⁵⁰, T. Holm ²², T.R. Holmes ³⁵,
 M. Holzbock ¹¹², L.B.A.H. Hommels ³⁰, B.P. Honan ⁹⁸, T.M. Hong ¹³⁵, J.C. Honig ⁵⁰, A. Hönle ¹¹²,
 B.H. Hooberman ¹⁶⁹, W.H. Hopkins ⁵, Y. Horii ¹¹⁴, P. Horn ⁴⁶, L.A. Horyn ³⁵, S. Hou ¹⁵⁵, J. Howarth ⁵⁵,
 J. Hoya ⁸⁶, M. Hrabovsky ¹²⁷, A. Hrynevich ¹⁰⁶, T. Hryn'ova ⁴, P.J. Hsu ⁶¹, S.-C. Hsu ¹⁴⁵, Q. Hu ³⁷, S. Hu ^{58c},
 Y.F. Hu ^{13a,13d,am}, D.P. Huang ⁹², X. Huang ^{13c}, Y. Huang ^{58a}, Y. Huang ^{13a}, Z. Hubacek ¹³⁸, F. Hubaut ⁹⁹,

M. Huebner²², F. Huegging²², T.B. Huffman¹³¹, M. Huhtinen³⁴, R. Hulsken⁵⁶, N. Huseynov^{77,ab},
 J. Huston¹⁰⁴, J. Huth⁵⁷, R. Hyneman¹⁵⁰, S. Hyrych^{26a}, G. Iacobucci⁵², G. Iakovidis²⁷, I. Ibragimov¹⁴⁸,
 L. Iconomidou-Fayard⁶², P. Iengo³⁴, R. Ignazzi³⁸, O. Igonkina¹¹⁷, R. Iguchi¹⁶⁰, T. Iizawa⁵², Y. Ikegami⁷⁹,
 A. Ilg¹⁸, N. Ilic¹⁶³, H. Imam^{33a}, G. Introzzi^{68a,68b}, M. Iodice^{72a}, V. Ippolito^{70a,70b}, M. Ishino¹⁶⁰,
 W. Islam¹²⁶, C. Issever^{17,44}, S. Istin^{11c,an}, J.M. Iturbe Ponce^{60a}, R. Iuppa^{73a,73b}, A. Ivina¹⁷⁶, J.M. Izen⁴¹,
 V. Izzo^{67a}, P. Jacka¹³⁷, P. Jackson¹, R.M. Jacobs⁴⁴, B.P. Jaeger¹⁴⁹, C.S. Jagfeld¹¹¹, G. Jäkel¹⁷⁸,
 K.B. Jakobi⁹⁷, K. Jakobs⁵⁰, T. Jakoubek¹⁷⁶, J. Jamieson⁵⁵, K.W. Janas^{81a}, G. Jarlskog⁹⁴, A.E. Jaspan⁸⁸,
 N. Javadov^{77,ab}, T. Javůrek³⁴, M. Javurkova¹⁰⁰, F. Jeanneau¹⁴¹, L. Jeanty¹²⁸, J. Jejelava^{156a,ac}, P. Jenni^{50,e},
 S. Jézéquel⁴, J. Jia¹⁵², Z. Jia^{13c}, Y. Jiang^{58a}, S. Jiggins⁵⁰, J. Jimenez Pena¹¹², S. Jin^{13c}, A. Jinaru^{25b},
 O. Jinnouchi¹⁶¹, H. Jivan^{31e}, P. Johansson¹⁴⁶, K.A. Johns⁶, C.A. Johnson⁶³, E. Jones¹⁷⁴, R.W.L. Jones⁸⁷,
 T.J. Jones⁸⁸, J. Jovicevic³⁴, X. Ju¹⁶, J.J. Junggeburth³⁴, A. Juste Rozas^{12,x}, A. Kaczmarska⁸²,
 M. Kado^{70a,70b}, H. Kagan¹²⁴, M. Kagan¹⁵⁰, A. Kahn³⁷, C. Kahra⁹⁷, T. Kaji¹⁷⁵, E. Kajomovitz¹⁵⁷,
 C.W. Kalderon²⁷, A. Kaluza⁹⁷, A. Kamenshchikov¹²⁰, M. Kaneda¹⁶⁰, N.J. Kang¹⁴², S. Kang⁷⁶, Y. Kano¹¹⁴,
 J. Kanzaki⁷⁹, D. Kar^{31e}, K. Karava¹³¹, M.J. Kareem^{164b}, I. Karkanias¹⁵⁹, S.N. Karpov⁷⁷, Z.M. Karpova⁷⁷,
 V. Kartvelishvili⁸⁷, A.N. Karyukhin¹²⁰, E. Kasimi¹⁵⁹, C. Kato^{58d}, J. Katzy⁴⁴, K. Kawade¹⁴⁷, K. Kawagoe⁸⁵,
 T. Kawaguchi¹¹⁴, T. Kawamoto¹⁴¹, G. Kawamura⁵¹, E.F. Kay¹⁷², F.I. Kaya¹⁶⁶, S. Kazakos¹²,
 V.F. Kazanin^{119b,119a}, Y. Ke¹⁵², J.M. Keaveney^{31a}, R. Keeler¹⁷², J.S. Keller³², D. Kelsey¹⁵³, J.J. Kempster¹⁹,
 J. Kendrick¹⁹, K.E. Kennedy³⁷, O. Kepka¹³⁷, S. Kersten¹⁷⁸, B.P. Kerševan⁸⁹, S. Ketabchi Haghghat¹⁶³,
 M. Khandoga¹³², A. Khanov¹²⁶, A.G. Kharlamov^{119b,119a}, T. Kharlamova^{119b,119a}, E.E. Khoda¹⁷¹,
 T.J. Khoo¹⁷, G. Khorauli¹⁷³, E. Khramov⁷⁷, J. Khubua^{156b}, S. Kido⁸⁰, M. Kiehn³⁴, A. Kilgallon¹²⁸,
 E. Kim¹⁶¹, Y.K. Kim³⁵, N. Kimura⁹², A. Kirchhoff⁵¹, D. Kirchmeier⁴⁶, J. Kirk¹⁴⁰, A.E. Kiryunin¹¹²,
 T. Kishimoto¹⁶⁰, D.P. Kisliuk¹⁶³, V. Kitali⁴⁴, C. Kitsaki⁹, O. Kivernyk²², T. Klapdor-Kleingrothaus⁵⁰,
 M. Klassen^{59a}, C. Klein³², L. Klein¹⁷³, M.H. Klein¹⁰³, M. Klein⁸⁸, U. Klein⁸⁸, P. Klimek³⁴, A. Klimentov²⁷,
 F. Klimpel³⁴, T. Klingl²², T. Klioutchnikova³⁴, F.F. Klitzner¹¹¹, P. Kluit¹¹⁷, S. Kluth¹¹², E. Kneringer⁷⁴,
 T.M. Knight¹⁶³, A. Knue⁵⁰, D. Kobayashi⁸⁵, M. Kobel⁴⁶, M. Kocian¹⁵⁰, T. Kodama¹⁶⁰, P. Kodys¹³⁹,
 D.M. Koeck¹⁵³, P.T. Koenig²², T. Koffas³², N.M. Köhler³⁴, M. Kolb¹⁴¹, I. Koletsou⁴, T. Komarek¹²⁷,
 K. Köneke⁵⁰, A.X.Y. Kong¹, T. Kono¹²³, V. Konstantinides⁹², N. Konstantinidis⁹², B. Konya⁹⁴,
 R. Kopeliansky⁶³, S. Koperny^{81a}, K. Korcyl⁸², K. Kordas¹⁵⁹, G. Koren¹⁵⁸, A. Korn⁹², S. Korn⁵¹,
 I. Korolkov¹², E.V. Korolkova¹⁴⁶, N. Korotkova¹¹⁰, O. Kortner¹¹², S. Kortner¹¹², V.V. Kostyukhin^{146,162},
 A. Kotsokechagia⁶², A. Kotwal⁴⁷, A. Koulouris⁸, A. Kourkouveli-Charalampidi^{68a,68b}, C. Kourkoumelis⁸,
 E. Kourlitis⁵, R. Kowalewski¹⁷², W. Kozanecki¹⁴¹, A.S. Kozhin¹²⁰, V.A. Kramarenko¹¹⁰, G. Kramberger⁸⁹,
 D. Krasnopevtsev^{58a}, M.W. Krasny¹³², A. Krasznahorkay³⁴, J.A. Kremer⁹⁷, J. Kretzschmar⁸⁸, K. Kreul¹⁷,
 P. Krieger¹⁶³, F. Krieter¹¹¹, S. Krishnamurthy¹⁰⁰, A. Krishnan^{59b}, M. Krivos¹³⁹, K. Krizka¹⁶,
 K. Kroeninger⁴⁵, H. Kroha¹¹², J. Kroll¹³⁷, J. Kroll¹³³, K.S. Krowpman¹⁰⁴, U. Kruchonak⁷⁷, H. Krüger²²,
 N. Krumnack⁷⁶, M.C. Kruse⁴⁷, J.A. Krzysiak⁸², A. Kubota¹⁶¹, O. Kuchinskaia¹⁶², S. Kuday^{3b},
 D. Kuechler⁴⁴, J.T. Kuechler⁴⁴, S. Kuehn³⁴, T. Kuhl⁴⁴, V. Kukhtin⁷⁷, Y. Kulchitsky^{105,af}, S. Kuleshov^{143b},
 M. Kumar^{31e}, N. Kumari⁹⁹, M. Kuna⁵⁶, A. Kupco¹³⁷, T. Kupfer⁴⁵, O. Kuprash⁵⁰, H. Kurashige⁸⁰,
 L.L. Kurchaninov^{164a}, Y.A. Kurochkin¹⁰⁵, A. Kurova¹⁰⁹, M.G. Kurth^{13a,13d}, E.S. Kuwertz³⁴, M. Kuze¹⁶¹,
 A.K. Kvam¹⁴⁵, J. Kvita¹²⁷, T. Kwan¹⁰¹, C. Lacasta¹⁷⁰, F. Lacava^{70a,70b}, H. Lacker¹⁷, D. Lacour¹³²,
 N.N. Lad⁹², E. Ladygin⁷⁷, R. Lafaye⁴, B. Laforge¹³², T. Lagouri^{143c}, S. Lai⁵¹, I.K. Lakomic^{81a},
 N. Lalloue⁵⁶, J.E. Lambert¹²⁵, S. Lammers⁶³, W. Lampl⁶, C. Lampoudis¹⁵⁹, E. Lançon²⁷, U. Landgraf⁵⁰,
 M.P.J. Landon⁹⁰, V.S. Lang⁵⁰, J.C. Lange⁵¹, R.J. Langenberg¹⁰⁰, A.J. Lankford¹⁶⁷, F. Lanni²⁷, K. Lantzsch²²,
 A. Lanza^{68a}, A. Lapertosa^{53b,53a}, J.F. Laporte¹⁴¹, T. Lari^{66a}, F. Lasagni Manghi^{21b}, M. Lassnig³⁴,
 V. Latonova¹³⁷, T.S. Lau^{60a}, A. Laudrain⁹⁷, A. Laurier³², M. Lavorgna^{67a,67b}, S.D. Lawlor⁹¹,
 M. Lazzaroni^{66a,66b}, B. Le⁹⁸, A. Lebedev⁷⁶, M. LeBlanc³⁴, T. LeCompte⁵, F. Ledroit-Guillon⁵⁶,
 A.C.A. Lee⁹², C.A. Lee²⁷, G.R. Lee¹⁵, L. Lee⁵⁷, S.C. Lee¹⁵⁵, S. Lee⁷⁶, L.L. Leeuw^{31c}, B. Lefebvre^{164a},
 H.P. Lefebvre⁹¹, M. Lefebvre¹⁷², C. Leggett¹⁶, K. Lehmann¹⁴⁹, N. Lehmann¹⁸, G. Lehmann Miotto³⁴,
 W.A. Leight⁴⁴, A. Leisos^{159,w}, M.A.L. Leite^{78c}, C.E. Leitgeb⁴⁴, R. Leitner¹³⁹, K.J.C. Leney⁴⁰, T. Lenz²²,
 S. Leone^{69a}, C. Leonidopoulos⁴⁸, A. Leopold¹³², C. Leroy¹⁰⁷, R. Les¹⁰⁴, C.G. Lester³⁰, M. Levchenko¹³⁴,
 J. Levêque⁴, D. Levin¹⁰³, L.J. Levinson¹⁷⁶, D.J. Lewis¹⁹, B. Li^{13b}, B. Li¹⁰³, C. Li^{58a}, C.-Q. Li^{58c,58d}, H. Li^{58a},
 H. Li^{58b}, J. Li^{58c}, K. Li¹⁴⁵, L. Li^{58c}, M. Li^{13a,13d}, Q.Y. Li^{58a}, S. Li^{58d,58c,c}, X. Li⁴⁴, Y. Li⁴⁴, Z. Li^{58b}, Z. Li¹³¹,
 Z. Li¹⁰¹, Z. Li⁸⁸, Z. Liang^{13a}, M. Liberatore⁴⁴, B. Liberti^{71a}, K. Lie^{60c}, K. Lin¹⁰⁴, R.A. Linck⁶³,
 R.E. Lindley⁶, J.H. Lindon², A. Linss⁴⁴, A.L. Lioni⁵², E. Lipeles¹³³, A. Lipniacka¹⁵, T.M. Liss^{169,aj},

A. Lister¹⁷¹, J.D. Little⁷, B. Liu^{13a}, B.X. Liu¹⁴⁹, J.B. Liu^{58a}, J.K.K. Liu³⁵, K. Liu^{58d,58c}, M. Liu^{58a},
 M.Y. Liu^{58a}, P. Liu^{13a}, X. Liu^{58a}, Y. Liu⁴⁴, Y. Liu^{13c,13d}, Y.L. Liu¹⁰³, Y.W. Liu^{58a}, M. Livan^{68a,68b},
 A. Lleres⁵⁶, J. Llorente Merino¹⁴⁹, S.L. Lloyd⁹⁰, E.M. Lobodzinska⁴⁴, P. Loch⁶, S. Loffredo^{71a,71b},
 T. Lohse¹⁷, K. Lohwasser¹⁴⁶, M. Lokajicek¹³⁷, J.D. Long¹⁶⁹, R.E. Long⁸⁷, I. Longarini^{70a,70b}, L. Longo³⁴,
 R. Longo¹⁶⁹, I. Lopez Paz¹², A. Lopez Solis⁴⁴, J. Lorenz¹¹¹, N. Lorenzo Martinez⁴, A.M. Lory¹¹¹,
 A. Lösle⁵⁰, X. Lou^{43a,43b}, X. Lou^{13a}, A. Lounis⁶², J. Love⁵, P.A. Love⁸⁷, J.J. Lozano Bahilo¹⁷⁰, G. Lu^{13a},
 M. Lu^{58a}, S. Lu¹³³, Y.J. Lu⁶¹, H.J. Lubatti¹⁴⁵, C. Luci^{70a,70b}, F.L. Lucio Alves^{13c}, A. Lucotte⁵⁶,
 F. Luehring⁶³, I. Luise¹⁵², L. Luminari^{70a}, B. Lund-Jensen¹⁵¹, N.A. Luongo¹²⁸, M.S. Lutz¹⁵⁸, D. Lynn²⁷,
 H. Lyons⁸⁸, R. Lysak¹³⁷, E. Lytken⁹⁴, F. Lyu^{13a}, V. Lyubushkin⁷⁷, T. Lyubushkina⁷⁷, H. Ma²⁷, L.L. Ma^{58b},
 Y. Ma⁹², D.M. Mac Donell¹⁷², G. Maccarrone⁴⁹, C.M. Macdonald¹⁴⁶, J.C. MacDonald¹⁴⁶, R. Madar³⁶,
 W.F. Mader⁴⁶, M. Madugoda Ralalage Don¹²⁶, N. Madysa⁴⁶, J. Maeda⁸⁰, T. Maeno²⁷, M. Maerker⁴⁶,
 V. Magerl⁵⁰, J. Magro^{64a,64c}, D.J. Mahon³⁷, C. Maidantchik^{78b}, A. Maio^{136a,136b,136d}, K. Maj^{81a},
 O. Majersky^{26a}, S. Majewski¹²⁸, N. Makovec⁶², B. Malaescu¹³², Pa. Malecki⁸², V.P. Maleev¹³⁴,
 F. Malek⁵⁶, D. Malito^{39b,39a}, U. Mallik⁷⁵, C. Malone³⁰, S. Maltezos⁹, S. Malyukov⁷⁷, J. Mamuzic¹⁷⁰,
 G. Mancini⁴⁹, J.P. Mandalia⁹⁰, I. Mandić⁸⁹, L. Manhaes de Andrade Filho^{78a}, I.M. Maniatis¹⁵⁹,
 M. Manisha¹⁴¹, J. Manjarres Ramos⁴⁶, K.H. Mankinen⁹⁴, A. Mann¹¹¹, A. Manousos⁷⁴, B. Mansoulie¹⁴¹,
 I. Manthos¹⁵⁹, S. Manzoni¹¹⁷, A. Marantis^{159,w}, L. Marchese¹³¹, G. Marchiori¹³², M. Marcisovsky¹³⁷,
 L. Marcoccia^{71a,71b}, C. Marcon⁹⁴, M. Marjanovic¹²⁵, Z. Marshall¹⁶, S. Marti-Garcia¹⁷⁰, T.A. Martin¹⁷⁴,
 V.J. Martin⁴⁸, B. Martin dit Latour¹⁵, L. Martinelli^{72a,72b}, M. Martinez^{12,x}, P. Martinez Agullo¹⁷⁰,
 V.I. Martinez Outschoorn¹⁰⁰, S. Martin-Haugh¹⁴⁰, V.S. Martoiu^{25b}, A.C. Martyniuk⁹², A. Marzin³⁴,
 S.R. Maschek¹¹², L. Masetti⁹⁷, T. Mashimo¹⁶⁰, R. Mashinistov¹⁰⁸, J. Masik⁹⁸, A.L. Maslennikov^{119b,119a},
 L. Massa^{21b}, P. Massarotti^{67a,67b}, P. Mastrandrea^{69a,69b}, A. Mastroberardino^{39b,39a}, T. Masubuchi¹⁶⁰,
 D. Matakias²⁷, T. Mathisen¹⁶⁸, A. Matic¹¹¹, N. Matsuzawa¹⁶⁰, J. Maurer^{25b}, B. Maček⁸⁹,
 D.A. Maximov^{119b,119a}, R. Mazini¹⁵⁵, I. Maznas¹⁵⁹, S.M. Mazza¹⁴², C. Mc Ginn²⁷, J.P. Mc Gowan¹⁰¹,
 S.P. Mc Kee¹⁰³, T.G. McCarthy¹¹², W.P. McCormack¹⁶, E.F. McDonald¹⁰², A.E. McDougall¹¹⁷,
 J.A. MCFayden¹⁵³, G. Mchedlidze^{156b}, M.A. McKay⁴⁰, K.D. McLean¹⁷², S.J. McMahon¹⁴⁰,
 P.C. McNamara¹⁰², R.A. McPherson^{172,aa}, J.E. Mdhlluli^{31e}, Z.A. Meadows¹⁰⁰, S. Meehan³⁴, T. Megy³⁶,
 S. Mehlhase¹¹¹, A. Mehta⁸⁸, B. Meirose⁴¹, D. Melini¹⁵⁷, B.R. Mellado Garcia^{31e}, F. Meloni⁴⁴,
 A. Melzer²², E.D. Mendes Gouveia^{136a}, A.M. Mendes Jacques Da Costa¹⁹, H.Y. Meng¹⁶³, L. Meng³⁴,
 S. Menke¹¹², M. Mentink³⁴, E. Meoni^{39b,39a}, S.A.M. Merkt¹³⁵, C. Merlassino¹³¹, P. Mermod^{52,*},
 L. Merola^{67a,67b}, C. Meroni^{66a}, G. Merz¹⁰³, O. Meshkov^{110,108}, J.K.R. Meshreki¹⁴⁸, J. Metcalfe⁵,
 A.S. Mete⁵, C. Meyer⁶³, J-P. Meyer¹⁴¹, M. Michetti¹⁷, R.P. Middleton¹⁴⁰, L. Mijović⁴⁸, G. Mikenberg¹⁷⁶,
 M. Mikestikova¹³⁷, M. Mikuž⁸⁹, H. Mildner¹⁴⁶, A. Milic¹⁶³, C.D. Milke⁴⁰, D.W. Miller³⁵, L.S. Miller³²,
 A. Milov¹⁷⁶, D.A. Milstead^{43a,43b}, A.A. Minaenko¹²⁰, I.A. Minashvili^{156b}, L. Mince⁵⁵, A.I. Mincer¹²²,
 B. Mindur^{81a}, M. Mineev⁷⁷, Y. Minegishi¹⁶⁰, Y. Mino⁸³, L.M. Mir¹², M. Miralles Lopez¹⁷⁰,
 M. Mironova¹³¹, T. Mitani¹⁷⁵, V.A. Mitsou¹⁷⁰, M. Mittal^{58c}, O. Miu¹⁶³, P.S. Miyagawa⁹⁰, Y. Miyazaki⁸⁵,
 A. Mizukami⁷⁹, J.U. Mjörnmark⁹⁴, T. Mkrтчhyan^{59a}, M. Mlynarikova¹¹⁸, T. Moa^{43a,43b}, S. Mobius⁵¹,
 K. Mochizuki¹⁰⁷, P. Moder⁴⁴, P. Mogg¹¹¹, S. Mohapatra³⁷, G. Mokgatitswane^{31e}, B. Mondal¹⁴⁸,
 S. Mondal¹³⁸, K. Mönig⁴⁴, E. Monnier⁹⁹, A. Montalbano¹⁴⁹, J. Montejo Berlingen³⁴, M. Montella¹²⁴,
 F. Monticelli⁸⁶, N. Morange⁶², A.L. Moreira De Carvalho^{136a}, M. Moreno Llácer¹⁷⁰,
 C. Moreno Martinez¹², P. Morettini^{53b}, M. Morgenstern¹⁵⁷, S. Morgenstern¹⁷⁴, D. Mori¹⁴⁹, M. Morii⁵⁷,
 M. Morinaga¹⁶⁰, V. Morisbak¹³⁰, A.K. Morley³⁴, A.P. Morris⁹², L. Morvaj³⁴, P. Moschovakos³⁴,
 B. Moser¹¹⁷, M. Mosidze^{156b}, T. Moskalets⁵⁰, P. Moskvitina¹¹⁶, J. Moss^{29,o}, E.J.W. Moyse¹⁰⁰,
 S. Muanza⁹⁹, J. Mueller¹³⁵, D. Muenstermann⁸⁷, G.A. Mullier⁹⁴, J.J. Mullin¹³³, D.P. Mungo^{66a,66b},
 J.L. Munoz Martinez¹², F.J. Munoz Sanchez⁹⁸, M. Murin⁹⁸, P. Murin^{26b}, W.J. Murray^{174,140},
 A. Murrone^{66a,66b}, J.M. Muse¹²⁵, M. Muškinja¹⁶, C. Mwewa²⁷, A.G. Myagkov^{120,ag}, A.A. Myers¹³⁵,
 G. Myers⁶³, J. Myers¹²⁸, M. Myska¹³⁸, B.P. Nachman¹⁶, O. Nackenhorst⁴⁵, A. Nag Nag⁴⁶, K. Nagai¹³¹,
 K. Nagano⁷⁹, J.L. Nagle²⁷, E. Nagy⁹⁹, A.M. Nairz³⁴, Y. Nakahama¹¹⁴, K. Nakamura⁷⁹, H. Nanjo¹²⁹,
 F. Napolitano^{59a}, R. Narayan⁴⁰, I. Naryshkin¹³⁴, M. Naseri³², C. Nass²², T. Naumann⁴⁴, G. Navarro^{20a},
 J. Navarro-Gonzalez¹⁷⁰, P.Y. Nechaeva¹⁰⁸, F. Nechansky⁴⁴, T.J. Neep¹⁹, A. Negri^{68a,68b}, M. Negrini^{21b},
 C. Nellist¹¹⁶, C. Nelson¹⁰¹, K. Nelson¹⁰³, M.E. Nelson^{43a,43b}, S. Nemecek¹³⁷, M. Nessi^{34,g},
 M.S. Neubauer¹⁶⁹, F. Neuhaus⁹⁷, J. Neundorff⁴⁴, R. Newhouse¹⁷¹, P.R. Newman¹⁹, C.W. Ng¹³⁵, Y.S. Ng¹⁷,
 Y.W.Y. Ng¹⁶⁷, B. Ngair^{33e}, H.D.N. Nguyen⁹⁹, T. Nguyen Manh¹⁰⁷, R.B. Nickerson¹³¹, R. Nicolaidou¹⁴¹,

D.S. Nielsen ³⁸, J. Nielsen ¹⁴², M. Niemeyer ⁵¹, N. Nikiporou ¹⁰, V. Nikolaenko ^{120,ag}, I. Nikolic-Audit ¹³², K. Nikolopoulos ¹⁹, P. Nilsson ²⁷, H.R. Nindhito ⁵², A. Nisati ^{70a}, N. Nishu ², R. Nisius ¹¹², T. Nitta ¹⁷⁵, T. Nobe ¹⁶⁰, D.L. Noel ³⁰, Y. Noguchi ⁸³, I. Nomidis ¹³², M.A. Nomura ²⁷, M.B. Norfolk ¹⁴⁶, R.R.B. Norisam ⁹², J. Novak ⁸⁹, T. Novak ⁴⁴, O. Novgorodova ⁴⁶, L. Novotny ¹³⁸, R. Novotny ¹¹⁵, L. Nozka ¹²⁷, K. Ntekas ¹⁶⁷, E. Nurse ⁹², F.G. Oakham ^{32,ak}, J. Ocariz ¹³², A. Ochi ⁸⁰, I. Ochoa ^{136a}, J.P. Ochoa-Ricoux ^{143a}, K. O'Connor ²⁴, S. Oda ⁸⁵, S. Odaka ⁷⁹, S. Oerdek ⁵¹, A. Ogrodnik ^{81a}, A. Oh ⁹⁸, C.C. Ohm ¹⁵¹, H. Oide ¹⁶¹, R. Oishi ¹⁶⁰, M.L. Ojeda ¹⁶³, Y. Okazaki ⁸³, M.W. O'Keefe ⁸⁸, Y. Okumura ¹⁶⁰, A. Olariu ^{25b}, L.F. Oleiro Seabra ^{136a}, S.A. Olivares Pino ^{143c}, D. Oliveira Damazio ²⁷, D. Oliveira Goncalves ^{78a}, J.L. Oliver ¹, M.J.R. Olsson ¹⁶⁷, A. Olszewski ⁸², J. Olszowska ⁸², Ö.O. Öncel ²², D.C. O'Neil ¹⁴⁹, A.P. O'Neill ¹³¹, A. Onofre ^{136a,136e}, P.U.E. Onyisi ¹⁰, H. Oppen ¹³⁰, R.G. Oreamuno Madriz ¹¹⁸, M.J. Oreglia ³⁵, G.E. Orellana ⁸⁶, D. Orestano ^{72a,72b}, N. Orlando ¹², R.S. Orr ¹⁶³, V. O'Shea ⁵⁵, R. Ospanov ^{58a}, G. Otero y Garzon ²⁸, H. Otono ⁸⁵, P.S. Ott ^{59a}, G.J. Ottino ¹⁶, M. Ouchrif ^{33d}, J. Ouellette ²⁷, F. Ould-Saada ¹³⁰, A. Ouraou ^{141,*}, Q. Ouyang ^{13a}, M. Owen ⁵⁵, R.E. Owen ¹⁴⁰, V.E. Ozcan ^{11c}, N. Ozturk ⁷, S. Ozturk ^{11c}, J. Pacalt ¹²⁷, H.A. Pacey ³⁰, K. Pachal ⁴⁷, A. Pacheco Pages ¹², C. Padilla Aranda ¹², S. Pagan Griso ¹⁶, G. Palacino ⁶³, S. Palazzo ⁴⁸, S. Palestini ³⁴, M. Palka ^{81b}, P. Palni ^{81a}, D.K. Panchal ¹⁰, C.E. Pandini ⁵², J.G. Panduro Vazquez ⁹¹, P. Pani ⁴⁴, G. Panizzo ^{64a,64c}, L. Paolozzi ⁵², C. Papadatos ¹⁰⁷, S. Parajuli ⁴⁰, A. Paramonov ⁵, C. Paraskevopoulos ⁹, D. Paredes Hernandez ^{60b}, S.R. Paredes Saenz ¹³¹, B. Parida ¹⁷⁶, T.H. Park ¹⁶³, A.J. Parker ²⁹, M.A. Parker ³⁰, F. Parodi ^{53b,53a}, E.W. Parrish ¹¹⁸, J.A. Parsons ³⁷, U. Parzefall ⁵⁰, L. Pascual Dominguez ¹⁵⁸, V.R. Pascuzzi ¹⁶, F. Pasquali ¹¹⁷, E. Pasqualucci ^{70a}, S. Passaggio ^{53b}, F. Pastore ⁹¹, P. Pasuwan ^{43a,43b}, J.R. Pater ⁹⁸, A. Pathak ¹⁷⁷, J. Patton ⁸⁸, T. Pauly ³⁴, J. Parkes ¹⁵⁰, M. Pedersen ¹³⁰, L. Pedraza Diaz ¹¹⁶, R. Pedro ^{136a}, T. Peiffer ⁵¹, S.V. Peleganchuk ^{119b,119a}, O. Penc ¹³⁷, C. Peng ^{60b}, H. Peng ^{58a}, M. Penzin ¹⁶², B.S. Peralva ^{78a}, M.M. Perego ⁶², A.P. Pereira Peixoto ^{136a}, L. Pereira Sanchez ^{43a,43b}, D.V. Perepelitsa ²⁷, E. Perez Codina ^{164a}, M. Perganti ⁹, L. Perini ^{66a,66b}, H. Pernegger ³⁴, S. Perrella ³⁴, A. Perrevoort ¹¹⁷, K. Peters ⁴⁴, R.F.Y. Peters ⁹⁸, B.A. Petersen ³⁴, T.C. Petersen ³⁸, E. Petit ⁹⁹, V. Petousis ¹³⁸, C. Petridou ¹⁵⁹, P. Petroff ⁶², F. Petrucci ^{72a,72b}, M. Pettee ¹⁷⁹, N.E. Pettersson ³⁴, K. Petukhova ¹³⁹, A. Peyaud ¹⁴¹, R. Pezoa ^{143d}, L. Pezzotti ^{68a,68b}, G. Pezzullo ¹⁷⁹, T. Pham ¹⁰², P.W. Phillips ¹⁴⁰, M.W. Phipps ¹⁶⁹, G. Piacquadio ¹⁵², E. Pianori ¹⁶, F. Piazza ^{66a,66b}, A. Picazio ¹⁰⁰, R. Piegai ²⁸, D. Pietreanu ^{25b}, J.E. Pilcher ³⁵, A.D. Pilkington ⁹⁸, M. Pinamonti ^{64a,64c}, J.L. Pinfold ², C. Pitman Donaldson ⁹², D.A. Pizzi ³², L. Pizzimento ^{71a,71b}, A. Pizzini ¹¹⁷, M.-A. Pleier ²⁷, V. Plesanovs ⁵⁰, V. Pleskot ¹³⁹, E. Plotnikova ⁷⁷, P. Podberezko ^{119b,119a}, R. Poettgen ⁹⁴, R. Poggi ⁵², L. Poggioli ¹³², I. Pogrebnyak ¹⁰⁴, D. Pohl ²², I. Pokharel ⁵¹, G. Polesello ^{68a}, A. Poley ^{149,164a}, A. Policicchio ^{70a,70b}, R. Polifka ¹³⁹, A. Polini ^{21b}, C.S. Pollard ⁴⁴, Z.B. Pollock ¹²⁴, V. Polychronakos ²⁷, D. Ponomarenko ¹⁰⁹, L. Pontecorvo ³⁴, S. Popa ^{25a}, G.A. Popeneciu ^{25d}, L. Portales ⁴, D.M. Portillo Quintero ⁵⁶, S. Pospisil ¹³⁸, P. Postolache ^{25c}, K. Potamianos ¹³¹, I.N. Potrap ⁷⁷, C.J. Potter ³⁰, H. Potti ¹, T. Poulsen ⁴⁴, J. Poveda ¹⁷⁰, T.D. Powell ¹⁴⁶, G. Pownall ⁴⁴, M.E. Pozo Astigarraga ³⁴, A. Prades Ibanez ¹⁷⁰, P. Pralavorio ⁹⁹, M.M. Prapa ⁴², S. Prell ⁷⁶, D. Price ⁹⁸, M. Primavera ^{65a}, M.A. Principe Martin ⁹⁶, M.L. Proffitt ¹⁴⁵, N. Proklova ¹⁰⁹, K. Prokofiev ^{60c}, F. Prokoshin ⁷⁷, S. Protopopescu ²⁷, J. Proudfoot ⁵, M. Przybycien ^{81a}, D. Pudzha ¹³⁴, P. Puzo ⁶², D. Pyatizbyantseva ¹⁰⁹, J. Qian ¹⁰³, Y. Qin ⁹⁸, A. Quadt ⁵¹, M. Queitsch-Maitland ³⁴, G. Rabanal Bolanos ⁵⁷, F. Ragusa ^{66a,66b}, G. Rahal ⁹⁵, J.A. Raine ⁵², S. Rajagopalan ²⁷, K. Ran ^{13a,13d}, D.F. Rassloff ^{59a}, D.M. Rauch ⁴⁴, S. Rave ⁹⁷, B. Ravina ⁵⁵, I. Ravinovich ¹⁷⁶, M. Raymond ³⁴, A.L. Read ¹³⁰, N.P. Readioff ¹⁴⁶, D.M. Rebuszi ^{68a,68b}, G. Redlinger ²⁷, K. Reeves ⁴¹, D. Reikher ¹⁵⁸, A. Reiss ⁹⁷, A. Rej ¹⁴⁸, C. Rembser ³⁴, A. Renardi ⁴⁴, M. Renda ^{25b}, M.B. Rendel ¹¹², A.G. Rennie ⁵⁵, S. Resconi ^{66a}, E.D. Resseguie ¹⁶, S. Rettie ⁹², B. Reynolds ¹²⁴, E. Reynolds ¹⁹, M. Rezaei Estabragh ¹⁷⁸, O.L. Rezanova ^{119b,119a}, P. Reznicek ¹³⁹, E. Ricci ^{73a,73b}, R. Richter ¹¹², S. Richter ⁴⁴, E. Richter-Was ^{81b}, M. Ridel ¹³², P. Rieck ¹¹², P. Riedler ³⁴, O. Rifki ⁴⁴, M. Rijssenbeek ¹⁵², A. Rimoldi ^{68a,68b}, M. Rimoldi ⁴⁴, L. Rinaldi ^{21b,21a}, T.T. Rinn ¹⁶⁹, M.P. Rinnagel ¹¹¹, G. Ripellino ¹⁵¹, I. Riu ¹², P. Rivadeneira ⁴⁴, J.C. Rivera Vergara ¹⁷², F. Rizatdinova ¹²⁶, E. Rizvi ⁹⁰, C. Rizzi ⁵², B.A. Roberts ¹⁷⁴, S.H. Robertson ^{101,aa}, M. Robin ⁴⁴, D. Robinson ³⁰, C.M. Robles Gajardo ^{143d}, M. Robles Manzano ⁹⁷, A. Robson ⁵⁵, A. Rocchi ^{71a,71b}, C. Roda ^{69a,69b}, S. Rodriguez Bosca ^{59a}, A. Rodriguez Rodriguez ⁵⁰, A.M. Rodríguez Vera ^{164b}, S. Roe ³⁴, J. Roggel ¹⁷⁸, O. Røhne ¹³⁰, R.A. Rojas ^{143d}, B. Roland ⁵⁰, C.P.A. Roland ⁶³, J. Roloff ²⁷, A. Romaniouk ¹⁰⁹, M. Romano ^{21b}, N. Rompotis ⁸⁸, M. Ronzani ¹²², L. Roos ¹³², S. Rosati ^{70a}, G. Rosin ¹⁰⁰, B.J. Rosser ¹³³, E. Rossi ¹⁶³, E. Rossi ⁴, E. Rossi ^{67a,67b}, L.P. Rossi ^{53b}, L. Rossini ⁴⁴, R. Rosten ¹²⁴, M. Rotaru ^{25b}, B. Rottler ⁵⁰, D. Rousseau ⁶², D. Rousso ³⁰,

G. Rovelli ^{68a,68b}, A. Roy ¹⁰, A. Rozanov ⁹⁹, Y. Rozen ¹⁵⁷, X. Ruan ^{31e}, A.J. Ruby ⁸⁸, T.A. Ruggeri ¹, F. Rühr ⁵⁰, A. Ruiz-Martinez ¹⁷⁰, A. Rummler ³⁴, Z. Rurikova ⁵⁰, N.A. Rusakovich ⁷⁷, H.L. Russell ³⁴, L. Rustige ³⁶, J.P. Rutherford ⁶, E.M. Rüttinger ¹⁴⁶, M. Rybar ¹³⁹, E.B. Rye ¹³⁰, A. Ryzhov ¹²⁰, J.A. Sabater Iglesias ⁴⁴, P. Sabatini ¹⁷⁰, L. Sabetta ^{70a,70b}, H.F.-W. Sadrozinski ¹⁴², R. Sadykov ⁷⁷, F. Safai Tehrani ^{70a}, B. Safarzadeh Samani ¹⁵³, M. Safdari ¹⁵⁰, P. Saha ¹¹⁸, S. Saha ¹⁰¹, M. Sahinsoy ¹¹², A. Sahu ¹⁷⁸, M. Saimpert ¹⁴¹, M. Saito ¹⁶⁰, T. Saito ¹⁶⁰, D. Salamani ⁵², G. Salamanna ^{72a,72b}, A. Salnikov ¹⁵⁰, J. Salt ¹⁷⁰, A. Salvador Salas ¹², D. Salvatore ^{39b,39a}, F. Salvatore ¹⁵³, A. Salzburger ³⁴, D. Sammel ⁵⁰, D. Sampsonidis ¹⁵⁹, D. Sampsonidou ^{58d,58c}, J. Sánchez ¹⁷⁰, A. Sanchez Pineda ⁴, V. Sanchez Sebastian ¹⁷⁰, H. Sandaker ¹³⁰, C.O. Sander ⁴⁴, I.G. Sanderswood ⁸⁷, J.A. Sandesara ¹⁰⁰, M. Sandhoff ¹⁷⁸, C. Sandoval ^{20b}, D.P.C. Sankey ¹⁴⁰, M. Sannino ^{53b,53a}, Y. Sano ¹¹⁴, A. Sansoni ⁴⁹, C. Santoni ³⁶, H. Santos ^{136a,136b}, S.N. Santpur ¹⁶, A. Santra ¹⁷⁶, K.A. Saoucha ¹⁴⁶, A. Saponov ⁷⁷, J.G. Saraiva ^{136a,136d}, J. Sardain ⁹⁹, O. Sasaki ⁷⁹, K. Sato ¹⁶⁵, C. Sauer ^{59b}, F. Sauerburger ⁵⁰, E. Sauvan ⁴, P. Savard ^{163,ak}, R. Sawada ¹⁶⁰, C. Sawyer ¹⁴⁰, L. Sawyer ⁹³, I. Sayago Galvan ¹⁷⁰, C. Sbarra ^{21b}, A. Sbrizzi ^{64a,64c}, T. Scanlon ⁹², J. Schaarschmidt ¹⁴⁵, P. Schacht ¹¹², D. Schaefer ³⁵, L. Schaefer ¹³³, U. Schäfer ⁹⁷, A.C. Schaffer ⁶², D. Schaile ¹¹¹, R.D. Schamberger ¹⁵², E. Schanet ¹¹¹, C. Scharf ¹⁷, N. Scharmberg ⁹⁸, V.A. Schegelsky ¹³⁴, D. Scheirich ¹³⁹, F. Schenck ¹⁷, M. Schernau ¹⁶⁷, C. Schiavi ^{53b,53a}, L.K. Schildgen ²², Z.M. Schillaci ²⁴, E.J. Schioppa ^{65a,65b}, M. Schioppa ^{39b,39a}, B. Schlag ⁹⁷, K.E. Schleicher ⁵⁰, S. Schlenker ³⁴, K. Schmieden ⁹⁷, C. Schmitt ⁹⁷, S. Schmitt ⁴⁴, L. Schoeffel ¹⁴¹, A. Schoening ^{59b}, P.G. Scholer ⁵⁰, E. Schopf ¹³¹, M. Schott ⁹⁷, J. Schovancova ³⁴, S. Schramm ⁵², F. Schroeder ¹⁷⁸, H.-C. Schultz-Coulon ^{59a}, M. Schumacher ⁵⁰, B.A. Schumm ¹⁴², Ph. Schune ¹⁴¹, A. Schwartzman ¹⁵⁰, T.A. Schwarz ¹⁰³, Ph. Schwemling ¹⁴¹, R. Schwienhorst ¹⁰⁴, A. Sciandra ¹⁴², G. Sciolla ²⁴, F. Scuri ^{69a}, F. Scutti ¹⁰², C.D. Sebastiani ⁸⁸, K. Sedlaczek ⁴⁵, P. Seema ¹⁷, S.C. Seidel ¹¹⁵, A. Seiden ¹⁴², B.D. Seidlitz ²⁷, T. Seiss ³⁵, C. Seitz ⁴⁴, J.M. Seixas ^{78b}, G. Sekhniaidze ^{67a}, S.J. Sekula ⁴⁰, L.P. Selem ⁴, N. Semprini-Cesari ^{21b,21a}, S. Sen ⁴⁷, C. Serfon ²⁷, L. Serin ⁶², L. Serkin ^{64a,64b}, M. Sessa ^{58a}, H. Severini ¹²⁵, S. Sevova ¹⁵⁰, F. Sforza ^{53b,53a}, A. Sfyrla ⁵², E. Shabalina ⁵¹, R. Shaheen ¹⁵¹, J.D. Shahinian ¹³³, N.W. Shaikh ^{43a,43b}, D. Shaked Renous ¹⁷⁶, L.Y. Shan ^{13a}, M. Shapiro ¹⁶, A. Sharma ³⁴, A.S. Sharma ¹, S. Sharma ⁴⁴, P.B. Shatalov ¹²¹, K. Shaw ¹⁵³, S.M. Shaw ⁹⁸, P. Sherwood ⁹², L. Shi ⁹², C.O. Shimmin ¹⁷⁹, Y. Shimogama ¹⁷⁵, M. Shimojima ¹¹³, J.D. Shinner ⁹¹, I.P.J. Shipsey ¹³¹, S. Shirabe ⁵², M. Shiyakova ⁷⁷, J. Shlomi ¹⁷⁶, M.J. Shochet ³⁵, J. Shojaii ¹⁰², D.R. Shope ¹⁵¹, S. Shrestha ¹²⁴, E.M. Shrif ^{31e}, M.J. Shroff ¹⁷², E. Shulga ¹⁷⁶, P. Sicho ¹³⁷, A.M. Sickles ¹⁶⁹, E. Sideras Haddad ^{31e}, O. Sidiropoulou ³⁴, A. Sidoti ^{21b}, F. Siegert ⁴⁶, Dj. Sijacki ¹⁴, M.V. Silva Oliveira ³⁴, S.B. Silverstein ^{43a}, S. Simion ⁶², R. Simoniello ³⁴, S. Simsek ^{11b}, P. Sinervo ¹⁶³, V. Sinetckii ¹¹⁰, S. Singh ¹⁴⁹, S. Sinha ⁴⁴, S. Sinha ^{31e}, M. Sioli ^{21b,21a}, I. Siral ¹²⁸, S.Yu. Sivoklokov ¹¹⁰, J. Sjölin ^{43a,43b}, A. Skaf ⁵¹, E. Skorda ⁹⁴, P. Skubic ¹²⁵, M. Slawinska ⁸², K. Sliwa ¹⁶⁶, V. Smakhtin ¹⁷⁶, B.H. Smart ¹⁴⁰, J. Smiesko ¹³⁹, S.Yu. Smirnov ¹⁰⁹, Y. Smirnov ¹⁰⁹, L.N. Smirnova ^{110,s}, O. Smirnova ⁹⁴, E.A. Smith ³⁵, H.A. Smith ¹³¹, M. Smizanska ⁸⁷, K. Smolek ¹³⁸, A. Smykiewicz ⁸², A.A. Snesarev ¹⁰⁸, H.L. Snoek ¹¹⁷, S. Snyder ²⁷, R. Sobie ^{172,aa}, A. Soffer ¹⁵⁸, F. Sohns ⁵¹, C.A. Solans Sanchez ³⁴, E.Yu. Soldatov ¹⁰⁹, U. Soldevila ¹⁷⁰, A.A. Solodkov ¹²⁰, S. Solomon ⁵⁰, A. Soloshenko ⁷⁷, O.V. Solovyanov ¹²⁰, V. Solovyev ¹³⁴, P. Sommer ¹⁴⁶, H. Son ¹⁶⁶, A. Sonay ¹², W.Y. Song ^{164b}, A. Sopczak ¹³⁸, A.L. Sapiro ⁹², F. Sopkova ^{26b}, S. Sottocornola ^{68a,68b}, R. Soualah ^{64a,64c}, A.M. Soukharev ^{119b,119a}, Z. Soumami ^{33e}, D. South ⁴⁴, S. Spagnolo ^{65a,65b}, M. Spalla ¹¹², M. Spangenberg ¹⁷⁴, F. Spanò ⁹¹, D. Sperlich ⁵⁰, T.M. Spieker ^{59a}, G. Spigo ³⁴, M. Spina ¹⁵³, D.P. Spiteri ⁵⁵, M. Spousta ¹³⁹, A. Stabile ^{66a,66b}, B.L. Stamas ¹¹⁸, R. Stamen ^{59a}, M. Stamenkovic ¹¹⁷, A. Stampekis ¹⁹, M. Standke ²², E. Stanecka ⁸², B. Stanislaus ³⁴, M.M. Stanitzki ⁴⁴, M. Stankaityte ¹³¹, B. Stapf ⁴⁴, E.A. Starchenko ¹²⁰, G.H. Stark ¹⁴², J. Stark ⁹⁹, D.M. Starke ^{164b}, P. Staroba ¹³⁷, P. Starovoitov ^{59a}, S. Stärz ¹⁰¹, R. Staszewski ⁸², G. Stavropoulos ⁴², P. Steinberg ²⁷, A.L. Steinhebel ¹²⁸, B. Stelzer ^{149,164a}, H.J. Stelzer ¹³⁵, O. Stelzer-Chilton ^{164a}, H. Stenzel ⁵⁴, T.J. Stevenson ¹⁵³, G.A. Stewart ³⁴, M.C. Stockton ³⁴, G. Stoicea ^{25b}, M. Stolarski ^{136a}, S. Stonjek ¹¹², A. Straessner ⁴⁶, J. Strandberg ¹⁵¹, S. Strandberg ^{43a,43b}, M. Strauss ¹²⁵, T. Strebler ⁹⁹, P. Strizeneč ^{26b}, R. Ströhmer ¹⁷³, D.M. Strom ¹²⁸, L.R. Strom ⁴⁴, R. Stroynowski ⁴⁰, A. Strubig ^{43a,43b}, S.A. Stucci ²⁷, B. Stugu ¹⁵, J. Stupak ¹²⁵, N.A. Styles ⁴⁴, D. Su ¹⁵⁰, S. Su ^{58a}, W. Su ^{58d,145,58c}, X. Su ^{58a}, N.B. Suarez ¹³⁵, K. Sugizaki ¹⁶⁰, V.V. Sulin ¹⁰⁸, M.J. Sullivan ⁸⁸, D.M.S. Sultan ⁵², S. Sultansoy ^{3c}, T. Sumida ⁸³, S. Sun ¹⁰³, S. Sun ¹⁷⁷, X. Sun ⁹⁸, O. Sunneborn Gudnadottir ¹⁶⁸, C.J.E. Suster ¹⁵⁴, M.R. Sutton ¹⁵³, M. Svatos ¹³⁷, M. Swiatlowski ^{164a}, T. Swirski ¹⁷³, I. Sykora ^{26a}, M. Sykora ¹³⁹, T. Sykora ¹³⁹, D. Ta ⁹⁷, K. Tackmann ^{44,y}, A. Taffard ¹⁶⁷, R. Tafirout ^{164a}, E. Tagiev ¹²⁰, R.H.M. Taibah ¹³², R. Takashima ⁸⁴, K. Takeda ⁸⁰, T. Takeshita ¹⁴⁷, E.P. Takeva ⁴⁸, Y. Takubo ⁷⁹, M. Talby ⁹⁹,

A.A. Talyshv^{119b,119a}, K.C. Tam^{60b}, N.M. Tamir¹⁵⁸, A. Tanaka¹⁶⁰, J. Tanaka¹⁶⁰, R. Tanaka⁶², Z. Tao¹⁷¹,
 S. Tapia Araya⁷⁶, S. Tapprogge⁹⁷, A. Tarek Abouelfadl Mohamed¹⁰⁴, S. Tarem¹⁵⁷, K. Tariq^{58b},
 G. Tarna^{25b,f}, G.F. Tartarelli^{66a}, P. Tas¹³⁹, M. Tasevsky¹³⁷, E. Tassi^{39b,39a}, G. Tateno¹⁶⁰, Y. Tayalati^{33e},
 G.N. Taylor¹⁰², W. Taylor^{164b}, H. Teagle⁸⁸, A.S. Tee⁸⁷, R. Teixeira De Lima¹⁵⁰, P. Teixeira-Dias⁹¹,
 H. Ten Kate³⁴, J.J. Teoh¹¹⁷, K. Terashi¹⁶⁰, J. Terron⁹⁶, S. Terzo¹², M. Testa⁴⁹, R.J. Teuscher^{163,aa},
 N. Themistokleous⁴⁸, T. Theveneaux-Pelzer¹⁷, D.W. Thomas⁹¹, J.P. Thomas¹⁹, E.A. Thompson⁴⁴,
 P.D. Thompson¹⁹, E. Thomson¹³³, E.J. Thorpe⁹⁰, Y. Tian⁵¹, V.O. Tikhomirov^{108,ah},
 Yu.A. Tikhonov^{119b,119a}, S. Timoshenko¹⁰⁹, P. Tipton¹⁷⁹, S. Tisserant⁹⁹, S.H. Tlou^{31e}, A. Tnourji³⁶,
 K. Todome^{21b,21a}, S. Todorova-Nova¹³⁹, S. Todt⁴⁶, M. Togawa⁷⁹, J. Tojo⁸⁵, S. Tokár^{26a}, K. Tokushuku⁷⁹,
 E. Tolley¹²⁴, R. Tombs³⁰, M. Tomoto^{79,114}, L. Tompkins¹⁵⁰, P. Tornambe¹⁰⁰, E. Torrence¹²⁸, H. Torres⁴⁶,
 E. Torrò Pastor¹⁷⁰, M. Toscani²⁸, C. Tosciri³⁵, J. Toth^{99,z}, D.R. Tovey¹⁴⁶, A. Traeet¹⁵, C.J. Treado¹²²,
 T. Trefzger¹⁷³, A. Tricoli²⁷, I.M. Trigger^{164a}, S. Trincaz-Duvoud¹³², D.A. Trischuk¹⁷¹, W. Trischuk¹⁶³,
 B. Trocme⁵⁶, A. Trofymov⁶², C. Troncon^{66a}, F. Trovato¹⁵³, L. Truong^{31c}, M. Trzebinski⁸², A. Trzuppek⁸²,
 F. Tsai¹⁵², A. Tsiamis¹⁵⁹, P.V. Tsiarehshka^{105,af}, A. Tsigotis^{159,w}, V. Tsiskaridze¹⁵², E.G. Tskhadadze^{156a},
 M. Tsopoulou¹⁵⁹, I.I. Tsukerman¹²¹, V. Tsulaia¹⁶, S. Tsuno⁷⁹, O. Tsur¹⁵⁷, D. Tsybychev¹⁵², Y. Tu^{60b},
 A. Tudorache^{25b}, V. Tudorache^{25b}, A.N. Tuna³⁴, S. Turchikhin⁷⁷, D. Turgeman¹⁷⁶, I. Turk Cakir^{3b,u},
 R.J. Turner¹⁹, R. Turra^{66a}, P.M. Tuts³⁷, S. Tzamarias¹⁵⁹, P. Tzanis⁹, E. Tzovara⁹⁷, K. Uchida¹⁶⁰,
 F. Ukegawa¹⁶⁵, G. Unal³⁴, M. Unal¹⁰, A. Undrus²⁷, G. Unel¹⁶⁷, F.C. Ungaro¹⁰², K. Uno¹⁶⁰, J. Urban^{26b},
 P. Urquijo¹⁰², G. Usai⁷, R. Ushioda¹⁶¹, Z. Uysal^{11d}, V. Vacek¹³⁸, B. Vachon¹⁰¹, K.O.H. Vadla¹³⁰,
 T. Vafeiadis³⁴, C. Valderanis¹¹¹, E. Valdes Santurio^{43a,43b}, M. Valente^{164a}, S. Valentinetti^{21b,21a},
 A. Valero¹⁷⁰, L. Valéry⁴⁴, R.A. Vallance¹⁹, A. Vallier⁹⁹, J.A. Valls Ferrer¹⁷⁰, T.R. Van Daalen¹²,
 P. Van Gemmeren⁵, S. Van Stroud⁹², I. Van Vulpen¹¹⁷, M. Vanadia^{71a,71b}, W. Vandelli³⁴,
 M. Vandenbroucke¹⁴¹, E.R. Vandewall¹²⁶, D. Vannicola^{70a,70b}, L. Vannoli^{53b,53a}, R. Vari^{70a},
 E.W. Varnes⁶, C. Varni^{53b,53a}, T. Varol¹⁵⁵, D. Varouchas⁶², K.E. Varvell¹⁵⁴, M.E. Vasile^{25b}, L. Vaslin³⁶,
 G.A. Vasquez¹⁷², F. Vazeille³⁶, D. Vazquez Furelos¹², T. Vazquez Schroeder³⁴, J. Veatch⁵¹, V. Vecchio⁹⁸,
 M.J. Veen¹¹⁷, I. Veliscek¹³¹, L.M. Veloce¹⁶³, F. Veloso^{136a,136c}, S. Veneziano^{70a}, A. Ventura^{65a,65b},
 A. Verbytskyi¹¹², M. Verducci^{69a,69b}, C. Vergis²², M. Verissimo De Araujo^{78b}, W. Verkerke¹¹⁷,
 A.T. Vermeulen¹¹⁷, J.C. Vermeulen¹¹⁷, C. Vernieri¹⁵⁰, P.J. Verschuuren⁹¹, M.L. Vesterbacka¹²²,
 M.C. Vetterli^{149,ak}, N. Viaux Maira^{143d}, T. Vickey¹⁴⁶, O.E. Vickey Boeriu¹⁴⁶, G.H.A. Viehhauser¹³¹,
 L. Vignani^{59b}, M. Villa^{21b,21a}, M. Villaplana Perez¹⁷⁰, E.M. Villhauer⁴⁸, E. Vilucchi⁴⁹, M.G. Vincker³²,
 G.S. Virdee¹⁹, A. Vishwakarma⁴⁸, C. Vittori^{21b,21a}, I. Vivarelli¹⁵³, V. Vladimirov¹⁷⁴, E. Voevodina¹¹²,
 M. Vogel¹⁷⁸, P. Vokac¹³⁸, J. Von Ahnen⁴⁴, S.E. von Buddenbrock^{31e}, E. Von Toerne²², V. Vorobel¹³⁹,
 K. Vorobev¹⁰⁹, M. Vos¹⁷⁰, J.H. Vosseveld⁸⁸, M. Vozak⁹⁸, N. Vranjes¹⁴, M. Vranjes Milosavljevic¹⁴,
 V. Vrba^{138,*}, M. Vreeswijk¹¹⁷, N.K. Vu⁹⁹, R. Vuillermet³⁴, I. Vukotic³⁵, S. Wada¹⁶⁵, C. Wagner¹⁰⁰,
 P. Wagner²², W. Wagner¹⁷⁸, S. Wahdan¹⁷⁸, H. Wahlberg⁸⁶, R. Wakasa¹⁶⁵, M. Wakida¹¹⁴,
 V.M. Walbrecht¹¹², J. Walder¹⁴⁰, R. Walker¹¹¹, S.D. Walker⁹¹, W. Walkowiak¹⁴⁸, A.M. Wang⁵⁷,
 A.Z. Wang¹⁷⁷, C. Wang^{58a}, C. Wang^{58c}, H. Wang¹⁶, J. Wang^{60a}, P. Wang⁴⁰, R.-J. Wang⁹⁷, R. Wang⁵⁷,
 R. Wang¹¹⁸, S.M. Wang¹⁵⁵, S. Wang^{58b}, T. Wang^{58a}, W.T. Wang^{58a}, W.X. Wang^{58a}, X. Wang¹⁶⁹,
 Y. Wang^{58a}, Z. Wang¹⁰³, C. Wanotayaroj³⁴, A. Warburton¹⁰¹, C.P. Ward³⁰, R.J. Ward¹⁹, N. Warrack⁵⁵,
 A.T. Watson¹⁹, M.F. Watson¹⁹, G. Watts¹⁴⁵, B.M. Waugh⁹², A.F. Webb¹⁰, C. Weber²⁷, M.S. Weber¹⁸,
 S.A. Weber³², S.M. Weber^{59a}, C. Wei^{58a}, Y. Wei¹³¹, A.R. Weidberg¹³¹, J. Weingarten⁴⁵, M. Weirich⁹⁷,
 C. Weiser⁵⁰, T. Wenaus²⁷, B. Wendland⁴⁵, T. Wengler³⁴, S. Wenig³⁴, N. Vermes²², M. Wessels^{59a},
 K. Whalen¹²⁸, A.M. Wharton⁸⁷, A.S. White⁵⁷, A. White⁷, M.J. White¹, D. Whiteson¹⁶⁷,
 W. Wiedenmann¹⁷⁷, C. Wiel⁴⁶, M. Wielers¹⁴⁰, N. Wieseotte⁹⁷, C. Wiglesworth³⁸, L.A.M. Wiik-Fuchs⁵⁰,
 D.J. Wilbern¹²⁵, H.G. Wilkens³⁴, L.J. Wilkins⁹¹, D.M. Williams³⁷, H.H. Williams¹³³, S. Williams³⁰,
 S. Willocq¹⁰⁰, P.J. Windischhofer¹³¹, I. Wingerter-Seez⁴, F. Winklmeier¹²⁸, B.T. Winter⁵⁰,
 M. Wittgen¹⁵⁰, M. Wobisch⁹³, A. Wolf⁹⁷, R. Wölker¹³¹, J. Wollrath¹⁶⁷, M.W. Wolter⁸²,
 H. Wolters^{136a,136c}, V.W.S. Wong¹⁷¹, A.F. Wongel⁴⁴, S.D. Worm⁴⁴, B.K. Wosiek⁸², K.W. Woźniak⁸²,
 K. Wraight⁵⁵, J. Wu^{13a,13d}, S.L. Wu¹⁷⁷, X. Wu⁵², Y. Wu^{58a}, Z. Wu^{141,58a}, J. Wuerzinger¹³¹, T.R. Wyatt⁹⁸,
 B.M. Wynne⁴⁸, S. Xella³⁸, J. Xiang^{60c}, X. Xiao¹⁰³, X. Xie^{58a}, I. Xiotidis¹⁵³, D. Xu^{13a}, H. Xu^{58a}, H. Xu^{58a},
 L. Xu^{58a}, R. Xu¹³³, T. Xu^{58a}, W. Xu¹⁰³, Y. Xu^{13b}, Z. Xu^{58b}, Z. Xu¹⁵⁰, B. Yabsley¹⁵⁴, S. Yacoob^{31a},
 N. Yamaguchi⁸⁵, Y. Yamaguchi¹⁶¹, M. Yamatani¹⁶⁰, H. Yamauchi¹⁶⁵, T. Yamazaki¹⁶, Y. Yamazaki⁸⁰,
 J. Yan^{58c}, Z. Yan²³, H.J. Yang^{58c,58d}, H.T. Yang¹⁶, S. Yang^{58a}, T. Yang^{60c}, X. Yang^{58a}, X. Yang^{13a},

Y. Yang¹⁶⁰, Z. Yang^{103,58a}, W.-M. Yao¹⁶, Y.C. Yap⁴⁴, H. Ye^{13c}, J. Ye⁴⁰, S. Ye²⁷, I. Yeletsikh⁷⁷,
M.R. Yexley⁸⁷, P. Yin³⁷, K. Yorita¹⁷⁵, K. Yoshihara⁷⁶, C.J.S. Young³⁴, C. Young¹⁵⁰, R. Yuan^{58b,j}, X. Yue^{59a},
M. Zaazoua^{33e}, B. Zabinski⁸², G. Zacharis⁹, E. Zaffaroni⁵², A.M. Zaitsev^{120,ag}, T. Zakareishvili^{156b},
N. Zakharchuk³², S. Zambito³⁴, D. Zanzi⁵⁰, S.V. Zeißner⁴⁵, C. Zeitnitz¹⁷⁸, G. Zemaityte¹³¹, J.C. Zeng¹⁶⁹,
O. Zenin¹²⁰, T. Ženiš^{26a}, S. Zenz⁹⁰, S. Zerradi^{33a}, D. Zerwas⁶², M. Zgubič¹³¹, B. Zhang^{13c}, D.F. Zhang^{13b},
G. Zhang^{13b}, J. Zhang⁵, K. Zhang^{13a}, L. Zhang^{13c}, M. Zhang¹⁶⁹, R. Zhang¹⁷⁷, S. Zhang¹⁰³, X. Zhang^{58c},
X. Zhang^{58b}, Z. Zhang⁶², P. Zhao⁴⁷, Y. Zhao¹⁴², Z. Zhao^{58a}, A. Zhemchugov⁷⁷, Z. Zheng¹⁰³, D. Zhong¹⁶⁹,
B. Zhou¹⁰³, C. Zhou¹⁷⁷, H. Zhou⁶, N. Zhou^{58c}, Y. Zhou⁶, C.G. Zhu^{58b}, C. Zhu^{13a,13d}, H.L. Zhu^{58a},
H. Zhu^{13a}, J. Zhu¹⁰³, Y. Zhu^{58a}, X. Zhuang^{13a}, K. Zhukov¹⁰⁸, V. Zhulanov^{119b,119a}, D. Zieminska⁶³,
N.I. Zimine⁷⁷, S. Zimmermann^{50,*}, M. Ziolkowski¹⁴⁸, L. Živković¹⁴, A. Zoccoli^{21b,21a}, K. Zoch⁵²,
T.G. Zorbas¹⁴⁶, O. Zormpa⁴², W. Zou³⁷, L. Zwalinski³⁴

¹ Department of Physics, University of Adelaide, Adelaide, Australia

² Department of Physics, University of Alberta, Edmonton AB, Canada

³ (a) Department of Physics, Ankara University, Ankara; (b) Istanbul Aydın University, Application and Research Center for Advanced Studies, Istanbul; (c) Division of Physics, TOBB University of Economics and Technology, Ankara, Turkey

⁴ LAPP, Univ. Savoie Mont Blanc, CNRS/IN2P3, Annecy, France

⁵ High Energy Physics Division, Argonne National Laboratory, Argonne IL, United States of America

⁶ Department of Physics, University of Arizona, Tucson AZ, United States of America

⁷ Department of Physics, University of Texas at Arlington, Arlington TX, United States of America

⁸ Physics Department, National and Kapodistrian University of Athens, Athens, Greece

⁹ Physics Department, National Technical University of Athens, Zografou, Greece

¹⁰ Department of Physics, University of Texas at Austin, Austin TX, United States of America

¹¹ (a) Bahcesehir University, Faculty of Engineering and Natural Sciences, Istanbul; (b) Istanbul Bilgi University, Faculty of Engineering and Natural Sciences, Istanbul; (c) Department of Physics, Bogazici University, Istanbul; (d) Department of Physics Engineering, Gaziantep University, Gaziantep, Turkey

¹² Institut de Física d'Altes Energies (IFAE), Barcelona Institute of Science and Technology, Barcelona, Spain

¹³ (a) Institute of High Energy Physics, Chinese Academy of Sciences, Beijing; (b) Physics Department, Tsinghua University, Beijing; (c) Department of Physics, Nanjing University, Nanjing;

(d) University of Chinese Academy of Science (UCAS), Beijing, China

¹⁴ Institute of Physics, University of Belgrade, Belgrade, Serbia

¹⁵ Department for Physics and Technology, University of Bergen, Bergen, Norway

¹⁶ Physics Division, Lawrence Berkeley National Laboratory and University of California, Berkeley CA, United States of America

¹⁷ Institut für Physik, Humboldt Universität zu Berlin, Berlin, Germany

¹⁸ Albert Einstein Center for Fundamental Physics and Laboratory for High Energy Physics, University of Bern, Bern, Switzerland

¹⁹ School of Physics and Astronomy, University of Birmingham, Birmingham, United Kingdom

²⁰ (a) Facultad de Ciencias y Centro de Investigaciones, Universidad Antonio Nariño, Bogotá; (b) Departamento de Física, Universidad Nacional de Colombia, Bogotá, Colombia

²¹ (a) Dipartimento di Fisica e Astronomia A. Righi, Università di Bologna, Bologna; (b) INFN Sezione di Bologna, Italy

²² Physikalisches Institut, Universität Bonn, Bonn, Germany

²³ Department of Physics, Boston University, Boston MA, United States of America

²⁴ Department of Physics, Brandeis University, Waltham MA, United States of America

²⁵ (a) Transilvania University of Brasov, Brasov; (b) Horia Hulubei National Institute of Physics and Nuclear Engineering, Bucharest; (c) Department of Physics, Alexandru Ioan Cuza University of Iasi, Iasi; (d) National Institute for Research and Development of Isotopic and Molecular Technologies, Physics Department, Cluj-Napoca; (e) University Politehnica Bucharest, Bucharest; (f) West University in Timisoara, Timisoara, Romania

²⁶ (a) Faculty of Mathematics, Physics and Informatics, Comenius University, Bratislava; (b) Department of Subnuclear Physics, Institute of Experimental Physics of the Slovak Academy of Sciences, Kosice, Slovak Republic

²⁷ Physics Department, Brookhaven National Laboratory, Upton NY, United States of America

²⁸ Departamento de Física (FCEN) and IFIBA, Universidad de Buenos Aires and CONICET, Buenos Aires, Argentina

²⁹ California State University, CA, United States of America

³⁰ Cavendish Laboratory, University of Cambridge, Cambridge, United Kingdom

³¹ (a) Department of Physics, University of Cape Town, Cape Town; (b) iThema Labs, Western Cape; (c) Department of Mechanical Engineering Science, University of Johannesburg, Johannesburg; (d) University of South Africa, Department of Physics, Pretoria; (e) School of Physics, University of the Witwatersrand, Johannesburg, South Africa

³² Department of Physics, Carleton University, Ottawa ON, Canada

³³ (a) Faculté des Sciences Ain Chock, Réseau Universitaire de Physique des Hautes Energies - Université Hassan II, Casablanca; (b) Faculté des Sciences, Université Ibn-Tofail, Kénitra;

(c) Faculté des Sciences Semlalia, Université Cadi Ayyad, LPHEA-Marrakech; (d) LPMR, Faculté des Sciences, Université Mohamed Premier, Oujda; (e) Faculté des sciences, Université Mohammed V, Rabat, Morocco

³⁴ CERN, Geneva, Switzerland

³⁵ Enrico Fermi Institute, University of Chicago, Chicago IL, United States of America

³⁶ LPC, Université Clermont Auvergne, CNRS/IN2P3, Clermont-Ferrand, France

³⁷ Nevis Laboratory, Columbia University, Irvington NY, United States of America

³⁸ Niels Bohr Institute, University of Copenhagen, Copenhagen, Denmark

³⁹ (a) Dipartimento di Fisica, Università della Calabria, Rende; (b) INFN Gruppo Collegato di Cosenza, Laboratori Nazionali di Frascati, Italy

⁴⁰ Physics Department, Southern Methodist University, Dallas TX, United States of America

⁴¹ Physics Department, University of Texas at Dallas, Richardson TX, United States of America

⁴² National Centre for Scientific Research "Demokritos", Agia Paraskevi, Greece

⁴³ (a) Department of Physics, Stockholm University; (b) Oskar Klein Centre, Stockholm, Sweden

⁴⁴ Deutsches Elektronen-Synchrotron DESY, Hamburg and Zeuthen, Germany

⁴⁵ Lehrstuhl für Experimentelle Physik IV, Technische Universität Dortmund, Dortmund, Germany

⁴⁶ Institut für Kern- und Teilchenphysik, Technische Universität Dresden, Dresden, Germany

⁴⁷ Department of Physics, Duke University, Durham NC, United States of America

⁴⁸ SUPA - School of Physics and Astronomy, University of Edinburgh, Edinburgh, United Kingdom

⁴⁹ INFN e Laboratori Nazionali di Frascati, Frascati, Italy

⁵⁰ Physikalisches Institut, Albert-Ludwigs-Universität Freiburg, Freiburg, Germany

⁵¹ II. Physikalisches Institut, Georg-August-Universität Göttingen, Göttingen, Germany

⁵² Département de Physique Nucléaire et Corpusculaire, Université de Genève, Genève, Switzerland

⁵³ (a) Dipartimento di Fisica, Università di Genova, Genova; (b) INFN Sezione di Genova, Italy

⁵⁴ II. Physikalisches Institut, Justus-Liebig-Universität Giessen, Giessen, Germany

- 55 SUPA - School of Physics and Astronomy, University of Glasgow, Glasgow, United Kingdom
- 56 LPSC, Université Grenoble Alpes, CNRS/IN2P3, Grenoble INP, Grenoble, France
- 57 Laboratory for Particle Physics and Cosmology, Harvard University, Cambridge MA, United States of America
- 58 (a) Department of Modern Physics and State Key Laboratory of Particle Detection and Electronics, University of Science and Technology of China, Hefei; (b) Institute of Frontier and Interdisciplinary Science and Key Laboratory of Particle Physics and Particle Irradiation (MOE), Shandong University, Qingdao; (c) School of Physics and Astronomy, Shanghai Jiao Tong University, Key Laboratory for Particle Astrophysics and Cosmology (MOE), SKLPPC, Shanghai; (d) Tsung-Dao Lee Institute, Shanghai, China
- 59 (a) Kirchhoff-Institut für Physik, Ruprecht-Karls-Universität Heidelberg, Heidelberg; (b) Physikalisches Institut, Ruprecht-Karls-Universität Heidelberg, Heidelberg, Germany
- 60 (a) Department of Physics, Chinese University of Hong Kong, Shatin, N.T., Hong Kong; (b) Department of Physics, University of Hong Kong, Hong Kong; (c) Department of Physics and Institute for Advanced Study, Hong Kong University of Science and Technology, Clear Water Bay, Kowloon, Hong Kong, China
- 61 Department of Physics, National Tsing Hua University, Hsinchu, Taiwan
- 62 IJCLab, Université Paris-Saclay, CNRS/IN2P3, 91405, Orsay, France
- 63 Department of Physics, Indiana University, Bloomington IN, United States of America
- 64 (a) INFN Gruppo Collegato di Udine, Sezione di Trieste, Udine; (b) ICTP, Trieste; (c) Dipartimento Politecnico di Ingegneria e Architettura, Università di Udine, Udine, Italy
- 65 (a) INFN Sezione di Lecce; (b) Dipartimento di Matematica e Fisica, Università del Salento, Lecce, Italy
- 66 (a) INFN Sezione di Milano; (b) Dipartimento di Fisica, Università di Milano, Milano, Italy
- 67 (a) INFN Sezione di Napoli; (b) Dipartimento di Fisica, Università di Napoli, Napoli, Italy
- 68 (a) INFN Sezione di Pavia; (b) Dipartimento di Fisica, Università di Pavia, Pavia, Italy
- 69 (a) INFN Sezione di Pisa; (b) Dipartimento di Fisica E. Fermi, Università di Pisa, Pisa, Italy
- 70 (a) INFN Sezione di Roma; (b) Dipartimento di Fisica, Sapienza Università di Roma, Roma, Italy
- 71 (a) INFN Sezione di Roma Tor Vergata; (b) Dipartimento di Fisica, Università di Roma Tor Vergata, Roma, Italy
- 72 (a) INFN Sezione di Roma Tre; (b) Dipartimento di Matematica e Fisica, Università Roma Tre, Roma, Italy
- 73 (a) INFN-TIFPA; (b) Università degli Studi di Trento, Trento, Italy
- 74 Institut für Astro- und Teilchenphysik, Leopold-Franzens-Universität, Innsbruck, Austria
- 75 University of Iowa, Iowa City IA, United States of America
- 76 Department of Physics and Astronomy, Iowa State University, Ames IA, United States of America
- 77 Joint Institute for Nuclear Research, Dubna, Russia
- 78 (a) Departamento de Engenharia Elétrica, Universidade Federal de Juiz de Fora (UFJF), Juiz de Fora; (b) Universidade Federal do Rio De Janeiro COPPE/EE/IF, Rio de Janeiro; (c) Instituto de Física, Universidade de São Paulo, São Paulo, Brazil
- 79 KEK, High Energy Accelerator Research Organization, Tsukuba, Japan
- 80 Graduate School of Science, Kobe University, Kobe, Japan
- 81 (a) AGH University of Science and Technology, Faculty of Physics and Applied Computer Science, Krakow; (b) Marian Smoluchowski Institute of Physics, Jagiellonian University, Krakow, Poland
- 82 Institute of Nuclear Physics Polish Academy of Sciences, Krakow, Poland
- 83 Faculty of Science, Kyoto University, Kyoto, Japan
- 84 Kyoto University of Education, Kyoto, Japan
- 85 Research Center for Advanced Particle Physics and Department of Physics, Kyushu University, Fukuoka, Japan
- 86 Instituto de Física La Plata, Universidad Nacional de La Plata and CONICET, La Plata, Argentina
- 87 Physics Department, Lancaster University, Lancaster, United Kingdom
- 88 Oliver Lodge Laboratory, University of Liverpool, Liverpool, United Kingdom
- 89 Department of Experimental Particle Physics, Jožef Stefan Institute and Department of Physics, University of Ljubljana, Ljubljana, Slovenia
- 90 School of Physics and Astronomy, Queen Mary University of London, London, United Kingdom
- 91 Department of Physics, Royal Holloway University of London, Egham, United Kingdom
- 92 Department of Physics and Astronomy, University College London, London, United Kingdom
- 93 Louisiana Tech University, Ruston LA, United States of America
- 94 Fysiska institutionen, Lunds universitet, Lund, Sweden
- 95 Centre de Calcul de l'Institut National de Physique Nucléaire et de Physique des Particules (IN2P3), Villeurbanne, France
- 96 Departamento de Física Teórica C-15 and CIAFF, Universidad Autónoma de Madrid, Madrid, Spain
- 97 Institut für Physik, Universität Mainz, Mainz, Germany
- 98 School of Physics and Astronomy, University of Manchester, Manchester, United Kingdom
- 99 CPPM, Aix-Marseille Université, CNRS/IN2P3, Marseille, France
- 100 Department of Physics, University of Massachusetts, Amherst MA, United States of America
- 101 Department of Physics, McGill University, Montreal QC, Canada
- 102 School of Physics, University of Melbourne, Victoria, Australia
- 103 Department of Physics, University of Michigan, Ann Arbor MI, United States of America
- 104 Department of Physics and Astronomy, Michigan State University, East Lansing MI, United States of America
- 105 B.I. Stepanov Institute of Physics, National Academy of Sciences of Belarus, Minsk, Belarus
- 106 Research Institute for Nuclear Problems of Byelorussian State University, Minsk, Belarus
- 107 Group of Particle Physics, University of Montreal, Montreal QC, Canada
- 108 P.N. Lebedev Physical Institute of the Russian Academy of Sciences, Moscow, Russia
- 109 National Research Nuclear University MEPhI, Moscow, Russia
- 110 D.V. Skobeltsyn Institute of Nuclear Physics, M.V. Lomonosov Moscow State University, Moscow, Russia
- 111 Fakultät für Physik, Ludwig-Maximilians-Universität München, München, Germany
- 112 Max-Planck-Institut für Physik (Werner-Heisenberg-Institut), München, Germany
- 113 Nagasaki Institute of Applied Science, Nagasaki, Japan
- 114 Graduate School of Science and Kobayashi-Maskawa Institute, Nagoya University, Nagoya, Japan
- 115 Department of Physics and Astronomy, University of New Mexico, Albuquerque NM, United States of America
- 116 Institute for Mathematics, Astrophysics and Particle Physics, Radboud University/Nikhef, Nijmegen, Netherlands
- 117 Nikhef National Institute for Subatomic Physics and University of Amsterdam, Amsterdam, Netherlands
- 118 Department of Physics, Northern Illinois University, DeKalb IL, United States of America
- 119 (a) Budker Institute of Nuclear Physics and NSU, SB RAS, Novosibirsk; (b) Novosibirsk State University Novosibirsk, Russia
- 120 Institute for High Energy Physics of the National Research Centre Kurchatov Institute, Protvino, Russia
- 121 Institute for Theoretical and Experimental Physics named by A.I. Alikhanov of National Research Centre "Kurchatov Institute", Moscow, Russia
- 122 Department of Physics, New York University, New York NY, United States of America
- 123 Ochanomizu University, Otsuka, Bunkyo-ku, Tokyo, Japan
- 124 Ohio State University, Columbus OH, United States of America
- 125 Homer L. Dodge Department of Physics and Astronomy, University of Oklahoma, Norman OK, United States of America
- 126 Department of Physics, Oklahoma State University, Stillwater OK, United States of America
- 127 Palacký University, Joint Laboratory of Optics, Olomouc, Czech Republic
- 128 Institute for Fundamental Science, University of Oregon, Eugene, OR, United States of America
- 129 Graduate School of Science, Osaka University, Osaka, Japan

- 130 Department of Physics, University of Oslo, Oslo, Norway
 131 Department of Physics, Oxford University, Oxford, United Kingdom
 132 LPNHE, Sorbonne Université, Université de Paris, CNRS/IN2P3, Paris, France
 133 Department of Physics, University of Pennsylvania, Philadelphia PA, United States of America
 134 Konstantinov Nuclear Physics Institute of National Research Centre "Kurchatov Institute", PNPI, St. Petersburg, Russia
 135 Department of Physics and Astronomy, University of Pittsburgh, Pittsburgh PA, United States of America
 136 ^(a) Laboratório de Instrumentação e Física Experimental de Partículas - LIP, Lisboa; ^(b) Departamento de Física, Faculdade de Ciências, Universidade de Lisboa, Lisboa; ^(c) Departamento de Física, Universidade de Coimbra, Coimbra; ^(d) Centro de Física Nuclear da Universidade de Lisboa, Lisboa; ^(e) Departamento de Física, Universidade do Minho, Braga; ^(f) Departamento de Física Teórica y del Cosmos, Universidad de Granada, Granada (Spain); ^(g) Dep Física and CEFITEC of Faculdade de Ciências e Tecnologia, Universidade Nova de Lisboa, Caparica; ^(h) Instituto Superior Técnico, Universidade de Lisboa, Lisboa, Portugal
 137 Institute of Physics of the Czech Academy of Sciences, Prague, Czech Republic
 138 Czech Technical University in Prague, Prague, Czech Republic
 139 Charles University, Faculty of Mathematics and Physics, Prague, Czech Republic
 140 Particle Physics Department, Rutherford Appleton Laboratory, Didcot, United Kingdom
 141 IRFU, CEA, Université Paris-Saclay, Gif-sur-Yvette, France
 142 Santa Cruz Institute for Particle Physics, University of California Santa Cruz, Santa Cruz CA, United States of America
 143 ^(a) Departamento de Física, Pontificia Universidad Católica de Chile, Santiago; ^(b) Universidad Andres Bello, Department of Physics, Santiago; ^(c) Instituto de Alta Investigación, Universidad de Tarapacá, Arica; ^(d) Departamento de Física, Universidad Técnica Federico Santa María, Valparaíso, Chile
 144 Universidade Federal de São João del Rei (UFSJ), São João del Rei, Brazil
 145 Department of Physics, University of Washington, Seattle WA, United States of America
 146 Department of Physics and Astronomy, University of Sheffield, Sheffield, United Kingdom
 147 Department of Physics, Shinshu University, Nagano, Japan
 148 Department Physik, Universität Siegen, Siegen, Germany
 149 Department of Physics, Simon Fraser University, Burnaby BC, Canada
 150 SLAC National Accelerator Laboratory, Stanford CA, United States of America
 151 Department of Physics, Royal Institute of Technology, Stockholm, Sweden
 152 Departments of Physics and Astronomy, Stony Brook University, Stony Brook NY, United States of America
 153 Department of Physics and Astronomy, University of Sussex, Brighton, United Kingdom
 154 School of Physics, University of Sydney, Sydney, Australia
 155 Institute of Physics, Academia Sinica, Taipei, Taiwan
 156 ^(a) E. Andronikashvili Institute of Physics, Iv. Javakishvili Tbilisi State University, Tbilisi; ^(b) High Energy Physics Institute, Tbilisi State University, Tbilisi, Georgia
 157 Department of Physics, Technion, Israel Institute of Technology, Haifa, Israel
 158 Raymond and Beverly Sackler School of Physics and Astronomy, Tel Aviv University, Tel Aviv, Israel
 159 Department of Physics, Aristotle University of Thessaloniki, Thessaloniki, Greece
 160 International Center for Elementary Particle Physics and Department of Physics, University of Tokyo, Tokyo, Japan
 161 Department of Physics, Tokyo Institute of Technology, Tokyo, Japan
 162 Tomsk State University, Tomsk, Russia
 163 Department of Physics, University of Toronto, Toronto ON, Canada
 164 ^(a) TRIUMF, Vancouver BC; ^(b) Department of Physics and Astronomy, York University, Toronto ON, Canada
 165 Division of Physics and Tomonaga Center for the History of the Universe, Faculty of Pure and Applied Sciences, University of Tsukuba, Tsukuba, Japan
 166 Department of Physics and Astronomy, Tufts University, Medford MA, United States of America
 167 Department of Physics and Astronomy, University of California Irvine, Irvine CA, United States of America
 168 Department of Physics and Astronomy, University of Uppsala, Uppsala, Sweden
 169 Department of Physics, University of Illinois, Urbana IL, United States of America
 170 Instituto de Física Corpuscular (IFC), Centro Mixto Universidad de Valencia - CSIC, Valencia, Spain
 171 Department of Physics, University of British Columbia, Vancouver BC, Canada
 172 Department of Physics and Astronomy, University of Victoria, Victoria BC, Canada
 173 Fakultät für Physik und Astronomie, Julius-Maximilians-Universität Würzburg, Würzburg, Germany
 174 Department of Physics, University of Warwick, Coventry, United Kingdom
 175 Waseda University, Tokyo, Japan
 176 Department of Particle Physics and Astrophysics, Weizmann Institute of Science, Rehovot, Israel
 177 Department of Physics, University of Wisconsin, Madison WI, United States of America
 178 Fakultät für Mathematik und Naturwissenschaften, Fachgruppe Physik, Bergische Universität Wuppertal, Wuppertal, Germany
 179 Department of Physics, Yale University, New Haven CT, United States of America

^a Also at Borough of Manhattan Community College, City University of New York, New York NY; United States of America.

^b Also at Bruno Kessler Foundation, Trento; Italy.

^c Also at Center for High Energy Physics, Peking University; China.

^d Also at Centro Studi e Ricerche Enrico Fermi; Italy.

^e Also at CERN, Geneva; Switzerland.

^f Also at CPPM, Aix-Marseille Université, CNRS/IN2P3, Marseille; France.

^g Also at Département de Physique Nucléaire et Corpusculaire, Université de Genève, Genève; Switzerland.

^h Also at Departament de Física de la Universitat Autònoma de Barcelona, Barcelona; Spain.

ⁱ Also at Department of Financial and Management Engineering, University of the Aegean, Chios; Greece.

^j Also at Department of Physics and Astronomy, Michigan State University, East Lansing MI; United States of America.

^k Also at Department of Physics and Astronomy, University of Louisville, Louisville, KY; United States of America.

^l Also at Department of Physics, Ben Gurion University of the Negev, Beer Sheva; Israel.

^m Also at Department of Physics, California State University, East Bay; United States of America.

ⁿ Also at Department of Physics, California State University, Fresno; United States of America.

^o Also at Department of Physics, California State University, Sacramento; United States of America.

^p Also at Department of Physics, King's College London, London; United Kingdom.

^q Also at Department of Physics, St. Petersburg State Polytechnical University, St. Petersburg; Russia.

^r Also at Department of Physics, University of Fribourg, Fribourg; Switzerland.

^s Also at Faculty of Physics, M.V. Lomonosov Moscow State University, Moscow; Russia.

^t Also at Faculty of Physics, Sofia University, 'St. Kliment Ohridski', Sofia; Bulgaria.

^u Also at Giresun University, Faculty of Engineering, Giresun; Turkey.

^v Also at Graduate School of Science, Osaka University, Osaka; Japan.

^w Also at Hellenic Open University, Patras; Greece.

- ^x Also at Institutio Catalana de Recerca i Estudis Avancats, ICREA, Barcelona; Spain.
- ^y Also at Institut für Experimentalphysik, Universität Hamburg, Hamburg; Germany.
- ^z Also at Institute for Particle and Nuclear Physics, Wigner Research Centre for Physics, Budapest; Hungary.
- ^{aa} Also at Institute of Particle Physics (IPP); Canada.
- ^{ab} Also at Institute of Physics, Azerbaijan Academy of Sciences, Baku; Azerbaijan.
- ^{ac} Also at Institute of Theoretical Physics, Ilia State University, Tbilisi; Georgia.
- ^{ad} Also at Instituto de Fisica Teorica, IFT-UAM/CSIC, Madrid; Spain.
- ^{ae} Also at Istanbul University, Dept. of Physics, Istanbul; Turkey.
- ^{af} Also at Joint Institute for Nuclear Research, Dubna; Russia.
- ^{ag} Also at Moscow Institute of Physics and Technology State University, Dolgoprudny; Russia.
- ^{ah} Also at National Research Nuclear University MEPhI, Moscow; Russia.
- ^{ai} Also at Physikalisches Institut, Albert-Ludwigs-Universität Freiburg, Freiburg; Germany.
- ^{aj} Also at The City College of New York, New York NY; United States of America.
- ^{ak} Also at TRIUMF, Vancouver BC; Canada.
- ^{al} Also at Università di Napoli Parthenope, Napoli; Italy.
- ^{am} Also at University of Chinese Academy of Sciences (UCAS), Beijing; China.
- ^{an} Also at Yeditepe University, Physics Department, Istanbul; Turkey.
- * Deceased.